SCUOLA DI DOTTORATO
UNIVERSITÀ DEGLI STUDI DI MILANO-BICOCCA

School of Medicine and Surgery

PhD program in Neuroscience XXIX Cycle

Curriculum in Molecular and Cellular Biology

Study of the autophagy-lysosome pathway in cellular models of Parkinson's disease

Marinig Daniele

Registration number 711903

Tutor: Prof. Carlo Ferrarese

Co-tutor: Dr. Gessica Sala

Coordinator: Prof. Guido Cavaletti

ACADEMIC YEAR 2015/2016

Table of Contents

Chapter 1:
Introduction

1.1 Parkinson's Disease

The first clinical description of Parkinson's disease (PD) dates back to 1817 when the English physician James Parkinson published a monograph entitled "*An essay on the Shaking Palsy*". The current name of the disease was given 60 years later, in 1877, by the neurologist Jean-Martin Charcot in honor of Dr. James Parkinson.

PD is the second most common neurodegenerative disorder, with an overall incidence rate of 17 out of 100,000 (de Lau and Breteler, 2006).

The cardinal symptoms of the disease include: bradykinesia, resting tremors, muscle rigidity and postural instability. Other symptoms may include gait disorders, such as a shorter step and a posture in flexion (camptocormia), hypophonia, dysphagia, sweating abnormalities, constipation, changes in the libido or blood pressure alterations. There may also be sleep and mood disorders, such as depression, anxiety and apathy while cognitive disorders may finally appear in more advanced stages of the disease.

1.1.1 Pathology and clinical features

The two major neuropathologic findings in PD are the loss of pigmented dopaminergic neurons of the *substantia nigra pars compacta* and the presence of Lewy bodies and Lewy neurites.

The *substantia nigra* is part of the basal ganglia, a group of subcortical nuclei situated at the base of the forebrain. The basal ganglia consist of four nuclei; the striatum, the pallidum, the subthalamic nucleus and the above-mentioned *substantia nigra*. Under physiological conditions, the striatum receives glutamatergic excitatory input from the cerebral cortex, whereas provide GABAergic inhibitory output to the *globus pallidus* and then to the thalamus via the so called direct and indirect pathways. In the direct pathway, neurons are projected directly to the internal segment of the globus

pallidus, while in the indirect pathway outputs pass by two intermediate stations, the globus pallidus exterior and the subthalamic nucleus.

Both pathways are modulated by dopamine released from the pigmented neurons of the *substantia nigra pars compacta*, which acts on distinct receptors located on striatal GABAergic neurons: dopamine exerts an excitatory effect on the direct pathway, through the interaction with D1 receptors localized on neurons containing substance P and dynorphin, and inhibits the indirect pathway through the D2 class receptors on cells containing enkephalins.

Thus, the loss of dopaminergic neurons of the *substantia nigra* observed in PD, results in the suppression of the nigrostriatal dopaminergic transmission (Obeso et al., 2008) causing an over-stimulation of the subthalamic nucleus and the internal *globus pallidus*, which exert in turn an inhibiting action on the thalamocortical excitatory projection. The typical clinical symptoms of the disease, occur when more than 60% of striatal dopaminergic neurons are already lost (Dauer et al., 2003).

However, neurodegeneration can be observed in other neuronal populations, such as noradrenergic systems of the *locus coeruleus* (Bertrand et al., 1997), serotonergic nuclei of the median raphe (Halliday et al., 1990) and cholinergic neurons of the nucleus basalis of Meynert (Rogers et al., 1985), as well as in the cerebral cortex (cingulate and entorhinal cortex), in the olfactory bulb and at the autonomic nervous system. The degeneration of hippocampal structures and cortical cholinergic input contributes to the high rate of PD-associated dementia, especially in elderly patients. However, the clinical correlation of injury to serotonergic and noradrenergic pathways are not so clearly characterized as for dopaminergic systems.

PD diagnosis is made on clinical criteria, and is classically based on the identification of three of four cardinal features: bradykinesia, tremor, rigidity, or postural instability. However, only pathology can confirm the diagnosis by the identification of Lewy bodies and the degeneration of nigral neurons (Litvan et al., 2003). Lewy bodies (Figure 1) are intracellular proteinaceous aggregates of alpha-synuclein, parkin, ubiquitin and neurofilaments and can be found in all the affected brain regions (Forno, 1996). Lewy bodies exceed 15 microns in diameter and are

characterized by an organized structure that contains a dense eosinophilic nucleus surrounded by a clear halo. These aggregates are not specific for PD and can be found in Alzheimer's disease or in other forms of dementia (dementia with Lewy bodies), as well as in elderly individuals (Gibb and Lees, 1988).

Figure 1. Lewy bodies in nigral neurons from a patient with PD (image from Dauer et al., 2003)

1.1.2 Etiopathogenesis

While until a few decades ago PD was considered a purely sporadic disease, it is now accepted that its onset is the result of a combination of environmental and genetic factors. Indeed, epidemiological studies have suggested a causative role for pesticides exposure, such as paraquat and rotenone, to the development of sporadic PD, and many familial forms of PD have been identified. Whatever the cause, the mechanisms underlying neuron degeneration may include oxidative stress, mitochondrial dysfunction, glutamate receptor mediated excitotoxicity, neuroinflammation, ubiquitin-proteosome system impairment and autophagy alterations. The most relevant data about these mechanisms will be briefly discussed in the next paragraphs.

1.1.2.1 Oxidative stress

Oxidative stress is probably the most common underlying mechanism of PD. As a matter of fact, increased levels of oxidized lipids, proteins and DNA and a compensatory increase of antioxidant systems can be found in the *substantia nigra* of PD patients (Floo and Wetzel, 1998; Saggu et al., 1989; Alam et al., 1997).

The brain is particularly susceptible to oxidative stress damage given its high metabolic activity and its reduced ability to replace the post-mitotic neuronal population when compared to other organs. The oxidative hypothesis then suggests that free radicals formed by the oxidation of dopamine

contained in the dopaminergic neurons of the *substantia nigra* may play a crucial role in PD progression. Dopaminergic neurons are very sensitive to oxidative damage, since dopamine can auto-oxidize forming toxic superoxide radicals, hydrogen peroxide and dopamine-quinone (Graham, 1978) resulting in an increased oxidative stress (Figure 2). Moreover, neuromelanin, responsible for the nigral neurons pigmentation, is very rich in iron, which is capable of triggering non-enzymatic oxidative processes.

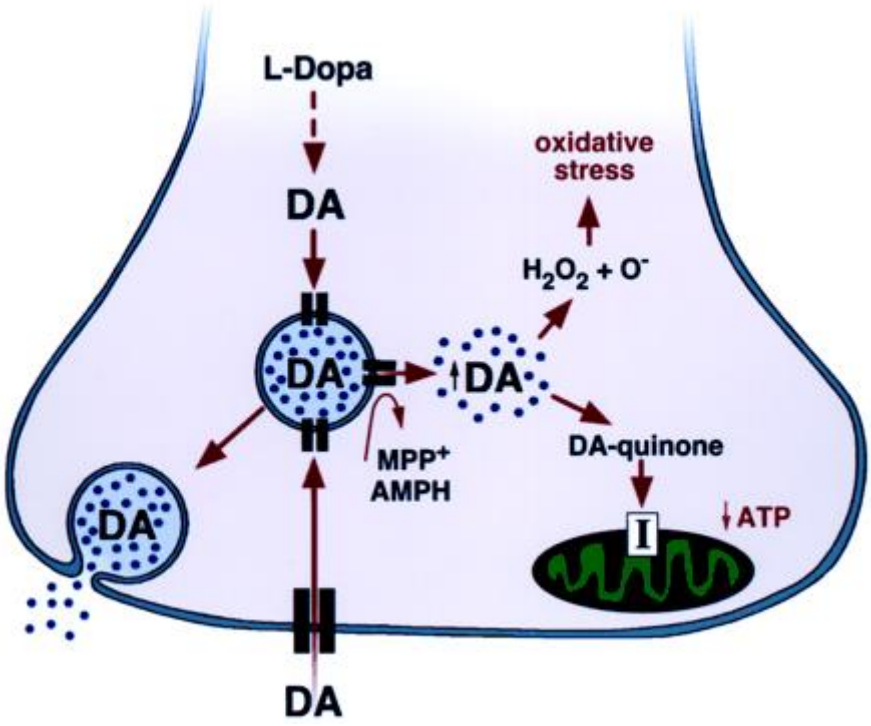

Figure 2. Schematic representation of dopamine catabolism and storage (image from Lotharius and Brundin, 2002).

Hydrogen peroxide is normally quickly eliminated by glutathione, a tripeptide with a reducing function on reactive oxygen species (ROS), through its oxidation to disulfide glutathione. If this mechanism does not function properly, hydrogen peroxide accumulation may lead to a highly reactive hydroxyl radical formation, through a reaction catalysed by iron. The observation that glutathione levels were decreased in the *substantia nigra* of PD patients compared to controls (Sian et al., 1994), suggests a lower level of protection for patients against the formation of free radicals and a more prominent effect of oxidative stress.

1.1.2.2 Mithocondrial dysfunction

ROS formation is closely associated with mitochondrial function since represents an inevitable consequence of mitochondrial respiration. During aerobic respiration a partial reduction of molecular oxygen to superoxide anion (O2-) takes place. This free radical can then be converted to highly reactive hydroxyl radical (OH •) through a Fenton reaction catalyzed by iron, or in peroxynitrite (ONOO-) reacting with nitric oxide (NO).

The first evidence of the role of mitochondrial dysfunction in PD came with a toxin, the 1-methyl-4-phenyl-1,2,3,6-tetrahydropyridine (MPTP), an impurity of desmethylprodine (MPPP), an analog of meperidine. People injecting such drug contaminated with MPTP rapidly developed a disorder similar to PD.

MPTP is a fat soluble molecule able to quickly penetrate the blood-brain barrier and, being amphipathic, it is captured in acid organelles, mostly lysosomes of astrocytes. The enzyme monoamine oxidase B (MAO-B) of astrocytes and serotonergic neurons converts MPTP to MPP+, which reaches the extracellular environment where it is moved in the intracellular space by the dopamine transporter DAT (Nicklas et al., 1985). Within the dopaminergic neurons, MPP+ accumulates in the mitochondria and inhibits the complex I of the electron transport chain abating the ATP production and increasing the formation of ROS, which in turn damage mitochondrial DNA, the components of the respiratory chain and other mitochondrial factors, triggering a vicious circle between block and mitochondrial oxidative stress. Thus, mitochondria can be either a source or a target for ROS and nigral dopaminergic neurons represent a particularly vulnerable population, given their high oxidative load and a reduced antioxidant capacity (Murphy, 2009).

Another important link between PD and mitochondrial dysfunctions is the previously mentioned formation of dopamine-quinone as part of dopamine oxidation. As a matter of fact, dopamine-quinone production results in an alteration of mitochondrial membrane permeability and in an increase in mitochondrial swelling (Berman and Hastings, 1999), indicating again the higher sensitivity of dopaminergic neurons to toxic stresses.

1.1.2.3 Excitotoxicity

Glutamate is a major excitatory neurotransmitter in mammals central nervous system acting in neural development, synaptic plasticity, learning and memory. However, a prolonged and strong activation of glutamate receptors may lead to a toxic phenomenon called excitotoxicity, introduced for the first time by Dr. Olney in 1969 (Olney, 1969). Excitotoxicity has been proposed as a mechanism of many neurodegenerative diseases (Albin and Greenamyre, 1992) including PD. Glutamate acts on two classes of postsynaptic receptors: ionotropic and metabotropic receptors. The ionotropic receptors include: the receptor for the N-methyl-D-aspartate (NMDA) which regulates calcium influx; the kainate receptor; and the α-amino-3-hydroxy-5-methyl-4-isoxazolepropionic acid (AMPA) receptor which regulate the sodium influx. Nigral neurons contain NMDA receptors and receive excitatory glutamatergic input from the subthalamic nucleus (Difazio et al., 1992). Glutamate receptor-mediated calcium overload can activate proteases, lipases and endonucleases and activate the nitric oxide synthase (NOS), causing an increase in nitric oxide production and in ROS formation. Moreover, calcium-mediated neurotoxicity involves the mitochondria, which represent one of the intracellular stores of this ion. If the amount of mitochondrial calcium exceeds a certain level, there is ROS formation, lower ATP production and release of pro-apoptotic factors (Beal, 1992). Thus, mitochondrial dysfunction is intimately connected to excitotoxicity since the damaged mitochondria are unable to sequester intracellular calcium during excitotoxic processes. In addition, the ATP depletion due to respiratory chain block determines an increased susceptibility to neuronal excitotoxicity as it decreases the activity of calcium transporters.

In PD, the subthalamic hyper-activation resulting from nigral neurons degeneration, may induce a further excitotoxic damage in the *substantia nigra*. A demonstration of this hypothesis has been observed as a disease progression slowdown in animal models after block of the glutamatergic transmission from the subthalamus to the *substantia nigra* through NMDA receptors antagonists (Blandini et al., 2001).

1.1.2.4. Neuroinflammation

Microglia activation as well as significantly increased levels of pro-inflammatory cytokines such as tumor necrosis factor (TNF), interleukin-1beta (IL-1β), interleukin-6 (IL-6), inducible nitric oxide

synthase (iNOS) and cyclooxygenase-2 (COX-2) have been reported in the striatum and *substantia nigra* of PD patients (Tansey et al., 2007). Microglia activation may be triggered by protein aggregation or by bacterial or viral infections or trauma. Brain samples from PD patients showed infiltrations of CD4+ and CD8+ cells, which were reproduced in a mouse model of PD during the course of neuronal degeneration (Brochard et al., 2009). In the same study, CD4+ deficient mice showed less neuronal death following treatment with MPTP, thus demonstrating the role of adaptive immunity in the development of the disease.

1.1.2.5. Role of alpha-synuclein

One of the hallmarks of PD is the formation of typical protein aggregates, Lewy bodies, which largely contain alpha-synuclein, a 140 amino acid protein, encoded by the SNCA gene on the chromosome 4q21 (Spillantini et al., 1995). Alpha-synuclein is predominantly expressed in the brain, at the level of the pre-synaptic terminals, in particular in the neocortex, hippocampus, striatum, thalamus, and cerebellum (Iwai et al., 1995). This synaptic localization suggests a possible role in neurotransmission and synaptic plasticity mechanisms. Actually, alpha-synuclein seems to regulate the activity of the enzymes involved in dopamine synthesis, such as tyrosine hydroxylase, the function of synaptic vesicles, the release of dopamine in the synaptic cleft and the trafficking of dopamine transporters to the cell surface (Venda et al., 2010). A direct correlation of alpha-synuclein and PD came with the identification of three missense mutations on SNCA gene: A53T, A30P and E46K, which segregated with the disease and caused PD with autosomal dominant transmission (Polymeropoulos et al., 1997; Kruger et al., 1998; Zarranz et al., 2004). Even duplication and triplications of SNCA have been associated with autosomal dominant forms of PD (Singleton et al., 2003; Chartier-Harlin et al., 2004) showing a correlation between the degree of over-expression and disease severity. Indeed, individuals with SNCA triplications develop an early-onset form of PD with a rapid cognitive decline and more severe non-motor symptoms, a wider neurodegeneration and a more rapid disease progression than patients with the gene duplications (Farrer al., 2004).

The monomeric form of the protein is natively unfolded in aqueous solution but can bind to membrane lipids forming alpha-helices. However, over-expressed or mutated unfolded monomers

may aggregate to form protofibrils which may in turn form amyloid fibrils, large insoluble protein aggregates with β-sheet architecture indigestible to cellular clearance mechanisms (Serpell, 2000). These aggregates collect other proteins forming the characteristics cytoplasmic inclusions of PD. However, other studies proposed that such toxic effect may be exerted by alpha-synuclein oligomers, rather than fibrils (Outeiro et al., 2008; Tetzlaff et al., 2008).

Anyway, alpha-synuclein oligomers-induced toxicity mechanism has not yet been fully elucidated, although probably includes a large number of different intra- and extracellular mechanisms. One of the possible mechanisms is the regulation of proteostasis where alpha-synuclein oligomers appear to inhibit *in vitro* the degree of protein refolding of the chaperone heat shock protein 70 (Hsp70) (Hinault et al., 2010) and proteasome activity (Lindersson et al., 2004). The block of proteostasis can induce chronic endoplasmic reticulum stress (ER stress) leading to cell death. In this regard, it has been recently observed that the formation of alpha-synuclein oligomers may occur inside the endoplasmic reticulum lumen sensitizing neurons to ER stress (Colla et al., 2012). Moreover, alpha-synuclein oligomers can compromise the stability of the cytoskeleton by binding to alpha-tubulin and microtubule protein tau, causing the inactivation and aggregation of the latter (Giasson et al., 2003).

In the extracellular space alpha-synuclein oligomers seem to exert different toxic mechanisms based on their morphology, which may be annular, spherical, chain or tubular. Oligomers in the annular conformation induce an increase in intracellular calcium *in vitro* since they seem to have the ability to create pores on the cell membrane, causing an influx of calcium ions with subsequent cell death, while globular oligomers may enter cells inducing aggregation of endogenous alpha-synuclein with a prion-like spreading behave (Danzer et al., 2007).

1.1.2.6. Protein quality systems

Protein misfolding, aggregation and accumulation are pathogenetic mechanisms already known for many neurodegenerative diseases. Protein aggregates may cause damage by deforming the cell or interfering with intracellular trafficking. Moreover, protein inclusions may sequester other proteins including those necessary for cell survival, which may suggest a direct correlation between inclusion formation and neurodegeneration. Conversely, another hypothesis suggests a protective

role for cytoplasmic protein inclusions, since they may be the result of an active sequestration of misfolded and potentially toxic proteins.

The two major proteolytic systems involved in the protein turnover and the removal of the aberrant and misfolded proteins are the ubiquitin-proteasome system (UPS) and the autophagy-lysosome pathway (ALP).

The UPS is the main pathway responsible for the selective degradation of intracellular soluble proteins in the cytosol, nucleus and endoplasmic reticulum (Coux et al., 1996). UPS-mediated protein degradation requires an elaborate sequence of events: a chain of activated ubiquitin monomers, a small globular protein, is covalently linked to lysine residues on the target protein, serving as a recognition sign for the proteasome, a multi-protein complex formed by different subunits having mutually complementary functions. The protease activity is carried out by the 20S subunit to which are linked two regulatory subunits 19S, which recognize ubiquitinated proteins and send to the 20S subunit. Moreover, the 19S subunits present ATP-binding sites since the proteasome degradative activity represents an energy-dependent process (Tanaka et al., 2012).

Following the discovery of highly ubiquitinated proteins in Lewy bodies (Kuzuhara et al., 1988), many other UPS components, such as subunits of the proteasome and ubiquitination enzymes, were found in the aggregates (Lowe et al., 1990; Kwak et al., 1991). Moreover, a significant reduction in proteasome activity has been observed in the *substantia nigra* of PD patients compared to healthy controls (McNaught et al., 2003). The demonstration that mutations in the Parkin gene (PARK2), a E3 ubiquitin ligase, and in UCH-L1 (PARK5), a ubiquitin hydrolase, cause monogenic forms of PD, suggested again the involvement of the UPS in the pathogenesis of the disease (Kitada et al., 1998; Zhang et al., 2000).

The role of ALP in the pathogenesis of PD will be presented and discussed in the next paragraph.

1.2 Autophagy-lysosome pathway

ALP is another catabolic mechanism for the removal of aberrant proteins, although it is also involved in the turnover of mitochondria (mitophagy) and other organelles as well as in regulating lipids metabolism (Singh et al., 2009), contributing to cell homeostasis. Autophagy participates to both innate and adaptive immunity (Levine and Deretic, 2007) and may exert a protective role against pathogens. Thus, it represents a cell survival mechanism under stress conditions, ensuring cellular integrity through the regeneration of metabolic precursors and the elimination of subcellular debris, although the formation of structures typical of an upregulated autophagy can be observed in a cell death phenomenon morphologically different to apoptosis (Scott et al., 2007) (Figure 3). However, it is not clear whether autophagy activation might be the cause of death or conversely a counteracting response.

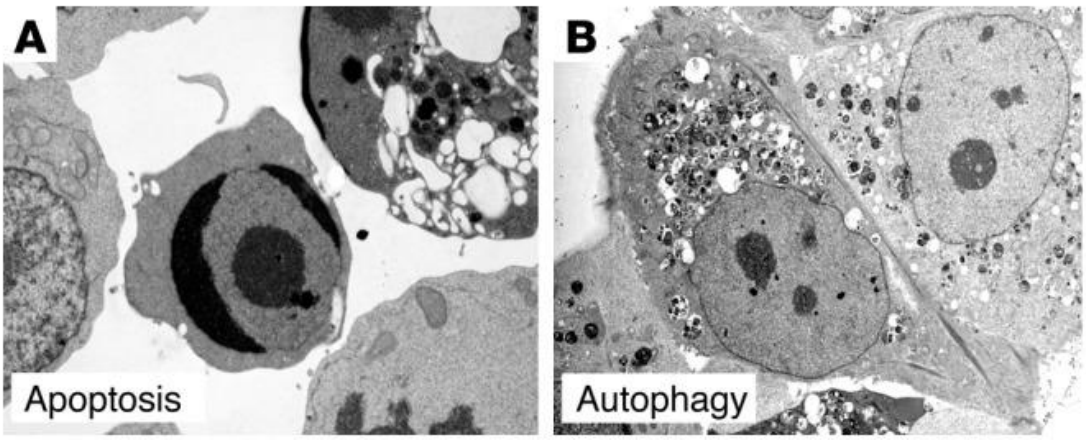

Figure 3. Electron micrographs of structural characteristics of apoptotic cells (A) or autophagy programmed cell death (B) (image from Levine and Yuan, 2005).

The routes through which the intracellular components to be degraded are conveyed to lysosomes are the basis for the distinction of the three known autophagy pathways: macroautophagy, chaperone-mediated autophagy (CMA) and microautophagy. Both macroautophagy and microautophagy digest large cellular structures by selective or non-selective mechanisms, while CMA selectively degrades only soluble proteins. All of them share a common point of arrival, the lysosomes, but differ in the substrates, regulatory mechanisms and activation conditions.

Although each autophagic pathway has its own unique characteristics, they seem to be interconnected since they can further increase their activity during a block of one of the other pathways. For example, blocking CMA induces the activation of macroautophagy (Massey et al., 2006) while macroautophagy dysfunction results in an increase of CMA (Kaushik et al., 2008). UPS is also connected to ALP since its inhibition may induce an upregulation of macroautophagy. Thus, ALP participates in the degradation of ubiquitinated proteins, previously thought as specific substrate of UPS (Figure 4), since its activation is effective in reducing the amount of ubiquitinated protein aggregates and in favoring cell survival, defining a cytoprotective effect for ALP in the presence of UPS dysfunction (Bjørkøy et al., 2005).

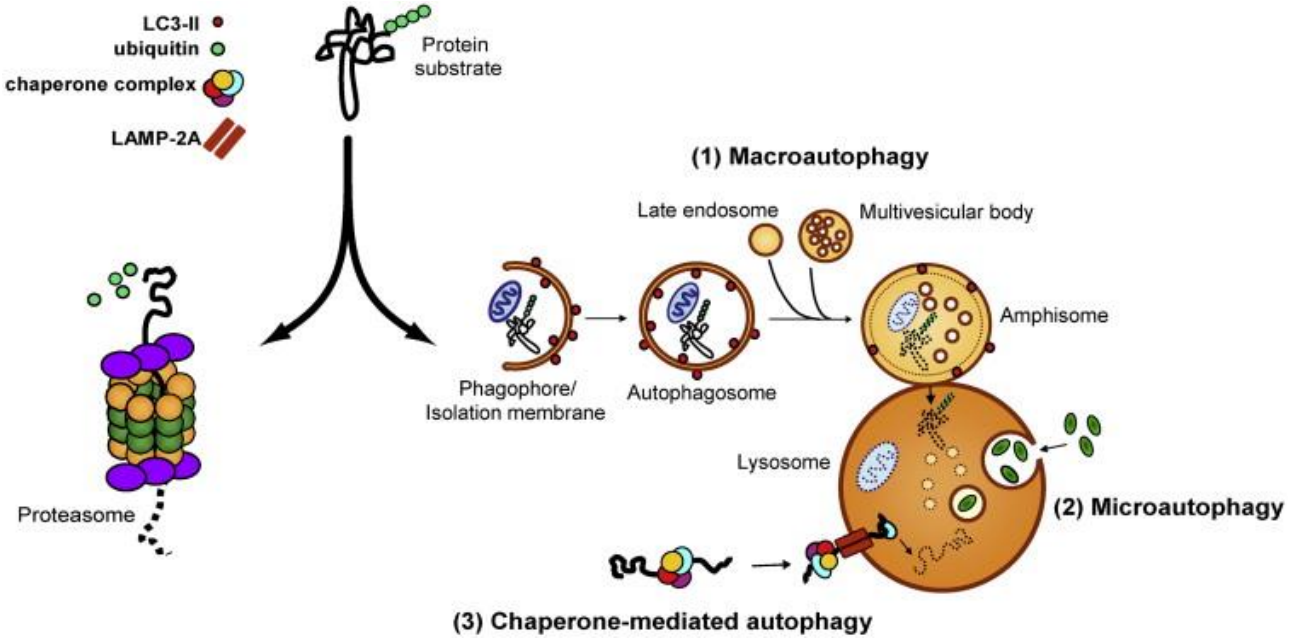

Figure 4. Schematic representation of UPS, macroautophagy, CMA and microautophagy (image from Nedelsky et al., 2008).

ALP activity and its connection with the UPS has become a topic of interest for neurodegenerative diseases for which the failure of catabolic systems has been proposed as one of the main pathogenic mechanisms. As a matter of fact, autophagy is involved in neuronal plasticity and cellular quality control through autophagy is crucial in neurons where abnormal proteins and damaged organelles cannot be reduced through mitotic divisions. In the following paragraphs the cellular and molecular mechanisms of macroautophagy and CMA as well as their potential involvement in PD pathogenesis will be introduced.

1.2.1 Macroautophagy

During macroautophagy process a portion of cytoplasm, including organelles, is enclosed by a double membrane vacuole, called autophagosome which will fuse with a lysosome, leading to cargo degradation. Macroautophagy initiation requires the assembly of the ULK complex, formed by ULK1, Atg13, FIP200 and Atg101, to the membrane in order to promote the formation of the autophagosome (Mizushima, 2010). The activation of the ULK complex requires the dissociation from mTORC1 (mammalian target of rapamycin complex 1) during cellular stress situations. mTORC1 contains mTOR, a kinase which inhibits autophagy via ULK1 and Atg13 phosphorylation. Rapamycin and nutrient starvation inactivate mTOR thus beginning the autophagosome formation. Alternatively, macroautophagy can also be induced with mTOR-independent mechanisms, such as altering the transcription of macroautophagy genes or reducing the levels of inositol 1,4,5-triphosphate (Vicencio et al., 2009).

The autophagosome formation then requires the nucleation and the expansion of the membranes to generate a vesicular structure. The nucleation involves the formation of the large protein complex Beclin1/phosphatidylinositol-3-kinase (PI3K) class III, coordinated by the interaction of many proteins including Beclin1, UVRAG, Atg14, Bcl-2, p150, AMBRA1, endophillin B1 and Vps34, which activates PI3K to produce phosphatidylinositol-3-phosphate. The formation of this complex is regulated by Bcl-2, a well-known anti-apoptotic factor that inhibits autophagy by binding Beclin1; during starvation Beclin1 dissociates from Bcl-2, allowing the formation of PI3K complex. Following nucleation, macroautophagy involves the recruitment of Atg proteins to the autophagosome membrane in order to promote the extension, expansion and the completion of autophagosome formation. During the elongation and expansion step, Atg7 and Atg10 help the formation of Atg5-Atg12 complex, which also interacts with Atg16L1 (Mizushima et al., 1998). The complex Atg5-Atg12-Atg16L1, together with Atg3, Atg4 and Atg7, promotes the conjugation of phosphatidylethanolamine (PE) to the microtubule-associated protein 1 light chain 3 (LC3)-I to form LC3-II, which is then translocated to the membrane of the pre-autophagosomes. In Figure 5 are shown the three steps of autophagosome formation.

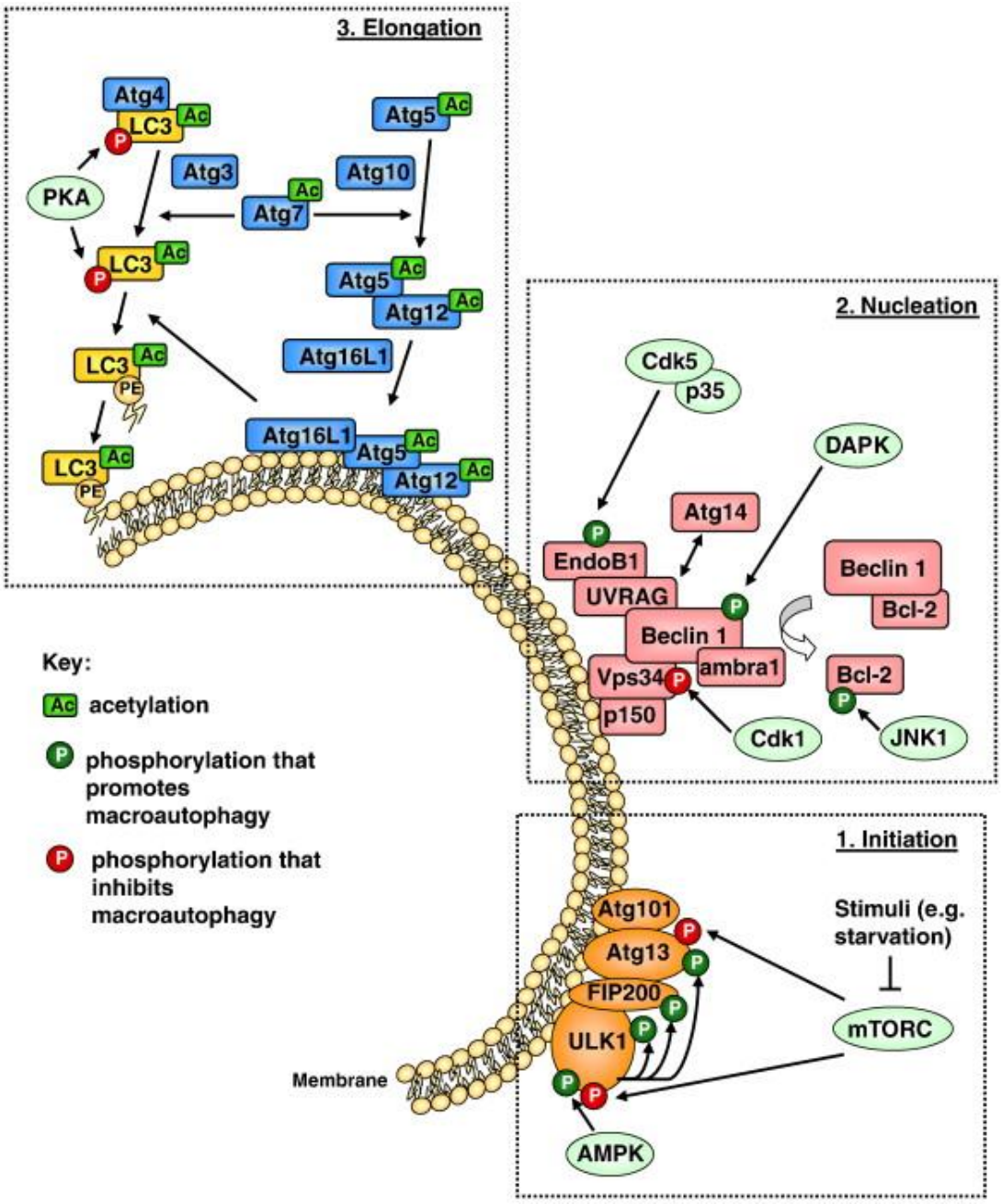

Figure 5. The three phases of autophagosome formation: 1) initiation, 2) nucleation and 3) elongation (image from Wong et al., 2011).

Following the expansion, the autophagosome fuses with a lysosome in a process known as maturation of the autophagosome, but can also fuse with different vesicles of the endosomal/lysosomal pathway such as late endosomes. Finally, the autophagosome maturation and the degradation require the action of a protein marker of late endosomes, Rab7 (Jäger et al., 2004), and the lysosomal associated membrane protein 2 (lamp2) which regulates fusion of the lysosome with the autophagosome (Eskelinen et al., 2002).

1.2.1.1 Macroautophagy and PD

The first evidence of an involvement of ALP in PD emerged with the observation of an accumulation of autophagic vacuoles in the *substantia nigra* of PD patients (Anglade et al., 1997). Interestingly, autophagy alterations may be found outside the brain since an increased conversion of LC3-I to LC3-II, indicative of an induced autophagic response, was observed in PD peripheral blood mononuclear cells (Prigione et al., 2010).

Moreover, alpha-synuclein overexpression seems to block macroautophagy machinery, inhibiting the autophagosome formation. This block appears to occur earlier than the autophagosome formation, involving Atg9, the protein responsible for the transport of the membrane to the autophagosome formation site (Reggiori et al., 2009). In fact, Atg9 is physiologically localized in the perinuclear area (the autophagosome formation site) while in the presence of alpha-synuclein overexpression is delocalized and distributed in the cytoplasm (Winslow et al., 2010). The same phenotype is observed in the case of RAB1A knock-down, a protein involved in the regulation of intracellular vesicular trafficking and recognized as a factor capable of inducing macroautophagy, suggesting that alpha-synuclein is able to block macroautophagy inhibiting the activity of RAB1A, causing the mislocalization of Atg9 and then the inhibition of autophagosome formation (Winslow et al., 2010).

One of the most important and more intriguing functions of macroautophagy linked to PD pathogenesis is the degradation of non-functioning mitochondria, a process called mitophagy. As already said, mitochondrial dysfunction is one of the mechanisms underlying PD pathogenesis. Interestingly, mutant A53T alpha-synuclein induced increased colocalization of autophagosomes and mitochondria and a decrease in the number and length of mitochondria *in vitro* (Choubey et al., 2011). Supporting the hypothesis of mitophagy in PD pathogenesis is the demonstration that Parkin, an ubiquitin ligase whose mutated form causes familial forms of PD, promotes autophagy of damaged mitochondria by mediating the engulfment of mitochondria by autophagosomes and the selective elimination of impaired mitochondria (Narendra et al., 2008). Parkin interacts with another PD-related protein, PINK1, a kinase anchored to the mitochondrial membrane. PINK1 is imported to the mitochondrial inner membrane in a membrane potential-dependent manner and here cleaved

by PARL protease (Jin et al., 2010). If mitochondria depolarization occurs, PINK1 accumulates on the outer membrane of damaged mitochondria by promoting the recruitment of Parkin, suggesting upstream action of the latter. Pathogenic mutations in both of these genes interfere with their mitophagyc functions (Matsuda et al., 2010), suggesting a role of mitophagy in PD.

1.2.2 Chaperone-mediated autophagy

CMA is a selective catabolic pathway involved in the degradation of specific cellular proteins. Thus, CMA represents an efficient machinery for the removal of specific damaged or aberrant proteins and an essential key-regulator in multiple cellular processes. CMA specificity is due to the presence in eligible substrates of a pentapeptide conserved motif biochemically related to KFERQ that consists of a glutamine (Q) residue at the beginning or end of the sequence, followed by a positively charged amino acid, a lysine (K) or arginine (R) residue, and one of the four hydrophobic amino acids phenylalanine (F), valine (V), leucine (L) or isoleucine (I) flanked by a negatively charged residue glutamic acid (E) or aspartic acid (D) (Dice, 1990). About 30% of soluble cytosolic proteins contain this motif while membrane proteins do not contain it, thus, not constituting substrates for CMA (Chiang HL and Dice, 1988). Actually, this motif is selectively recognized by the cytosolic chaperone heat shock cognate protein of 70 kDa, hsc70, which binds the substrate and translocates it to the lysosome membrane (Chiang et al., 1989). Hsc70, in association with a subset of molecular co-chaperones, participates to the unfolding of the substrate protein, an essential requirement for translocation to the lysosomes (Agarraberes and Dice, 2001). Then, the substrate is targeted to the lysosomal membrane where it binds with the lysosome-associated membrane protein type 2A (lamp2A) (Cuervo and Dice, 1996). Lamp2A, in association with other proteins, such as GFAP (glial fibrillary acidic protein) and EF1α (elongation factor 1α), forms a multi-protein complex which regulates the substrate translocation into the lysosomal lumen (Bandyopadhyay et al., 2008), a process which requires the presence of a specific form of hsc70 within the lysosomes (lys-hsc70). At the end of the process, lamp2A disassembles into monomers to initiate a new cycle of substrate uptake and degradation (Figure 6). Thus, the presence of lys-hsc70 discriminates the competent lysosomes for CMA. While only a small subset of lysosomes contains lys-hsc70, the

percentage of active lysosomes for the CMA (ie containing both lys-hsc70 and CMA substrates) increases in response to stress conditions, such as nutrients deprivation and oxidative stress, passing from a 20% at the baseline up to 80% of the lysosomal population (Cuervo et al., 1997).

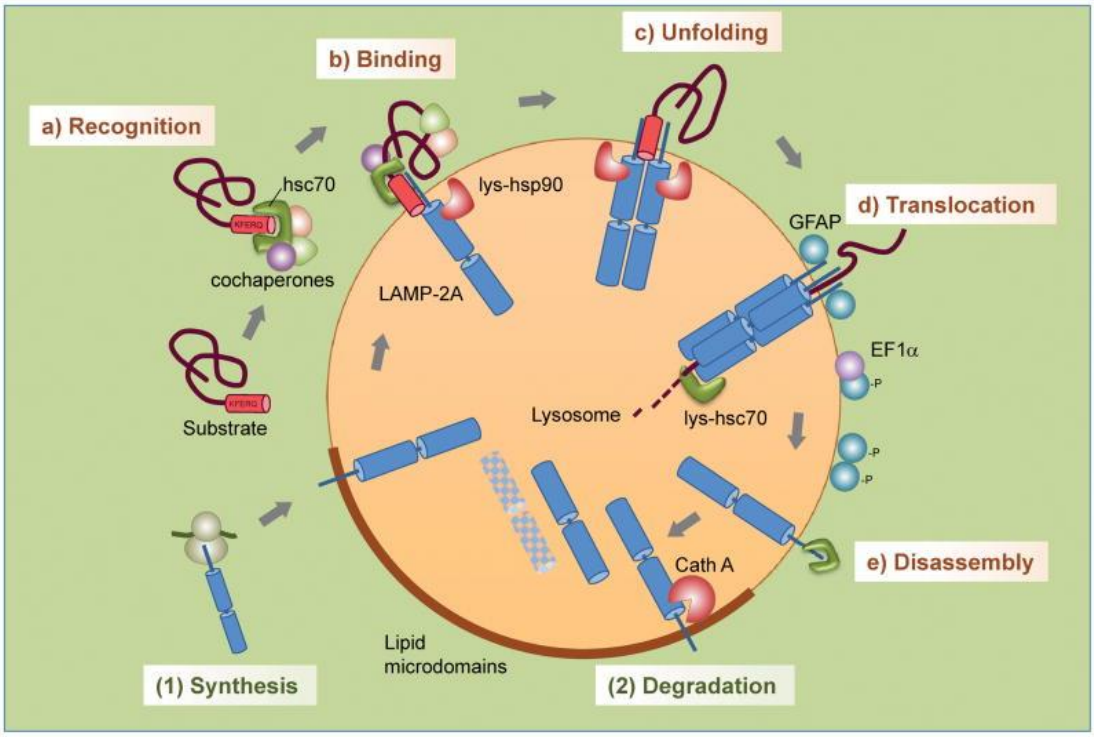

Figure 6. Schematic representation of chaperone-mediated autophagy (image from Kaushik and Cuervo, 2012).

Although the primary role of CMA may be amino acids recycling during starvation, CMA is more importantly involved in the protein quality control system. In fact, CMA represents the main catabolic mechanism for the removal of oxidized, aberrant and damaged proteins from the cell. Oxidative stress or exposure to toxins are able to upregulate CMA (Kiffin et al., 2004; Cuervo et al., 1995) and cells with reduced CMA activity resulted more susceptible to oxidative agents (Massey et al., 2006).

1.2.2.1 CMA and PD

The demonstration that CMA is crucial in regulating the intraneuronal levels of alpha-synuclein (Cuervo et al., 2004; Mak et al., 2010), lead to the hypothesis that dysfunctions in this selective catabolic pathway may be one of the pathogenic contributors to PD. Supporting this, an association of PD-related mutations to dysfunctions of CMA was evidenced in transgenic *in vitro* and *in vivo* models. Mutant A30P and A53T alpha-synuclein bind to lamp2A with a higher affinity without

being internalized and degraded (Cuervo et al., 2004) and mutations of the leucine-rich repeat kinase 2 (LRRK2), which cause the most common familial form of PD, is able to block CMA by inhibiting the translocation complex at the lysosome membrane (Orenstein et al., 2013). Wild-type alpha-synuclein overexpression is accompanied by an increase of lamp2A, but higher levels of alpha-synuclein will inevitably lead to the formation of oligomers undegradable by CMA (Xilouri et al., 2009). More importantly, a down-regulation of both hsc70 and lamp2A was observed in the *substantia nigra pars compacta* and amygdala of PD patient as compared to healthy controls (Alvarez-Erviti et al., 2010). The deleterious effect of the down-regulation of lamp2A has been evidenced in *in vitro* studies as an increased sensitivity to oxidative stressors (Massey et al., 2006) and an accumulation of soluble high molecular weight and detergent-insoluble species of alpha-synuclein (Vogiatzi et al., 2008). Finally, a very recent study showed that CMA impairment by lamp2A downregulation resulted in an increase of autophagic vacuoles in nigral neurons and a progressive loss of nigral dopaminergic neurons in rats (Xilouri et al., 2016). Anyway, CMA impairment may be partially compensated by macroautophagy, but it may be not sufficient in the long term or may itself cause cell death for autophagy during stressful conditions. On the contrary, *in vitro* studies showed that CMA upregulation by lamp2A over-expression protected cells from alpha-synuclein-induced neurotoxicity and was able to restore the nigrostriatal degeneration induced by alpha-synuclein and to reduce total alpha-synuclein levels as well as the generation of its aggregated and phosphorylated forms in rats (Xilouri et al., 2013). Thus, these evidences suggest that CMA dysregulations in PD may be a cause rather than a consequence of disease pathogenesis.

1.3 Aim of the thesis

Despite evidences for an involvement of dysfunction of ALP in PD pathogenesis have been already reported, little is known about the exact mechanisms underlying the potential noxious accumulation of undigested proteins within dopaminergic neurons. In particular, a more thorough comprehension of the link between CMA dysfunctions and PD is still required. Thus, this study aimed at fulfilling this point by assessing ALP in different *in vitro* models of PD with a more careful attention to CMA.

To this aim, we firstly investigated the potential role of hsc70 alteration in rotenone-induced PD cellular models. Indeed, hsc70 is the CMA effector responsible for the recognition and targeting of substrates to the lysosomal surface. However, other important functions and activities are ascribed to hsc70, including the slow-down of the assembly of alpha-synuclein into fibrils (Pemberton et al., 2011; Pemberton and Melki, 2012) and the fragmentation of alpha-synuclein fibrils into shorter non-toxic fibrils (Gao et al., 2015), suggesting that hsc70 abnormalities can play a crucial role in PD pathogenesis.

In the second part of the project, ALP was more widely assessed in fibroblasts from sporadic PD patients and in fibroblasts from PD patients carrying the G2019S mutation on LRRK2, in order to highlight possible molecular alterations of ALP in patient cells either under basal conditions or after different autophagy-modulator stimuli. Particular attention was paid to CMA, given its main involvement in alpha-synucelin degradation and the lack of data on this pathway in PD fibroblasts.

Chapter 2:
Rotenone down-regulates HSPA8/hsc70 chaperone protein in vitro: a new possible toxic mechanism contributing to Parkinson's disease

Adapted from:

Sala G[1], **Marinig D**[2], Riva C[3], Arosio A[3], Stefanoni G[4], Brighina L[5], Formenti M[6], Alberghina L[7], Colangelo AM[7], Ferrarese C[8]

Neurotoxicology. 2016 May;54:161-9. doi: 10.1016/j.neuro.2016.04.018. Epub 2016 Apr 28.

[1]Lab. of Neurobiology, School of Medicine and Surgery, University of Milano-Bicocca, Milano, Italy; NeuroMI Milan Center for Neuroscience, University of Milano-Bicocca, Milano, Italy. Electronic address: gessica.sala@unimib.it.

[2]Lab. of Neurobiology, School of Medicine and Surgery, University of Milano-Bicocca, Milano, Italy; PhD Program in Neuroscience, University of Milano-Bicocca, Milano, Italy; NeuroMI Milan Center for Neuroscience, University of Milano-Bicocca, Milano, Italy.

[3]Lab. of Neurobiology, School of Medicine and Surgery, University of Milano-Bicocca, Milano, Italy; NeuroMI Milan Center for Neuroscience, University of Milano-Bicocca, Milano, Italy.

[4]Lab. of Neurobiology, School of Medicine and Surgery, University of Milano-Bicocca, Milano, Italy; Dept. of Neurology, San Gerardo Hospital, Monza, Milano, Italy.

[5]Dept. of Neurology, San Gerardo Hospital, Monza, Milano, Italy; NeuroMI Milan Center for Neuroscience, University of Milano-Bicocca, Milano, Italy.

[6]Lab. of Neuroscience R. Levi-Montalcini, Dept. of Biotechnology and Biosciences, University of Milano-Bicocca, Milano, Italy; SYSBIO Centre of Systems Biology, University of Milano-Bicocca, Milano, Italy.

[7]Lab. of Neuroscience R. Levi-Montalcini, Dept. of Biotechnology and Biosciences, University of Milano-Bicocca, Milano, Italy; SYSBIO Centre of Systems Biology, University of Milano-Bicocca, Milano, Italy; NeuroMI Milan Center for Neuroscience, University of Milano-Bicocca, Milano, Italy.

[8]Lab. of Neurobiology, School of Medicine and Surgery, University of Milano-Bicocca, Milano, Italy; Dept. of Neurology, San Gerardo Hospital, Monza, Milano, Italy; NeuroMI Milan Center for Neuroscience, University of Milano-Bicocca, Milano, Italy.

Abstract

HSPA8/hsc70 (70-kDa heat shock cognate) chaperone protein exerts multiple protective roles. Beside its ability to confer to the cells a generic resistance against several metabolic stresses, it is also involved in at least two critical processes whose activity is essential in preventing Parkinson's disease (PD) pathology. Actually, hsc70 protein acts as the main carrier of chaperone-mediated autophagy (CMA), a selective catabolic pathway for alpha-synuclein, the main pathogenic protein that accumulates in degenerating dopaminergic neurons in PD. Furthermore, hsc70 efficiently fragments alpha-synuclein fibrils in vitro and promotes depolymerization into non-toxic alpha-synuclein monomers.

Considering that the mitochondrial complex I inhibitor rotenone, used to generate PD animal models, induces alpha-synuclein aggregation, this study was designed in order to verify whether rotenone exposure leads to hsc70 alteration possibly contributing to alpha-synuclein aggregation. To this aim, human SH-SY5Y neuroblastoma cells were treated with rotenone and hsc70 mRNA and protein expression were assessed; the effect of rotenone on hsc70 was compared with that exerted by hydrogen peroxide, a generic oxidative stress donor with no inhibitory activity on mitochondrial complex I. Furthermore, the effect of rotenone on hsc70 was verified in primary mouse cortical neurons. The possible contribution of macroautophagy to rotenone-induced hsc70 modulation was explored and the influence of hsc70 gene silencing on neurotoxicity was assessed. We demonstrated that rotenone, but not hydrogen peroxide, induced a significant reduction of hsc70 mRNA and protein expression. We also observed that the toxic effect of rotenone on alpha-synuclein levels was amplified when macroautophagy was inhibited, although rotenone-induced hsc70 reduction was independent from macroautophagy. Finally, we demonstrated that hsc70 gene silencing up-regulated alpha-synuclein mRNA and protein levels without affecting cell viability and without altering rotenone- and hydrogen peroxide-induced cytotoxicity.

These findings demonstrate the existence of a novel mechanism of rotenone toxicity mediated by hsc70 and indicate that dysfunction of both CMA and macroautophagy can synergistically

exacerbate alpha-synuclein toxicity, suggesting that hsc70 up-regulation may represent a valuable therapeutic strategy for PD.

2.1 Introduction

HSPA8/hsc70 (70-kDa heat shock cognate) protein represents a constitutively expressed protein belonging to the heat shock protein 70 (hsp70) chaperone family (Liu et al., 2012). Hsc70 is mainly localized in the intracellular space, possesses a highly conserved amino acid sequence and plays a critical role in a variety of cellular mechanisms including endocytosis, protein folding and degradation (Stricher et al., 2013).

Recent studies reported that hsc70 is able to confer to the cells resistance against metabolic stress, hyperthermia and oxidative challenges (Chong et al., 2013; Wang et al., 2013a). Furthermore, particularly relevant is the involvement of hsc70 protein in the autophagic pathway known as chaperone-mediated autophagy (CMA), a selective device for the degradation of aberrant proteins containing the consensus peptide sequence KFERQ, which are directly transported to the lysosomes by a translocation system constituted by specific carrier proteins including cytosolic hsc70. Hsc70 is also localized into the lysosomal lumen where it allows the translocation of the substrate protein across the lysosomal membrane (Cuervo and Wong, 2014). Dysfunction of the CMA pathway is known to be closely associated with Parkinson's disease (PD) (Alvarez-Erviti et al., 2010; Cuervo et al., 2004; Kabuta et al., 2008; Xilouri et al., 2009); in particular, a significant reduction of hsc70 levels was evidenced in the *substantia nigra pars compacta* and amygdala of PD brains (Alvarez-Erviti et al., 2010) and in lymphomonocytes obtained from sporadic PD patients (Sala et al., 2014).

A significant downregulation of HSPA8/hsc70 was also observed in Alzheimer's disease post-mortem brain tissues (Silva et al., 2014), suggesting that loss of expression of this molecular chaperone should play a critical role in the neuronal death associated not only with PD but also with other neurodegenerative diseases.

Since a crucial pathogenic role in PD is recognized to be played by intraneuronal accumulation and aggregation of alpha-synuclein, the demonstration that CMA represents the main catabolic system for alpha-synuclein (Cuervo et al., 2004; Mak et al., 2010) has strengthened the link between CMA dysfunction and PD pathology. Further reinforcing the connection between hsc70 and PD, hsc70 has been demonstrated *in vitro* to bind to both soluble alpha-synuclein, slowing down its assembly

into fibrils, and fibrillar form even with higher affinity (Pemberton et al., 2011; Pemberton and Melki, 2012), thus limiting the prion-like alpha-synuclein spreading known to amplify PD-associated neurodegeneration. Lastly, a very recent study demonstrated that HSPA8/hsc70 represents the main constituent of a disaggregase system that efficiently fragments alpha-synuclein fibrils *in vitro* into shorter fibrils and promotes their depolymerization into non-toxic alpha-synuclein monomers (Gao et al., 2015). These findings identify other protective mechanisms exerted by hsc70 against the cytotoxicity associated with alpha-synuclein aggregation and inter-neuronal propagation occurring in PD.

It is well known that exposure to rotenone, an inhibitor of the mitochondrial complex I, is able to reproduce PD pathology both in animal and cellular models, as indicated by the degeneration of nigrostriatal dopaminergic neurons and the formation in nigral neurons of alpha-synuclein-positive cytoplasmic inclusions (Betarbet et al., 2000; Gao et al., 2002; Sherer et al., 2003), although with some important limitations (Höglinger et al., 2006). Considering that rotenone induces alpha-synuclein aggregation and that hsc70 has a disaggregant effect on alpha-synuclein, this study was designed in order to verify whether rotenone exposure leads to hsc70 alteration possibly contributing to alpha-synuclein aggregation. To this aim, human SH-SY5Y neuroblastoma cells were treated with rotenone and hsc70 mRNA and protein expression was assessed. The protein levels of other heat shock proteins, hsp70 and hsp90, were evaluated to examine the specificity of rotenone-induced hsc70 reduction; the effect of rotenone on hsc70 was compared with that exerted by hydrogen peroxide, a generic oxidative stress donor with no inhibitory activity on mitochondrial complex I. Furthermore, the effect of rotenone on hsc70 was confirmed in primary mouse cortical neurons. As we observed a rotenone-induced autophagosome accumulation, the possible contribution of macroautophagy to rotenone-induced modulation of hsc70 was explored. The influence of hsc70 reduction on neurotoxicity was verified through HSPA8/hsc70 gene silencing.

2.2 Material and methods

2.2.1 Cell cultures

Human neuroblastoma SH-SY5Y cells were grown in Dulbecco's modified Eagle's medium-F12 (EuroClone) supplemented with 10% fetal bovine serum (EuroClone), 100 U/mL penicillin (EuroClone), 100 μg/mL streptomycin (EuroClone) and 2 mM L-glutamine (EuroClone), at 37°C in an atmosphere of 5% CO_2 in air. SH-SY5Y cells were used at a number of passages of growth ranging from thirteen to seventeen.

Cortical neurons were prepared as previously described (Cirillo et al., 2014). Animal experiments were carried out using protocols approved by the University of Milano-Bicocca Animal Care and Use Committee and by the Italian Ministry of Health (protocol number 14–2011). This study complies with the ARRIVE guidelines. Briefly, cortices were dissected from neonatal (P1-P2) C57BL/6J mice (Charles River Laboratories), washed in dissociation medium and digested by trypsin (0.15%) with deoxyribonuclease (DNAse, 1 mg/ml, Sigma-Aldrich) at 37°C for 20 min. After mechanical dissociation, cells ($1x10^6$/ml) were plated onto poly-D-lysine (1 mg/ml) coated dishes in Neurobasal medium (NB; Invitrogen) containing B27 (Invitrogen), bFGF 10 ng/ml (Invitrogen), glutamine 1mM (Sigma-Aldrich) and antibiotics (Sigma-Aldrich). Cultures were maintained at 37°C in 5% CO_2 and used after 8 days *in vitro* (DIV). To evaluate purity of cultures (99-99.5 %), cells were plated onto 12 mm poly-D-lysine coated coverslip (5000/well) and assessed by immunocytochemistry using anti-βIII-tubulin (Cell Signaling), as previously described (Cirillo et al., 2014). Neurons were imaged under a reversed microscope Olympus CX40 (X20) equipped with an Olympus camera.

2.2.2 Cytotoxicity assays

The effect of rotenone or hydrogen peroxide on cell viability was assessed by the MTT assay based on reduction of the yellow tetrazolium salts (MTT) to the purple formazan by mitochondrial dehydrogenases. After exposure to rotenone (from 100 to 800 nM) or hydrogen peroxide (from 50 to 200 μM) for 6 or 24 hours, SH-SY5Y cells were incubated with 0.5 mg/ml MTT (Sigma-Aldrich) in standard medium for 45 min at 37°C in an atmosphere of 5% CO_2 in air. The effect on

cell viability of 5 mM 3-methyladenine (3-MA) for 24 hours, alone or in combination with 200 -400 nM rotenone, was also assessed in SH-SY5Y cells. Similarly, cortical neurons (5000 cells/well) at DIV8 were treated with rotenone (from 100 to 800 nM) for 6 or 24 hours and incubated with MTT (0.5 mg/ml) for 4 hours. After cell solubilization with DMSO, absorbance was quantified (wavelength 570 nm) using a multi-mode microplate reader (FLUOstar Omega, BMG LABTECH) and cell viability expressed as % vs. vehicle-treated cells. Since rotenone affects mitochondrial function, rotenone-induced cell death was also evaluated with the Trypan blue exclusion test in order to independently confirm results obtained at MTT assay.

2.2.3 Whole-cell reactive oxygen species (ROS) levels

The dye 2',7'-dichlorofluorescein diacetate (DCF-DA, Sigma-Aldrich) was used to quantify the levels of whole-cell ROS. After medium removal, cells were exposed to 10 μM DCF-DA in Locke's buffer (154 mM NaCl, 5.6 mM KCl, 3.6 mM $NaHCO_3$, 2.3 mM $CaCl_2$, 5.6 mM glucose, 5 mM Hepes, 1.2 mM $MgCl_2$, pH 7.4) for 45 min at 37°C in an atmosphere of 5% CO_2 in air. Cells were washed in Locke's buffer without glucose, harvested and lysed. Fluorescence units (FU) were quantified (excitation 488 nm, emission 525 nm) and related to the total protein content assessed using the method of Bradford.

2.2.4 RNA extraction and cDNA synthesis

Total RNA was extracted using the RNeasy Mini kit (Qiagen), according to the manufacturer instructions. RNA concentration was determined spectrophotometrically at 260 nm. RNA (2 μg) was retro-transcribed into cDNA using the SuperScript® VILO™ cDNA Synthesis Kit (Invitrogen) at the following conditions: 10 min at 25°C and 60 min at 42°C. The reaction was terminated at 85°C for 5 min and cDNAs stored at -20°C.

2.2.5 Real-time quantitative PCR (qPCR)

cDNAs obtained from RNA (50 ng for hsc70 and 100 ng for alpha-synuclein) were amplified in triplicate in the ABI Prism 7500 HTSequence Detection System (Applied Biosystems) using the Platinum® SYBR® Green qPCR SuperMix-UDG (Invitrogen) at the following conditions: 50°C for 2 min, 95°C for 10 min, 40 cycles of: 95°C for 15 sec, 60°C for 30 sec. The following primer pairs

were used: human hsc70-F (CAGGTTTATGAAGGCGAGCGTGCC) and human hsc70-R (GGGTGCAGGAGGTATGCCTGTGA); human alpha-synuclein-F (GCAGCCACTGGCTTTGTCAA) and human alpha-synuclein-R (AGGATCCACAGGCATATCTTCCA); human beta-actin-F (TGTGGCATCCACGAAACTAC) and human beta-actin-R (GGAGCAATGATCTTGATCTTCA); mouse hsc70-F (CCTCGGAAAGACCGTTACCA) and mouse hsc70-R (TTTGTTGCCTGTCGCTGAGA); mouse beta-actin-F (GTCGAGTCGCGTCCACC) and mouse beta-actin-R (GTCATCCATGGCGAACTGGT). For relative quantification of each target vs. beta-actin mRNA, the comparative C_T method was used as previously described (Sala et al., 2010).

2.2.6 Western blotting

Cell pellets were lysed in cell extraction buffer (Invitrogen) supplemented with 1 mM PMSF and protease inhibitor cocktail (Sigma-Aldrich) and protein concentrations determined by Bradford's method. After denaturation, 10 and 30 μg (for mouse and human hsc70, respectively), 30 μg (for hsp70, hsp90 and beclin-1) or 50 μg (for LC3II and alpha-synuclein) proteins were separated by electrophoresis in 8% or 4-12% SDS-PAGE and transferred to nitrocellulose. Blots were blocked for 1 hour, incubated overnight at 4°C with specific primary antibodies (hsc70 Abcam, 1:3,000 dilution, hsp70 Enzo Life Sciences, 1:3,000 dilution, hsp90 Cell Signaling, 1:1,000 dilution, beclin-1 Cell Signaling, 1:1,000 dilution; LC3B Cell Signaling, 1:500 dilution; alpha-synuclein BD Biosciences, 1:1,000 dilution) and then with the HRP-linked anti-mouse or –rabbit IgG for 1 hour. Beta-actin (Sigma, 1:30,000 dilution) was used as internal standard. Signals were revealed by chemiluminescence, visualized on X-ray film and quantified by GS-710 Imaging Densitometer (Bio-Rad).

2.2.7 siRNA transfection

Gene silencing by small interfering RNA (siRNA) was carried out by transfecting cells with a siRNA-lipid complex composed by 10 nM Silencer® Select siRNA (Ambion® by Life Technologies) targeted to HSPA8/hsc70 gene and Lipofectamine® RNAiMAX Transfection Reagent (Invitrogen by Life Technologies) in 1:1 ratio. 10 nM Silencer® Select Negative Control

siRNA (Ambion® by Life Technologies) was used as non-targeting negative control. After 48 hours, transfection reagents were washed out and cells were pelleted or stimulated for 24 hours with 400 nM rotenone or 100 μM hydrogen peroxide.

2.2.8 Statistical analysis

All data are shown as mean ± standard deviation (SD). Statistical analysis was performed using GraphPad Prism 4.0. Repeated measures ANOVA, followed by Dunnett's or Tukey's multiple comparison test, was used to assess the significance of differences between groups.

2.3 Results

2.3.1 Effect of rotenone and hydrogen peroxide on hsc70 mRNA and protein expression in human SH-SY5Y cells

Preliminary experiments were carried out to establish rotenone and hydrogen peroxide concentrations able to evoke similar cytotoxic and pro-oxidant effects in SH-SY5Y cells. While rotenone is a specific mitochondrial complex I inhibitor that secondarily results in cell damage by promoting generation of peroxides, hydrogen peroxide is a well-known oxidative stress donor. Exposure for 24 hours to rotenone concentrations ranging from 100 to 800 nM or hydrogen peroxide (from 50 to 200 μM) causes a dose-dependent cell death, as shown in Figure 1A. Whole-cell intracellular ROS production was also quantified as index of rotenone- and hydrogen peroxide-induced oxidative stress. Exposure for 24 hours to 200 or 400 nM rotenone caused a significant increase (65 and 90 %, respectively; $p<0.01$) of ROS production with respect to vehicle-treated cells (Figure 1B). Similarly, 24 hours treatment with hydrogen peroxide (50 or 100 μM) results in a 30% ($p<0.05$) and 80% ($p<0.01$) ROS increase (Figure 1B).

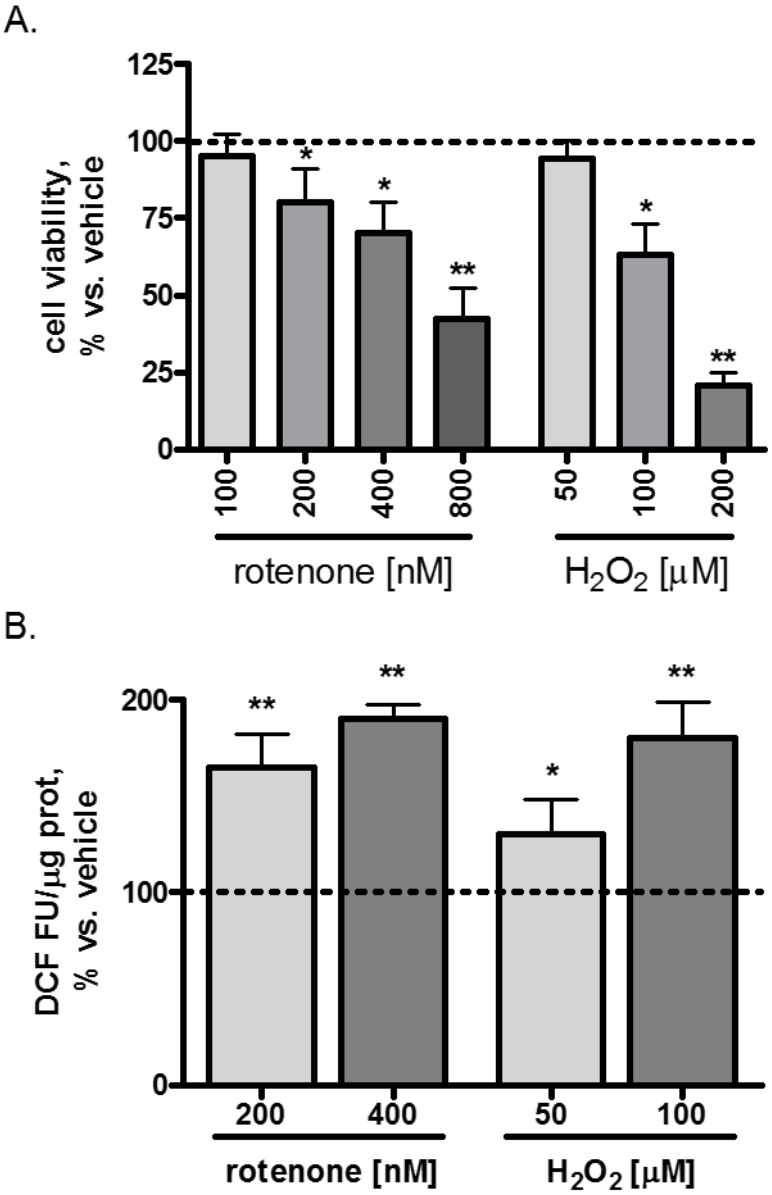

Figure 1. (A) Cytotoxicity studies. Cell viability was assessed by MTT assay after 24 hours exposure to 100-800 nM rotenone and 50-200 µM hydrogen peroxide (H_2O_2). Values are expressed as % vs. vehicle. N=6, repeated measures ANOVA test, followed by Dunnett's post-test; * $p<0.05$, ** $p<0.01$ vs. vehicle. **(B) Whole-cell intracellular ROS production.** The effect on ROS production of 24 hours exposure to 200-400 nM rotenone or 50-100 µM hydrogen peroxide (H_2O_2) was shown and expressed as % vs. vehicle of dichlorofluorescein fluorescence units (DCF FU) normalized to protein content. N=4, repeated measures ANOVA test, followed by Dunnett's post-test; * $p<0.05$, ** $p<0.01$ vs. vehicle.

Based on results derived from cytotoxicity studies, we decided to evaluate hsc70 gene and protein expression levels after treatment with rotenone or hydrogen peroxide at concentrations responsible

for a mild to moderate cytotoxic effects after 24 hours exposure. Therefore, SH-SY5Y cells were exposed to 200 and 400 nM rotenone or 50 and 100 μM hydrogen peroxide for 24 hours. The same concentrations of toxins was also administered to the cells for 6 hours when no cytotoxic effect of rotenone was evidenced and only a 20% cell death ($p<0.05$) was observed after exposure to 100 μM hydrogen peroxide. After treatment with rotenone for 6 or 24 hours, levels of mRNA encoding for hsc70 were quantified by real-time PCR. Relative quantification (RQ) of hsc70 normalized to beta-actin in SH-SY5Y is represented in Figure 2A. Rotenone induced a significant dose- and time-dependent decrease of mRNA encoding for hsc70, as compared to vehicle-treated cells. Interestingly, instead, western blot analyses showed that 6 hours treatment with rotenone (200 or 400 nM) resulted in a progressive increase of hsc70 protein levels, while prolonged incubation of SH-SY5Y cells with the same rotenone concentrations for 24 hours caused a dose-dependent reduction of hsc70 protein expression (Figure 2B-C).

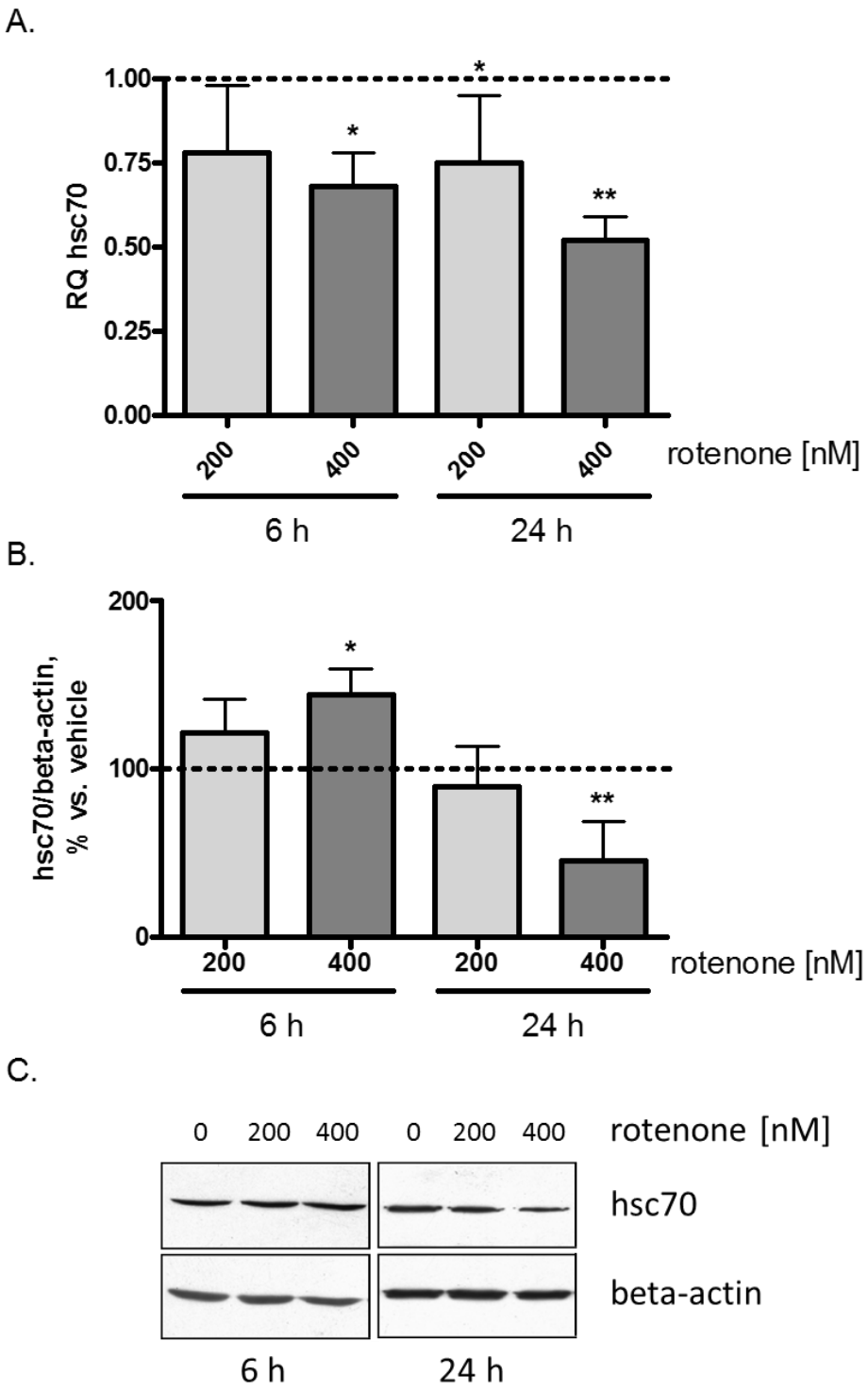

Figure 2. Effect of rotenone treatment on hsc70 mRNA and protein levels in human SH-SY5Y cells. **(A)** Relative quantification (RQ) of hsc70 mRNA levels after treatment with rotenone (200-400 nM) for 6 or 24 hours. Hsc70 mRNA levels were calculated as ratio to beta-actin and expressed as –fold change vs. vehicle (RQ = 1). **(B)** Hsc70 protein levels normalized to beta-actin and expressed as % vs. vehicle. **(C)** Representative Western blot image showing the effect of 6 or 24 hours rotenone exposure on hsc70 protein expression. Immunoreactivity of beta-actin, used as internal standard, was also shown. N=10, repeated measures ANOVA test, followed by Dunnett's post-test; * $p<0.05$, ** $p<0.01$ vs. vehicle.

To examine the specificity of rotenone-induced hsc70 reduction, the expression of other two molecular chaperones, hsp70 and hsp90, constitutively expressed under normal conditions to maintain protein homeostasis and induced upon environmental stress, was assessed. The exposure to 200 and 400 nM rotenone for 24 hours resulted in a 40 and 60% reduction ($p<0.01$) of hsp70 protein levels, while no significant change was observed for hsp90 (Figure 3A-B).

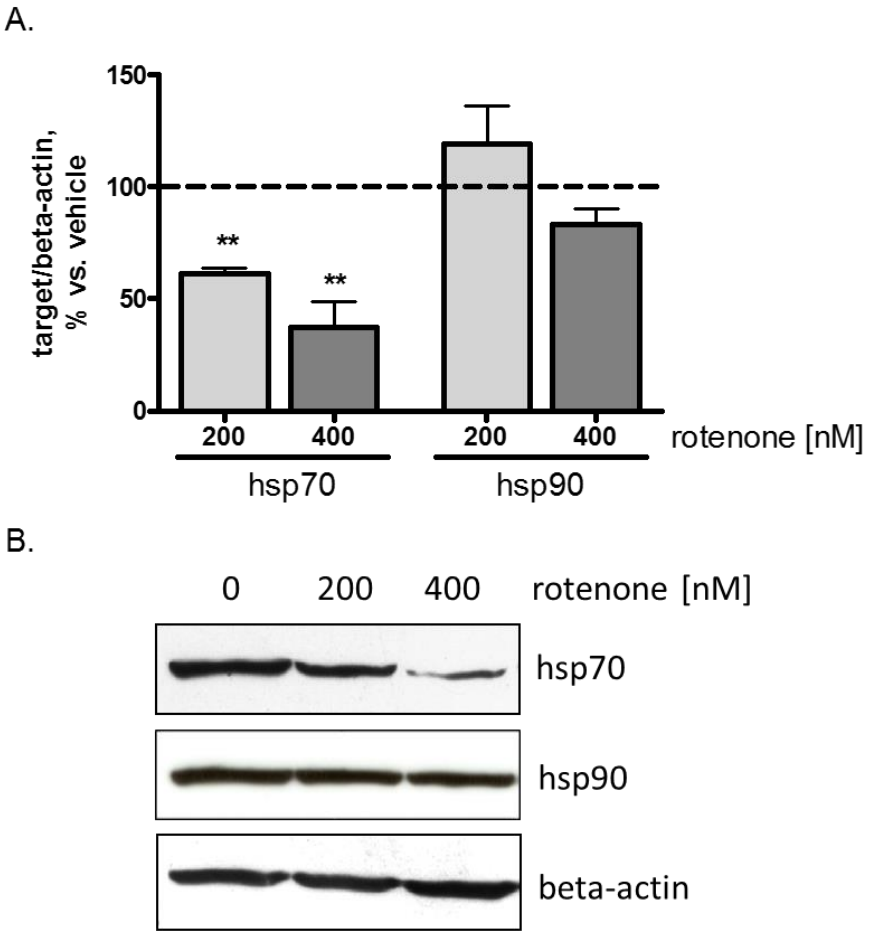

Figure 3. Effect of rotenone treatment on hsp70 and hsp90 protein levels in human SH-SY5Y cells. Cells were treated with 200-400 nM rotenone for 24 hours. **(A)** Hsp70 and hsp90 protein levels normalized to beta-actin and expressed as % vs. vehicle. **(B)** Representative Western blot image showing the effect of 24 hours rotenone exposure on hsp70 and hsp90 protein expression. Immunoreactivity of beta-actin, used as internal standard, was also shown. N=4, repeated measures ANOVA test, followed by Dunnett's post-test; ** $p<0.01$ vs. vehicle.

Hsc70 expression was also assessed after exposure to hydrogen peroxide, used as paradigm of oxidative stress. No significant change in hsc70 mRNA and protein levels was observed after 24

hours exposure to 50 or 100 μM hydrogen peroxide (Figure 4). No change was evidenced in hsc70 gene and protein levels after 6 hours treatment with hydrogen peroxide (data not shown).

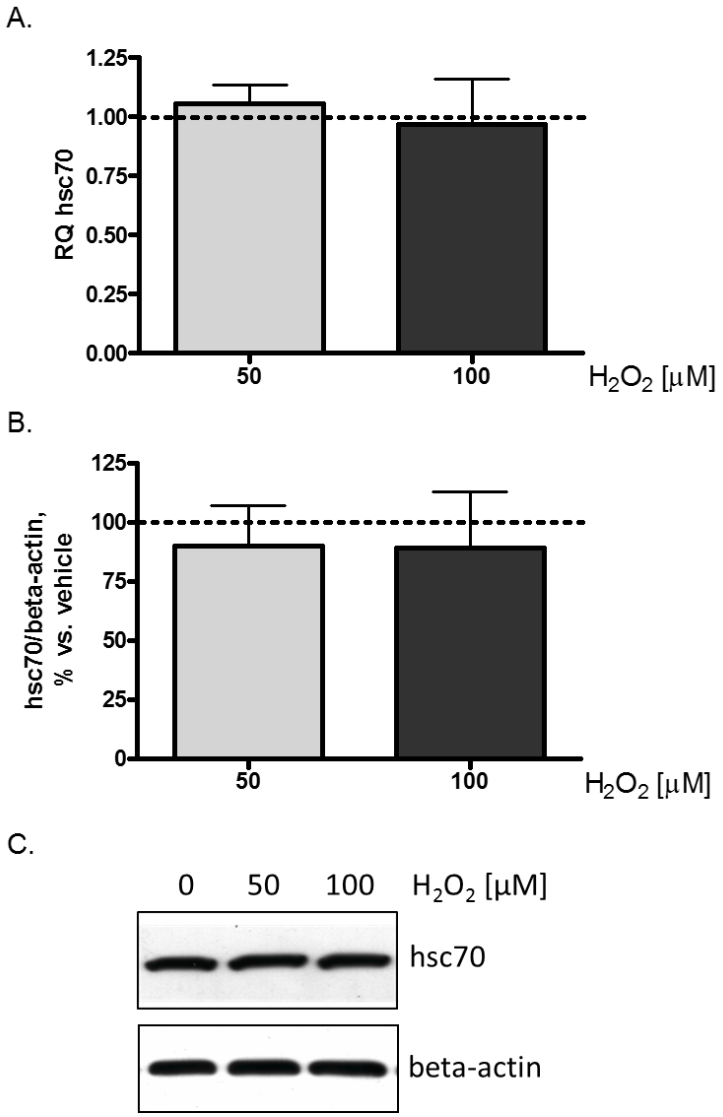

Figure 4. Effect of 24 hours hydrogen peroxide (H_2O_2) treatment on hsc70 mRNA and protein levels in human SH-SY5Y cells. (A) Relative quantification (RQ) of hsc70 mRNA levels calculated as ratio to beta-actin and expressed as –fold change vs. vehicle (RQ = 1). **(B)** Hsc70 protein levels, expressed as % vs. vehicle of the ratio between hsc70 and beta-actin optical density. **(C)** Representative Western blot image showing the effect of 24 hours H_2O_2 exposure on hsc70 protein expression. The immunoreactivity of beta-actin, used as internal standard, was also shown. N=10, repeated measures ANOVA test.

2.3.2 Effect of rotenone on hsc70 mRNA and protein expression in mouse cortical neurons

To validate the neurotoxic effect of rotenone on hsc70 expression, we used mouse cortical neurons. As shown in Figure 5A, exposure of cortical neurons to increasing concentrations of rotenone (100-800 nM) for 24 hours caused a dose-dependent cell death, while progressively increasing their loss of neuronal branched morphology (Figure 5B). No significant cytotoxic effect was evidenced on cortical neurons after 6 hours exposure to all tested rotenone concentrations (data not shown).

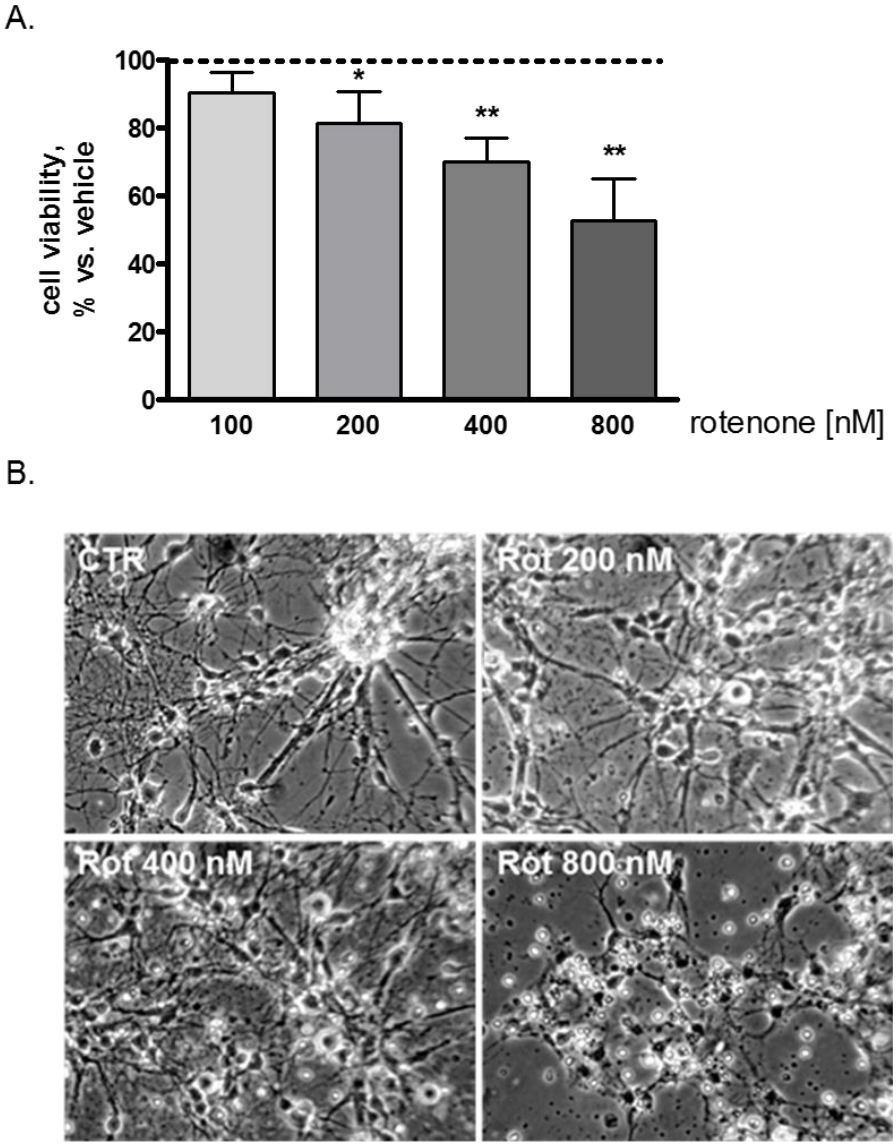

Figure 5. Survival of mouse cortical neurons exposed to rotenone for 24 hours. A. Cell viability was assessed by MTT assay after 24 hours exposure to 100-800 nM rotenone. Values, expressed as % vs. vehicle, are the mean ± SD of two separate experiments, each including five separate samples for each condition. * $p<0.05$, ** $p<0.01$ vs. vehicle; ANOVA test, followed by Dunnett's multiple comparisons test. **B.** Representative images of cortical neurons exposed for 24 hours to rotenone at the indicated concentrations.

Neurons were imaged under a reversed microscope Olympus CX40 (X20) equipped with an Olympus camera.

Hsc70 mRNA levels in primary neurons challenged with 200-400 nM rotenone for 6 or 24 hours showed a trend similar to that observed in neuroblastoma cells, as indicated by the significant time-dependent reduction of hsc70 mRNA levels (Figure 6A). Western blot analyses showed that 6 hours treatment with rotenone did not affect hsc70 protein levels, while an increased hsc70 protein level was observed at 6 hours in SH-SY5Y cells. Instead, similarly to SH-SY5Y cells, exposure to rotenone (200-400 nM) for 24 hours caused a significant reduction of hsc70 protein expression (Figure 6B-C).

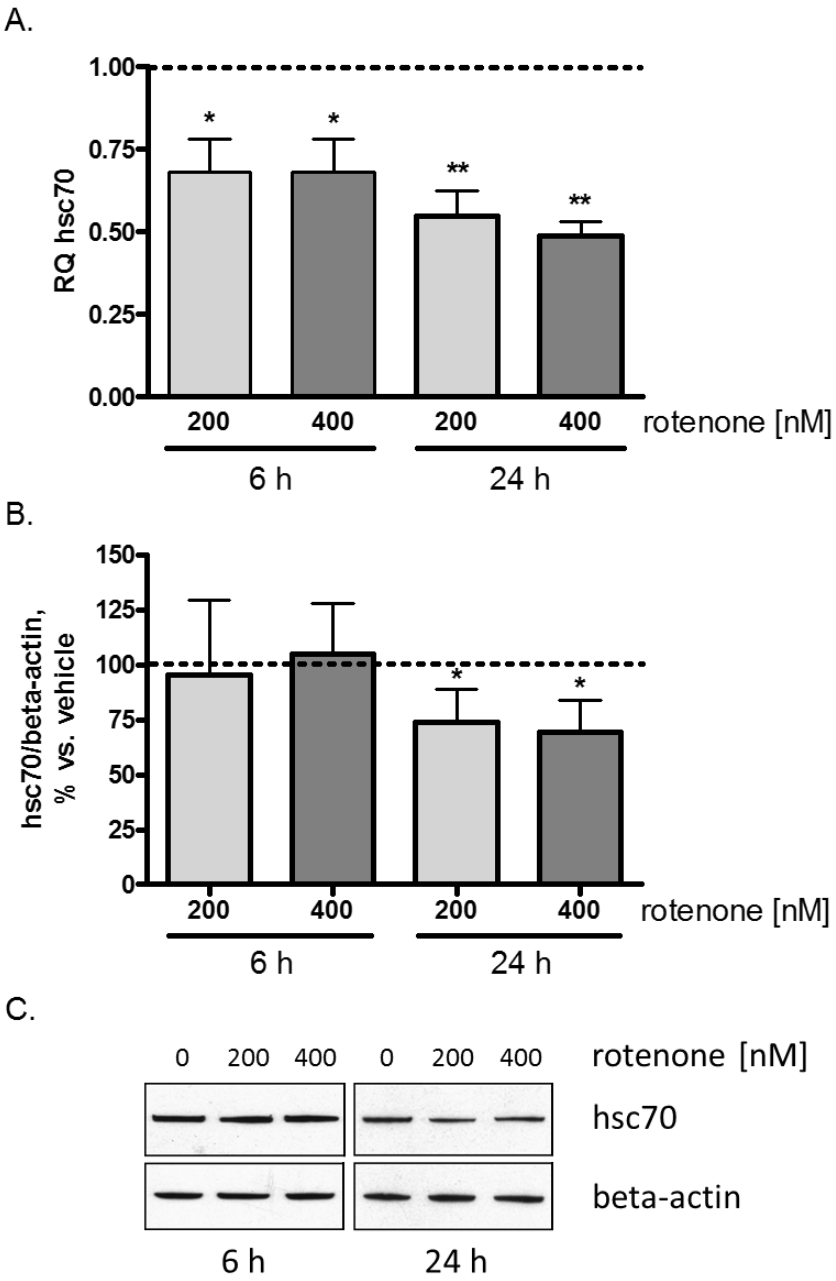

Figure 6. Effect of rotenone treatment on hsc70 mRNA and protein levels in mouse cortical neurons. **A.** Relative quantification (RQ) of hsc70 mRNA levels after treatment with rotenone (200-400 nM) for 6 or 24 hours. Hsc70 mRNA content was calculated as ratio to beta-actin and expressed as –fold change vs. vehicle (RQ = 1). **B.** Hsc70 protein levels normalized to beta-actin and expressed as % vs. vehicle. **C.** Representative Western blot image showing the effect of 6 or 24 hours rotenone exposure on hsc70 protein expression. Immunoreactivity of beta-actin, used as internal standard, was also shown. N=4, repeated measures ANOVA test, followed by Dunnett's post-test; * $p<0.05$, ** $p<0.01$ vs. vehicle.

2.3.3 Effect of macroautophagy inhibition on rotenone-induced hsc70 and alpha-synuclein modulation in SH-SY5Y cells

Next, we evaluated whether rotenone induces macroautophagy in SH-SY5Y cells. To this end, expression of LC3II and beclin-1, two proteins typically used to monitor macroautophagy, were assessed in SH-SY5Y cells exposed to 100-400 nM rotenone for 24 hours. Western blot analysis revealed that rotenone induced a significant increase of LC3II, while no change in beclin-1 protein expression was observed in rotenone-treated cells (Figure 7A-B).

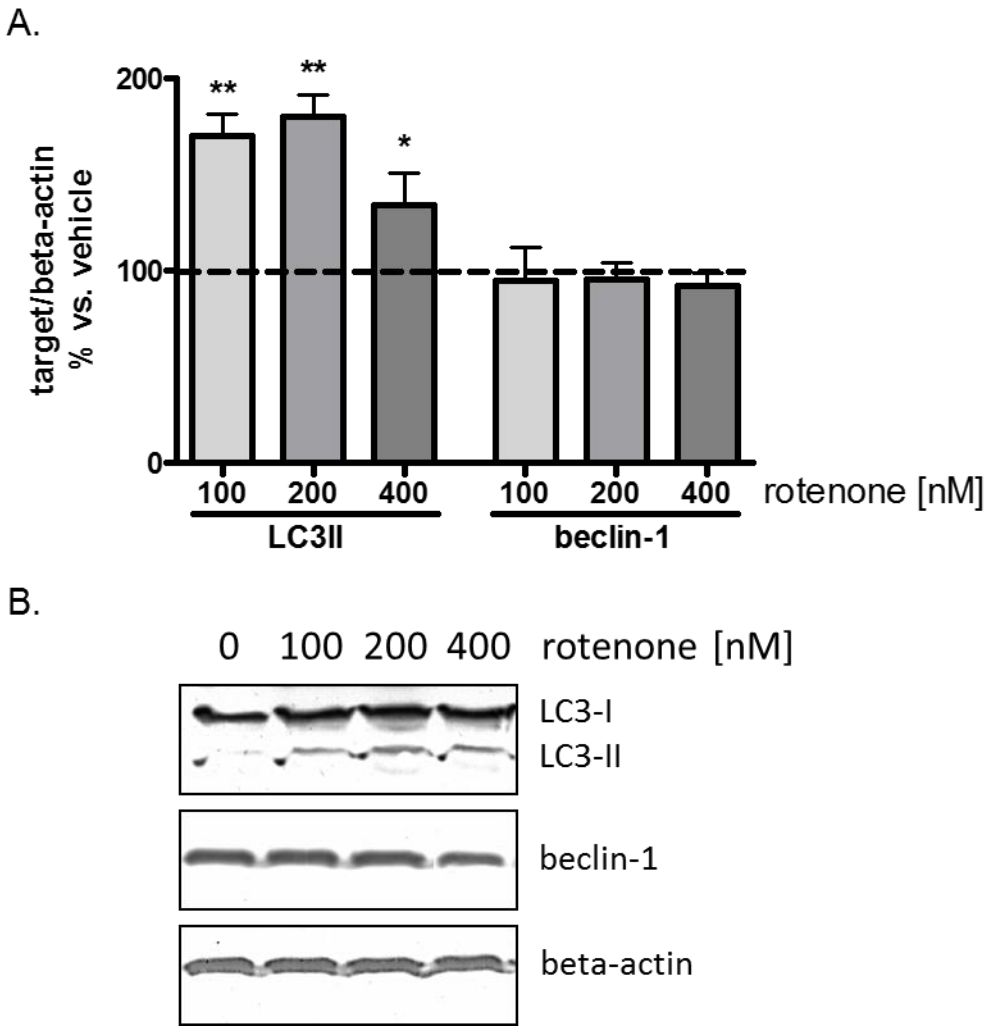

Figure 7. Effect of rotenone on macroautophagy. A. LC3II and beclin-1 protein levels after treatment with rotenone (100-400 nM) for 24 hours. Hsc70 mRNA content was , expressed as % vs. vehicle of the ratio between target protein and beta-actin optical density. **B.** Representative Western blot image showing the effect of rotenone treatment for 24 hours on LC3II and beclin-1 protein expression. Immunoreactivity of beta-actin, used as internal standard, was also shown. N=6, repeated measures ANOVA test, followed by Dunnett's post-test; * $p<0.05$, ** $p<0.01$ vs. vehicle.

To explore a putative role for macroautophagy in rotenone-induced modulation of hsc70, hsc70 mRNA and protein levels were assessed in presence of a specific macroautophagy inhibitor, 3-methyladenine (3-MA, 5mM, 1 hour before rotenone treatment). We observed that 3-MA, while was able to prevent or partially counteract cell death induced by 200 or 400 nM rotenone (Figure 8A), did not affect hsc70 mRNA and protein levels and did not modify the reduction of hsc70 mRNA (Figure 8B) and protein levels caused by rotenone exposure (Figure 8C-D). Furthermore, the effect of macroautophagy inhibition was also verified on alpha-synuclein expression during rotenone toxicity. Treatment with 3-MA resulted in a significant reduction (-37%, $p<0.05$) of alpha-synuclein mRNA levels (Figure 8B) and increase of its protein levels (+41%, $p<0.05$) (Figure 8C-D). As previously reported (Sala et al., 2013), exposure to rotenone caused an increase of alpha-synuclein mRNA and protein levels and macroautophagy inhibition resulted in a further increase of alpha-synuclein mRNA (+42% vs. rotenone-treated cells, $p<0.05$) and protein (+49% vs. rotenone-treated cells, $p<0.05$) levels (Figure 8).

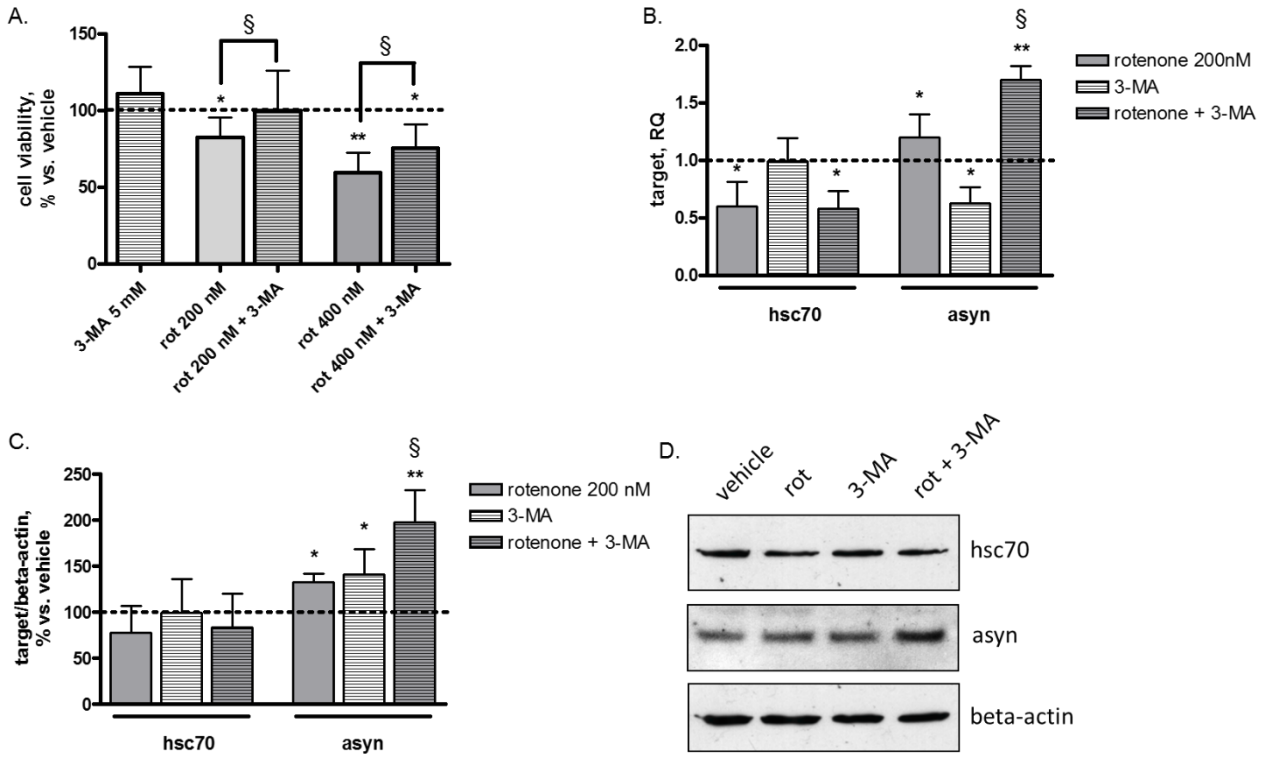

Figure 8. Effect of macroautophagy inhibition on rotenone-induced cell death and modulation of hsc70 and alpha-synuclein expression. 3-methyladenine (3-MA, 5mM) was used to inhibit macroautophagy and

administered 1 hour before rotenone treatment (200 nM, 24 hours). **A.** Cell viability was assessed by MTT assay. Values are expressed as % vs. vehicle. N=4, repeated measures ANOVA test, followed by Tukey's post-test; * $p<0.05$, ** $p<0.01$ vs. vehicle, § $p<0.01$ vs. rotenone-treated cells. **B.** Relative quantification (RQ) of hsc70 and alpha-synuclein (asyn) mRNA levels calculated as ratio to beta-actin and expressed as – fold change vs. vehicle (RQ = 1). **C.** Hsc70 and asyn protein levels, expressed as % vs. vehicle of the ratio between target proteins and beta-actin optical density. **D.** Representative Western blot image showing the effect of rotenone, 3-MA or rot/3-MA co-treatment on hsc70 and asyn protein expression. Immunoreactivity of beta-actin, used as internal standard, was also shown. N=3, repeated measures ANOVA test, followed by Tukey's post-test; * $p<0.05$, ** $p<0.01$ vs. vehicle; § $p<0.05$ vs. rotenone-treated cells.

2.3.4 Effect of HSPA8/hsc70 silencing on neurotoxicity

To test whether HSPA8/hsc70 gene silencing influenced neurotoxicity, SH-SY5Y cells were subjected to 48 hours transfection with a specific siRNA recognizing hsc70. Hsc70 silencing was confirmed through the assessment of hsc70 mRNA and protein expression by qPCR and Western blot, respectively. Hsc70 siRNA resulted in about 60% reduction of mRNA (Figure 9A) and 50% decrease of protein levels (Figure 9B-C) with respect to negative control. Hsc70 silencing resulted in a significant 2.5-fold increase of alpha-synuclein mRNA levels ($p<0.01$, Figure 9A) paralleled by an increase of its protein expression (+80%, $p<0.01$, Figure 9B-C). Furthermore, we demonstrated that hsc70 silencing did not affect cell viability and did not alter the cytotoxic effect exerted by 24 hours exposure to 400 nM rotenone or 100 μM hydrogen peroxide (Figure 9D).

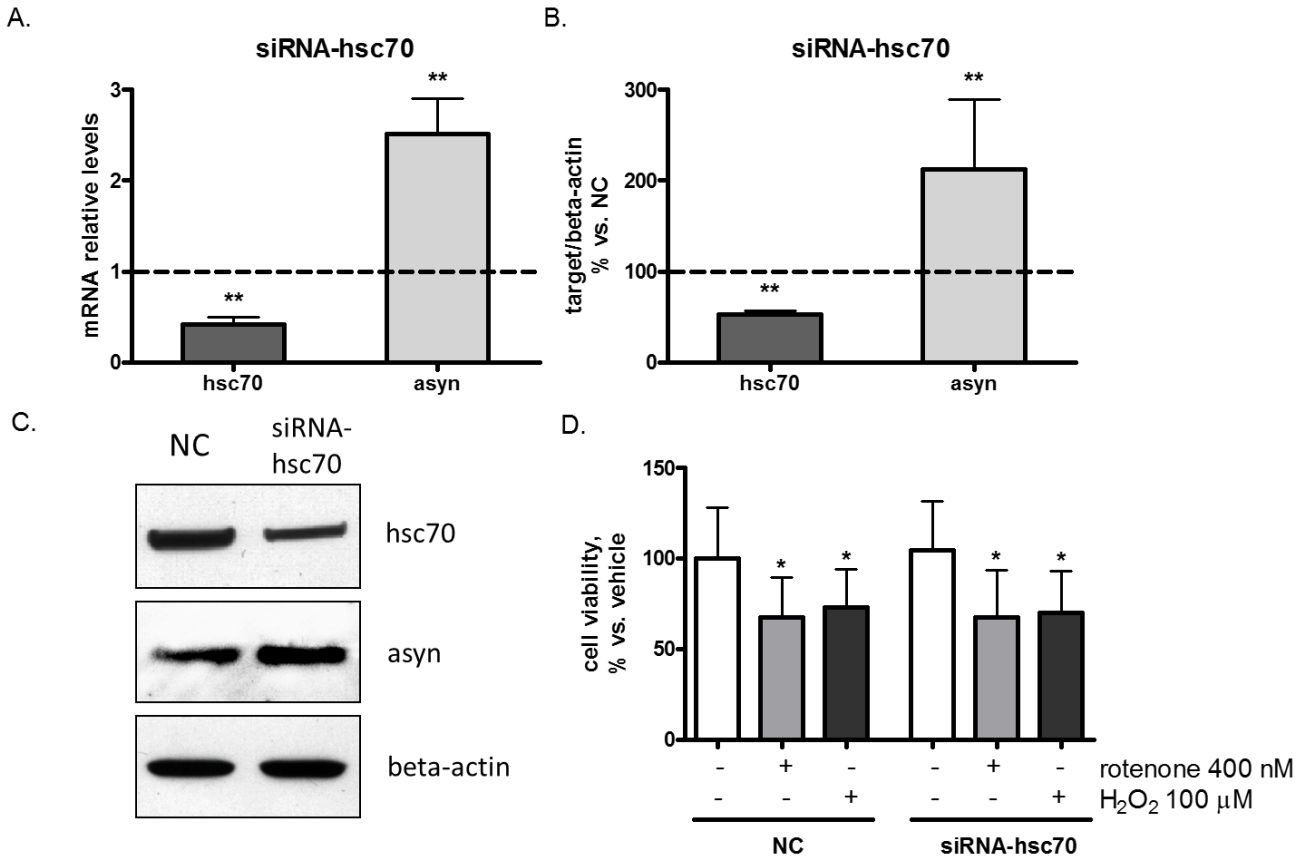

Figure 9. Effect of HSPA8/hsc70 silencing on neurotoxicity. Analysis of 48 hours hsc70 silencing on alpha-synuclein (asyn) gene (**A**) and protein levels (**B-C**) and on cytotoxicity (**D**) in SH-SY5Y cells. **A.** Hsc70 and asyn mRNA levels were normalized on beta-actin levels and expressed as –fold change vs. negative control (NC, mRNA level = 1). **B.** Hsc70 and asyn protein levels, expressed as % vs. negative control (NC) of the ratio between target proteins and beta-actin optical density. **C.** Representative Western blot image showing hsc70 and asyn protein expression in cells transfected with siRNA-hsc70 or NC. Immunoreactivity of beta-actin, used as internal standard, was also shown. **D.** Cell viability was assessed by MTT assay in cells transfected with siRNA-hsc70 or NC for 48 hours and then treated with 400 nM rotenone or 100 μM hydrogen peroxide (H_2O_2) for 24 hours. Values are expressed as % vs. vehicle. N=4, repeated measures ANOVA test, followed by Dunnett's post-test; * $p<0.05$ vs. corresponding vehicle (NC or siRNA-hsc70); ** $p<0.01$ vs. NC.

2.4 Discussion

Based on knowledge that hsc70 is a chaperone protein endowed with a critical role in several intracellular mechanisms known to be closely associated with PD, the aim of this study was to establish the existence of a possible modulation of hsc70 following exposure to PD-related stimuli.

No previous study specifically explored the effect of rotenone on the constitutively expressed HSPA8/hsc70 chaperone protein. Therefore, we assessed hsc70 mRNA and protein expression after mitochondrial inhibition by rotenone (a well-known inhibitor of the mitochondrial complex I) and oxidative stress, two major pathogenic mechanisms contributing to the loss of dopaminergic neurons in PD (Jenner and Olanow, 1998; Schapira et al., 1998). To this purpose, we used human neuroblastoma SH-SY5Y cells, a neuron-like cell line expressing dopaminergic markers and widely used to study PD pathomechanisms, and primary mouse cortical cultures, representing a neuronal population affected in late-stage PD. Maintaining proper levels of hsc70 appears fundamental for at least three processes whose dysfunction is known to lead to PD; in fact, hsc70 i) is required for the physiological activity of the CMA pathway, being hsc70 the principal carrier protein of CMA also essential to allow the entry of substrates into the lysosomal lumen (Cuervo and Wong, 2014); ii) it also cooperates to confer resistance against different metabolic cellular stresses (Chong et al., 2013; Wang et al., 2013a); iii) it prevents alpha-synuclein deposition and propagation through the binding to both soluble and fibrillar forms (Pemberton et al., 2011; Pemberton and Melki, 2012) and efficiently fragments alpha-synuclein fibrils *in vitro* into shorter fibrils and promotes depolymerization into non-toxic alpha-synuclein monomers (Gao et al., 2015).

Based on these considerations, we exposed SH-SY5Y cells to different concentrations of rotenone for 6 and 24 hours and we measured the effects of this treatment on hsc70 expression. We found that rotenone determined a dose- and time-dependent reduction of hsc70 mRNA levels, together with an initial (6 hours) increase of hsc70 protein levels followed by a dose-dependent reduction after 24 hours rotenone exposure (Figure 2). These findings suggest that, after 24 hours rotenone exposure, the reduction of hsc70 protein expression is ascribable to the down-regulation of its synthesis. Instead, the rotenone-induced increase of hsc70 protein levels observed at 6 hours can be interpreted as a consequence of an involvement of other mechanisms possibly affected by rotenone, such as a compromised protein degradation, that overcome and hide, at least for a limited time lapse, the reduced hsc70 synthesis. The observed reduction of hsp70 protein levels after rotenone exposure indicates that the influence of rotenone is not specific for hsc70, but rather involves other

heat shock proteins as already described in several brain areas of rotenone-treated rats (Sonia Angeline et al., 2012; Thakur and Nehru, 2014). Nevertheless, our findings identify for the first time hsc70 as adjunctive target of rotenone toxicity possibly contributing to alpha-synuclein accumulation.

The rotenone-induced reduction of hsc70 mRNA levels observed in SH-SY5Y cells was also confirmed in primary cortical neurons, which showed a similar trend in hsc70 mRNA levels when challenged with rotenone (Figure 6). While after 24 hours rotenone exposure a significant reduction of hsc70 protein levels was observed also in primary cortical neurons, differently from what found in SH-SY5Y cells, no alteration in hsc70 protein expression emerged after 6 hours treatment (Figure 6). This last result seems to indicate that in cortical neurons hsc70 protein expression after 6 hours rotenone treatment does not reflect the reduced synthesis, as well as already reported for neuroblastoma cells which even showed increased hsc70 protein levels at this time point.

We then compared the effect of the mitochondrial inhibitor rotenone, which also causes oxidative stress, versus the oxidative stress donor hydrogen peroxide. It was noteworthy to observe that concentrations of rotenone and hydrogen peroxide that caused similar cytotoxicity and intracellular ROS raise in SH-SY5Y cells differently affected hsc70 expression. In fact, while rotenone significantly reduced hsc70 gene expression (Figure 2A), hydrogen peroxide did not affect hsc70 mRNA and protein levels (Figure 4). These data suggest that mechanisms used by rotenone to reduce hsc70 expression may involve mitochondrial inhibition, but they are not necessarily directly linked to increased oxidative stress. Rather, it is conceivable that the effect of rotenone on hsc70 expression might be directly or indirectly linked to decreased mitochondrial bioenergetics, a primary outcome of mitochondrial complex I inhibition, leading to decreased ATP levels and induction of macroautophagy. Indeed, we found that treatment of SH-SY5Y cells with rotenone for 24 hours caused an increase of LC3-II levels, while leaving unchanged beclin-1 expression (Figure 7), in line with the rotenone-induced autophagosome accumulation already observed in these cells (Mader et al., 2012). Although we did not perform a complete study with specific pharmacological inhibitors of the autophagic steps, these data are indicative of a block of the autophagic flux caused

by rotenone, as also previously reported in both *in vitro* and *in vivo* studies (Giordano et al., 2014; Mader et al., 2012; Wu et al., 2015).

Using a specific inhibitor, we demonstrated that macroautophagy inhibition, although was able to partially prevent rotenone-induced cell death (Figure 8A), did not influence hsc70 expression, as evidenced by the similar rotenone-induced reduction in mRNA and protein hsc70 levels observed in the presence or absence of 3-MA (Figure 8B-D). These findings support the view that the effect of rotenone on hsc70 gene and protein expression is not ascribable to the rotenone cytotoxicity and that the protective effect of 3-MA on rotenone-induced cell death might be due to an induction of CMA, which represents a cellular protective mechanism against necrosis and massive cell death. Furthermore, we demonstrated that macroautophagy inhibition by 3-MA did not modify *per se* hsc70 mRNA and protein levels under basal conditions. Based on knowledge that macroautophagy participates, together with CMA, to alpha-synuclein degradation (Webb et al., 2003), through macroautophagy inhibition, we also explored the specific contribution of CMA in the accumulation of alpha-synuclein caused by rotenone, as previously demonstrated in both *in vivo* and *in vitro* models (Betarbet et al., 2006; Betarbet et al., 2000; Sala et al., 2013). Interestingly, we observed that macroautophagy inhibition by 3-MA was able to cause a significant increase of alpha-synuclein protein levels (Figure 8B-C), according to the knowledge that this protein is physiologically partially degraded by this pathway. Accumulation of alpha-synuclein protein (Figure 8B) could represent an inhibitory feedback responsible for the decrease of alpha-synuclein synthesis, as indicated by the reduction of mRNA levels in presence of 3-MA (Figure 8A). The increase of alpha-synuclein mRNA and protein levels induced by rotenone was further enhanced by macroautophagy inhibition, which likely renders cells more susceptible to rotenone toxicity, thus confirming the need of a proper activity of both CMA and macroautophagy for maintaining the cellular homeostasis.

Finally, hsc70 gene silencing allowed us to demonstrate that hsc70 reduction is *per se* sufficient to cause an up-regulation of alpha-synuclein gene and protein expression that is likely to favor protein accumulation and aggregation typical of PD and other synucleinopathies.

2.5 Conclusions

The main finding of this study is the demonstration that the constitutively expressed HSPA8/hsc70 chaperone protein represents a new intracellular target of rotenone toxicity. Our data suggest that mechanisms used by rotenone to reduce hsc70 expression may involve mitochondrial inhibition, although a role for increased oxidative stress cannot be excluded. This finding implies the existence of an adjunctive toxic mechanism of rotenone possibly contributing to PD pathogenesis and worthy of study in the attempt of identifying new therapeutic targets for the disease. Further studies exploring the molecular mechanisms responsible for rotenone-induced hsc70 reduction are needed, including the possible involvement of specific microRNA deregulation already reported to be associated with hsc70 reduction in PD (Alvarez-Erviti et al., 2013; Wang et al., 2013b), as well as a better understanding of specific mechanisms involved in hsc70-mediated modulation of alpha-synuclein.

Acknowledgements

This work was carried out within the framework of the Ivascomar project, Cluster Tecnologico Nazionale Scienze della Vita ALISEI, Italian Ministry of Research (MIUR, to CF and AMC). This work was also supported by MIUR grants (PRIN2007 to AMC; SYSBIONET-Italian ROADMAP ESFRI Infrastructures to LA and AMC) and Associazione Levi-Montalcini (fellowships to MF).

Chapter 3:
Altered regulation of autophagy in fibroblasts from patients with sporadic and LRRK2 mutant Parkinson's disease

Manuscript in preparation

Daniele Marinig[1,2], Chiara Riva[1], Chiara Zoia[1], Carlo Ferrarese[1,3], Gessica Sala[1]

[1]Lab. of Neurobiology, School of Medicine and Surgery, Milan Center for Neuroscience (NeuroMI), University of Milano-Bicocca; [2]PhD program in Neuroscience, University of Milano-Bicocca; [3]Dept. of Neurology, San Gerardo Hospital, Monza, Italy.

Abstract

Alterations of the intracellular catabolic mechanisms have already been observed in Parkinson's disease (PD). The evidence that the major constituent of Lewy bodies, alpha-synuclein, is selectively targeted by the chaperone-mediated autophagy (CMA) has raised great interest in the study of this mechanism in PD. Moreover, the PD-related mutation G2019S on the gene LRRK2 is able to block the multimerization of the lysosomal receptor lamp2A leading to accumulation of CMA substrates.

Aim: to study the effect of mutant LRRK2 on autophagy in primary fibroblast cell lines from G2019S mutant PD patients as compared to sporadic PD patients (sPD) and healthy controls.

Methods: the protein expression of the two key-regulators and a substrate of CMA, hsc70, lamp2A and MEF2D, as well as of the macroautophagy markers, LC3, beclin1 and p62 were measured in fibroblasts under basal conditions and after 24 hours exposure to autophagy inducers (serum starvation, rapamycin) or inhibitors (ammonium chloride, 3-methyladenine). The effects on autophagy parameters of the molecular chaperone drug ambroxol or the mitochondrial inhibitor rotenone were also tested.

Results: no difference in hsc70, lamp2A or beclin1 basal levels was observed in G2019S LRRK2 or sPD fibroblasts with respect to controls, while G2019S LRRK2 showed a significant increase of LC3-II and p62. Serum starvation and rapamycin resulted in a decrease of hsc70, while rapamycin significantly increased lamp2A levels in control fibroblasts. 3-methyladenine increased lamp2A levels in control fibroblasts, while ammonium chloride resulted in an accumulation of LC3-II and p62 in all cell lines. Ambroxol increased the levels of p62 and LC3-II in all cell lines and rotenone differently affect hsc70 expression in patient vs. control fibroblasts

Discussion: these findings indicate that G2019S LRRK2 fibroblasts display a macroautophagy alteration under basal condition and that both sporadic and G2019S LRRK2 fibroblasts have a different susceptibility to autophagy modulators. Moreover, the ambroxol-induced accumulation of p62 and LC3-II indicates that this drug is involved in macroautophagy modulation, while the exposure to rotenone further support the existence of a different regulation of CMA in patient vs.

control fibroblast.

Keywords

Autophagy, Parkinson's disease, LRRK2, fibroblasts

3.1 Introduction

Intracellular degradation systems are one of the most attractive research focus in the field of neurodegenerative diseases during the last decade. As a matter of fact, an efficient catabolic machinery seems to be crucial in preventing the onset of the so-called "proteinopathies" such as Alzheimer's disease and Parkinson's disease (PD). PD in particular is characterized by the presence of Lewy bodies, abnormal aggregates of alpha-synuclein, ubiquitin and other proteins within degenerating neurons, which deposition seems to be favored by alterations of protein catabolic systems, as suggested by ubiquitin-proteasome system (UPS) alterations observed in patients with familial forms of PD (McNaught and Olanow, 2003) or increased number of autophagic vacuoles found in the *substantia nigra* of PD patients (Anglade et al., 1997). The involvement of the autophagy-lysosome pathway (ALP) in the pathogenesis of PD has been also suggested by the demonstration that mutant forms of alpha-synuclein as well as its overexpression are able to impair chaperone-mediated autophagy (CMA) by binding the lysosome-associated membrane protein type 2A (lamp2A) with higher affinity (Cuervo et al., 2004; Xilouri et al., 2009). Lamp2A is a key regulator of CMA acting on the lysosomal membrane as a receptor for substrate proteins of CMA (Cuervo and Dice, 2000); thus, an abnormal binding of alpha-synuclein to lamp2A may inhibit not only its own but also the degradation of other potential neurotoxic substrates. This aberrant interaction has been also recently demonstrated for G2019S mutant forms of the leucine-rich repeat kinase 2 (LRRK2), a large multidomain protein involved in neurite outgrowth regulation in developing neurons (Cookson, 2010), which represents the most frequent autosomal-dominant familial form of PD (Paisan-Ruiz et al., 2004; Zimprich et al., 2004). Mutant forms of LRRK2 can block CMA by preventing lamp2A multimerization and, consequently, the formation of the

translocation complex at the lysosome membrane (Orenstein et al., 2013). Together with the observation that the two main effectors of CMA, heat shock cognate protein 70 kDa (hsc70) and lamp2A were downregulated in the *substantia nigra pars compacta* and amygdala of PD brains (Alvarez-Erviti et al., 2010), all these evidences support the hypothesis that the accumulation of toxic substrates within dopaminergic neurons following ALP impairment is one of the major event involved in the pathogenesis of PD. Thus, a deeper insight of ALP altered mechanisms, and in particular of CMA, the major catabolic system for alpha-synuclein (Cuervo et al., 2004; Mak et al.,2010), in PD may ameliorate the current knowledge of the PD pathogenesis and favor the identification of new biomarkers or novel therapeutic approaches. Interestingly, a reduction of hsc70 expression was observed in lymphomonocytes obtained from sporadic PD patients (Sala et al., 2014; Papagiannakis et al., 2015), and a reduction of lamp2 (not lamp2A) protein levels as well as increased levels of the autophagosome marker LC3-II were also reported in these cells (Prigione et al., 2010; Wu et al., 2011), highlighting the existence of a systemic alteration of autophagy in PD. According to this assumption, many other studies have investigated PD pathomechanisms using patient-derived skin fibroblasts. Fibroblasts indeed represent a very useful and suitable experimental model for studying PD-related alterations for at least 3 reasons: 1) fibroblasts can be easily isolated from punch skin biopsies; 2) they are a robust cell line which can be cultured and replicated several times allowing to test the effects of toxins and other compounds 3) they mirror the polygenic risk factors of patients and the bioenergetic deficits typically found in degenerating dopaminergic midbrain neurons (Auberger et al., 2012; Mytilineou et al., 1994; Wiedemann et al., 1999; Musanti et al., 1993; Hoyo et al., 2010). In this study we evaluated steady-state parametrs of the two major autophagic pathways, macroautophagy and CMA, in cultured fibroblasts obtained from sporadic PD patients and PD patients carrying the G2019S mutation on LRRK2 compared to healthy controls. Furthermore, we compared the effect of exposure to different autophagy modulators or to the mithocondrial inhibitor rotenone on macroautophagy and CMA in patient vs. control fibroblasts. Finally, we also investigated the effects of ambroxol hydrochloride on autophagy, and old secretolytic agent which is raising great interest as a potential novel candidate for the treatment of

Parkinson disease and neuronopathic Gaucher disease (Ambrosi et al., 2015; McNeill et al., 2014; Migdalska-Richards et al., 2016).

3.2 Materials and methods

3.2.1 Cell cultures

Fibroblast cell lines from 6 sporadic PD patients with no familial history, 3 PD patients carrying the G2019S LRRK2 mutation and 5 age- and sex-matched healthy controls were analyzed (Table 1). G2019S LRRK2 cell lines were provided by the "Cell line and DNA biobank from patients affected by genetic diseases" and "Parkinson Institute Biobank" (Filocamo et al., 2014). Cell lines were cultured in Dulbecco's modified Eagle's medium (DMEM), supplemented with 10% heat-inactivated fetal bovine serum, penicillin (100 U/ml) and streptomycin (100 µg/ml), at 37 °C in an atmosphere of 5% CO_2 (Sala et al., 2009). Fresh medium was renewed every 48 hours and 24 hours before each experiment. Cells used in experiments were expanded up to 15 passages in order to avoid artifacts due to *in vitro* aging.

Table 1. Demographic and clinical characteristics of subjects from which fibroblasts were obtained. Values are shown as mean ± standard deviation.

	Controls	*Sporadic PD*	*G2019S LRRK2*
Number	5	6	3
Age (years)	63.2 ± 8.8	64.3 ± 8.9	68 ± 6.6
Sex (M/F)	2/3	2/4	1/2
Age at onset (years)	n.a.	62 ± 3.4	52 ± 6.6
Disease duration (years)	n.a.	6.5 ± 1.3	16 ± 1.7

n.a. = not applicable

3.2.2 Reagents

All reagents were obtained from Sigma-Aldrich unless otherwise stated. Rotenone and ambroxol hydrochloride were dissolved in dimethylsulphoxide (DMSO) while ammonium chloride (NH_4Cl) and 3-methyladenine (3-MA) were dissolved in phosphate buffer saline (PBS). Rapamycin was

used as a ready-to-use solution in DMSO. All the reagents were prepared and diluted in fresh medium before each experiment.

3.2.3 RNA extraction and cDNA synthesis

RNA was extracted from cultured fibroblasts using the RNeasy Mini kit (Qiagen), according to the manufacturer instructions, and retro-transcribed into cDNA using the SuperScript® VILO™ cDNA Synthesis Kit (Invitrogen) at the following conditions: 10 min at 25°C and 60 min at 42°C. The reaction was terminated at 85°C for 5 min and cDNAs stored at -20°C for the next experiments.

3.2.4 Real-time quantitative PCR (qPCR)

cDNAs obtained from 50 ng RNA were amplified in triplicate in the ABI Prism 7500 HTSequence Detection System (Applied Biosystems) using 5x HOT FIREPol® EvaGreen® qPCR Mix Plus (ROX) (Solis BioDyne) at the following conditions: 95°C for 15 min, 40 cycles of: 95°C for 15 sec, 62.5°C for 20 sec, 72°C for 20 sec. The following primer pairs were used: hsc70-F (CAGGTTTATGAAGGCGAGCGTGCC) and hsc70-R (GGGTGCAGGAGGTATGCCTGTGA); lamp2A-F (GCAGTGCAGATGAAGACAAC) and lamp2A-R (AGTATGATGGCGCTTGAGAC); beclin-1-F (ATCTCGAGAAGGTCCAGGCT) and beclin-1-R (CTGTCCACTGTGCCAGATGT); LC3B-F (CAGCATCCAACCAAAATCCC) and LC3B-R (GTTGACATGGTCAGGTACAAG); beta-actin-F (TGTGGCATCCACGAAACTAC) and beta-actin-R (GGAGCAATGATCTTGATCTTCA). For relative quantification of each target vs. beta-actin mRNA, the comparative C_T method was used as previously described (Sala et al., 2010).

3.2.5 Western blotting

Cell pellets were lysed in cell extraction buffer (Invitrogen) supplemented with 1 mM PMSF and protease inhibitor cocktail (Sigma-Aldrich) and protein concentrations determined by Bradford's method. After denaturation, 20 μg of proteins were separated by electrophoresis in 8% or 15% SDS-PAGE and transferred to nitrocellulose. Blots were blocked for 1 hour at room temperature in 5% non-fat dried milk in TBS-T buffer (50 mM Tris–HCl (pH 7.6), 200 mM NaCl, 0.1% Tween 20), incubated overnight at 4°C with specific primary antibodies hsc70 (1:3,000) and lamp2A (1:500), Abcam; beclin-1 (1:1,000), LC3 (1:500) and p62/SQSTM1 (1:1,000), Cell Signaling;

MEF2D (1:1,000), BD Biosciences, and then with the HRP-linked anti-mouse or -rabbit IgG for 1 hour. Beta-actin (Sigma, 1:40,000 dilution) was used as internal standard. Signals were revealed by chemiluminescence, visualized on X-ray film and quantified using ImageJ software.

3.2.7 Statistical analysis

All data are shown as mean ± standard error of the mean (SEM) of at least 3 independent experiments. Statistical analysis was performed using GraphPad Prism 4.0. Repeated measures ANOVA, followed by Tukey's multiple comparison post-hoc test, was used to assess the significance of differences between groups.

3.3 Results

3.3.1 Expression of autophagic markers in fibroblasts from sporadic and mutant LRRK2 PD patients

The gene and protein expression of CMA effectors (hsc70 and lamp2A) as well as of macroautophagy markers (beclin1 and LC3) was evaluated in fibroblasts from healthy subjects, sporadic PD (sPD) patients and mutant G2019S LRRK2 PD patients under basal condition.

No difference in hsc70, lamp2A, beclin1 and LC3 mRNA levels was observed between sPD, G2019S LRRK2 and healthy controls fibroblasts (Figure 1).

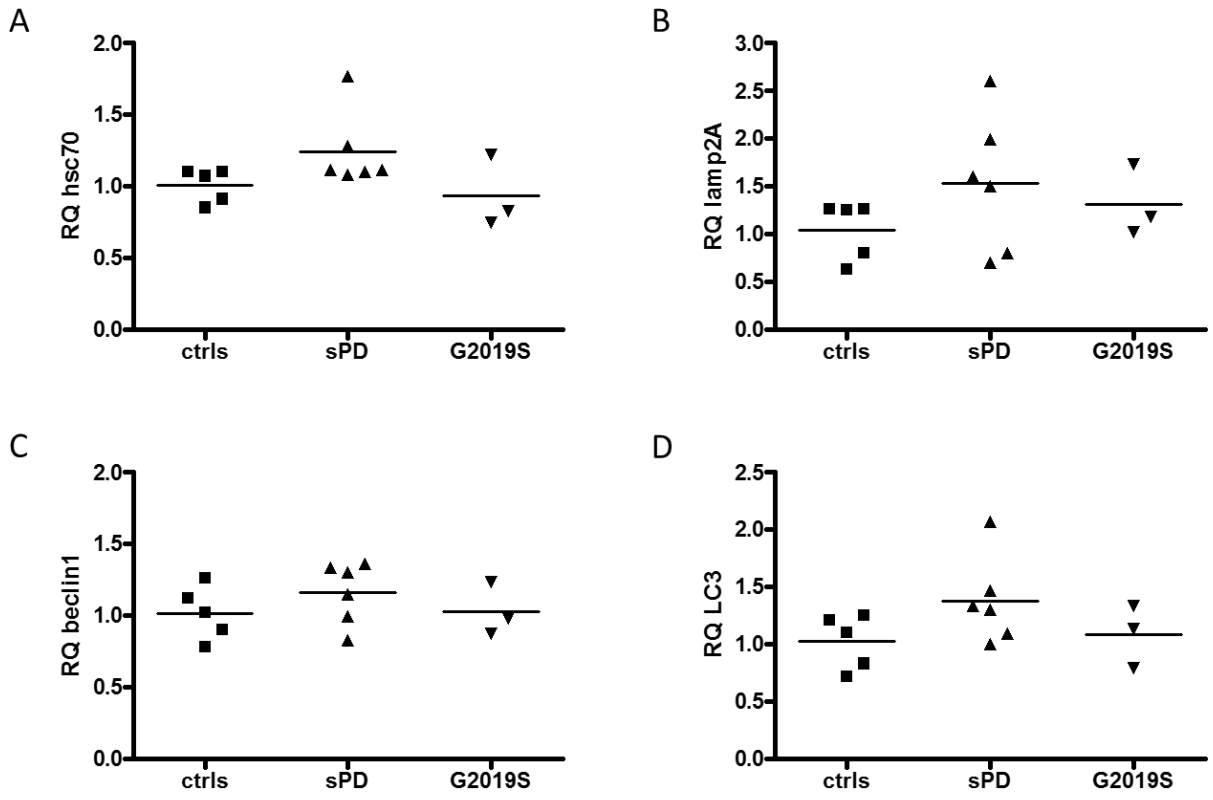

Figure 1. Gene expression of CMA and macroautophagy markers. Relative quantification (RQ) of hsc70 (A), lamp2A (B), beclin1 (C) and LC3 (D) mRNA levels in fibroblasts from healthy controls (ctrls), sporadic PD patients (sPD) and patients with G2019S LRRK2 mutation (G2019S). Hsc70, lamp2A, beclin1 and LC3 mRNA levels were calculated as ratio to beta-actin. One-way ANOVA, followed by Tukey's multiple comparison test (ctrls n = 5; sPD n = 6; G2019S n = 3).

No significant difference emerged in hsc70, lamp2A and beclin1 protein levels among the three groups, while G2019S LRRK2 fibroblasts showed significantly higher protein levels of LC3-II with respect to controls (Figure 2).

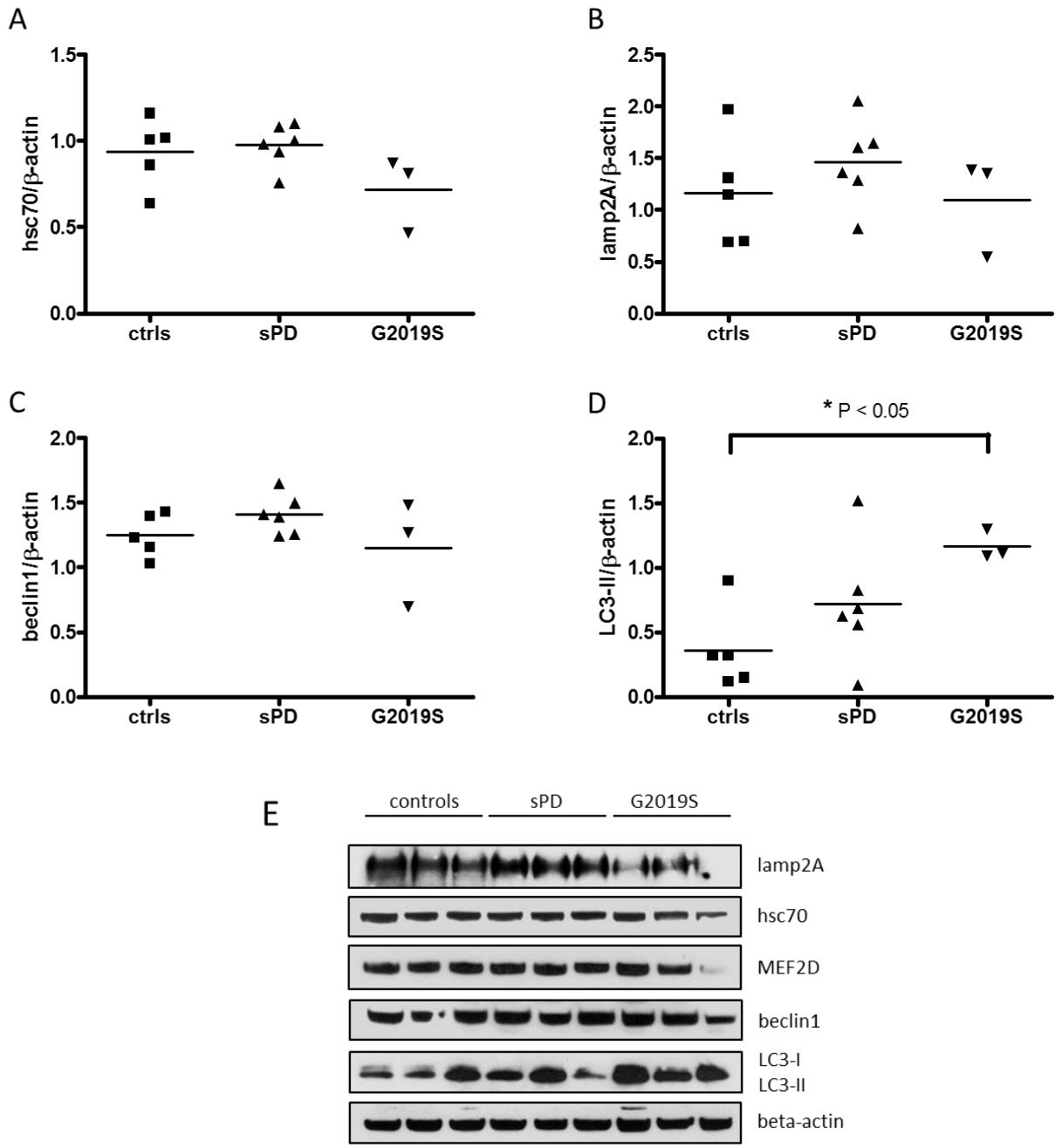

Figure 2. Protein levels of CMA and macroautophagy markers. Protein levels of hsc70 (A), lamp2A (B), beclin1 (C) and LC3-II (D) in fibroblasts from healthy controls (ctrls), sporadic PD patients (sPD) and patients with G2019S LRRK2 mutation. Hsc70, lamp2A, beclin1 and LC3-II protein levels were normalized to beta-actin. Representative Western blot image (E) showing hsc70, lamp2A, beclin1 and LC3-II protein levels in control (n = 3), sPD (n = 3) and G2019S LRRK2 fibroblasts (n=3). Immunoreactivity of beta-actin, used as internal standard, was also shown. One-way ANOVA, followed by Tukey's multiple comparison test (*$p < 0.05$) (ctrls n = 5; sPD n = 6; G2019S n = 3).

The expression of two autophagy substrates was also evaluated as indirect parameter of autophagic activity. Specifically, protein levels of myocyte enhancer factor 2D (MEF2D), a specific CMA substrate and transcription factor implicated in neuronal survival (Yang et al., 2009), and p62/SQSTM1, a macroautophagy substrate used as marker of autophagic flux (Bjørkøy et al., 2009), were analyzed in all cell lines. No significant difference was observed in MEF2D protein levels among sPD, G2019S LRRK2 and healthy control fibroblasts (Figure 3A), while a significant increase was found in p62 protein levels in G2019S LRRK2 fibroblasts compared to both control and sPD fibroblasts (Figure 3B).

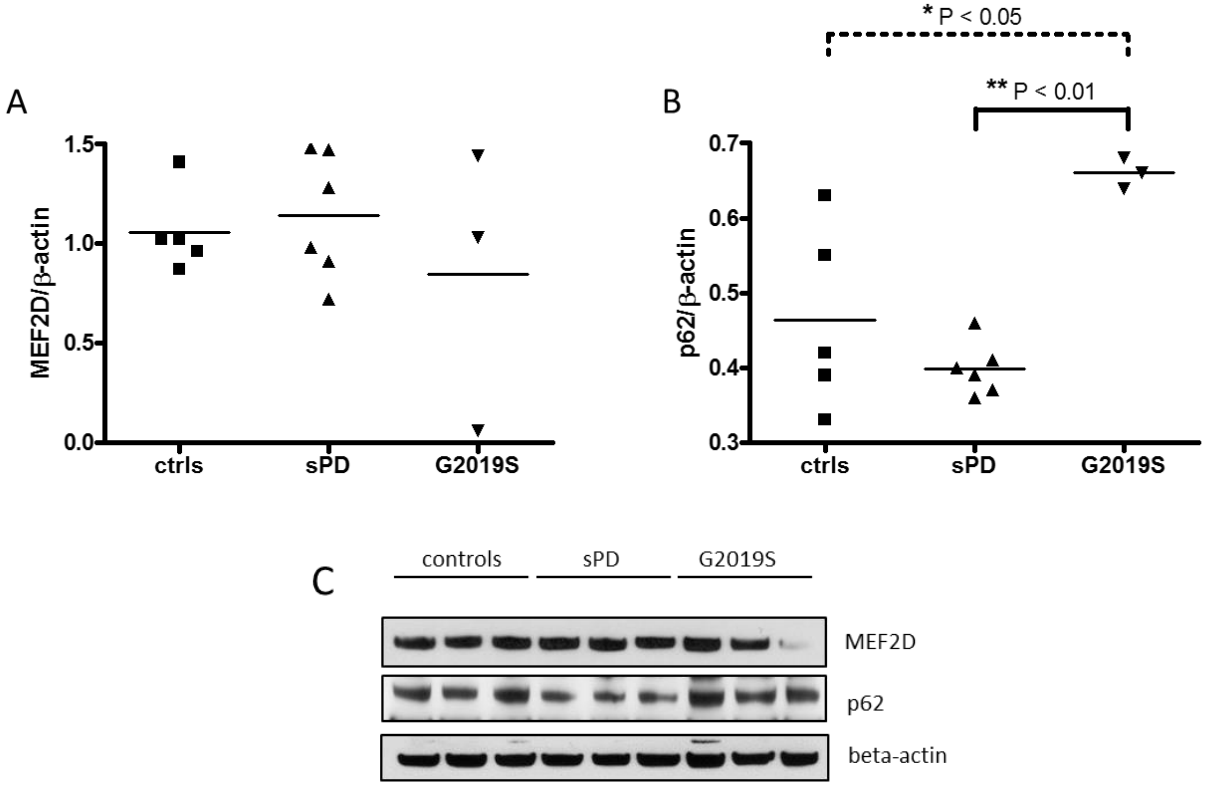

Figure 3. Protein levels of MEF2D and p62/SQSTM1. Protein levels of MEF2D (A) and p62 (B) in fibroblasts from healthy controls (ctrls), sporadic PD patients (sPD) and patients with G2019S LRRK2 mutation (G2019S). MEF2D and p62 protein levels were normalized to beta-actin. Representative Western blot image (C) showing MEF2D and p62 protein levels in control (n = 3), sPD (n = 3) and G2019S LRRK2 fibroblasts (n=3). Immunoreactivity of beta-actin, used as internal standard, was also shown. One-way ANOVA, followed by Tukey's multiple comparison test (*p < 0.05 vs. ctrls; **p < 0.01 vs. sPD) (ctrls n = 5; sPD n = 6; G2019S n = 3).

3.3.2 Effects of autophagy inducers serum starvation and rapamycin on CMA and macroautophagy

In order to evaluate possible different responses of fibroblasts from the three groups in terms of autophagy regulation, cultured fibroblasts were challenged with different autophagy modulators. Protein levels of autophagy key effectors were examined after 24-hours serum starvation, a non-specific autophagy stimulus, or after 24-hours exposure to 10 μM rapamycin, a specific macroautophagy inducer. Serum starvation resulted in a significant reduction of hsc70 levels in all fibroblasts cell lines with a more prominent effect in sPD and G2019S LRRK2 fibroblasts (-40%, $p < 0.05$ vs. vehicle in ctrls and -70%, $p < 0.01$ vs. vehicle in sPD and G2019S), while rapamycin significantly reduced hsc70 levels in fibroblasts from healthy controls and sPD patients only (-70%, $p < 0.01$ and -50%, $p < 0.05$ vs. vehicle, respectively), with no significant effects on G2019S LRRK2 fibroblasts (Figure 4A). No significant effect was exerted by serum starvation on lamp2A protein expression, while an increase of about 60% of lamp2A protein levels was observed only in control fibroblasts after rapamycin exposure (Figure 4B). No appreciable effects of starvation and rapamycin were observed on the macroautophagy marker beclin1 (Figure 4C). A significant increase of LC3-II was observed in G2019S LRRK2 fibroblasts after rapamycin treatment (+38%, $p < 0.05$ vs. vehicle, Figure 4D). Furthermore, a significant reduction of the protein levels of MEF2D was observed only in G2019S LRRK2 fibroblasts after serum starvation (-32%, $p < 0.05$ vs vehicle, Figure 4E), while no effect emerged after rapamycin exposure. No appreciable effects were observed on p62 levels following starvation or rapamycin treatment (Figure 4F).

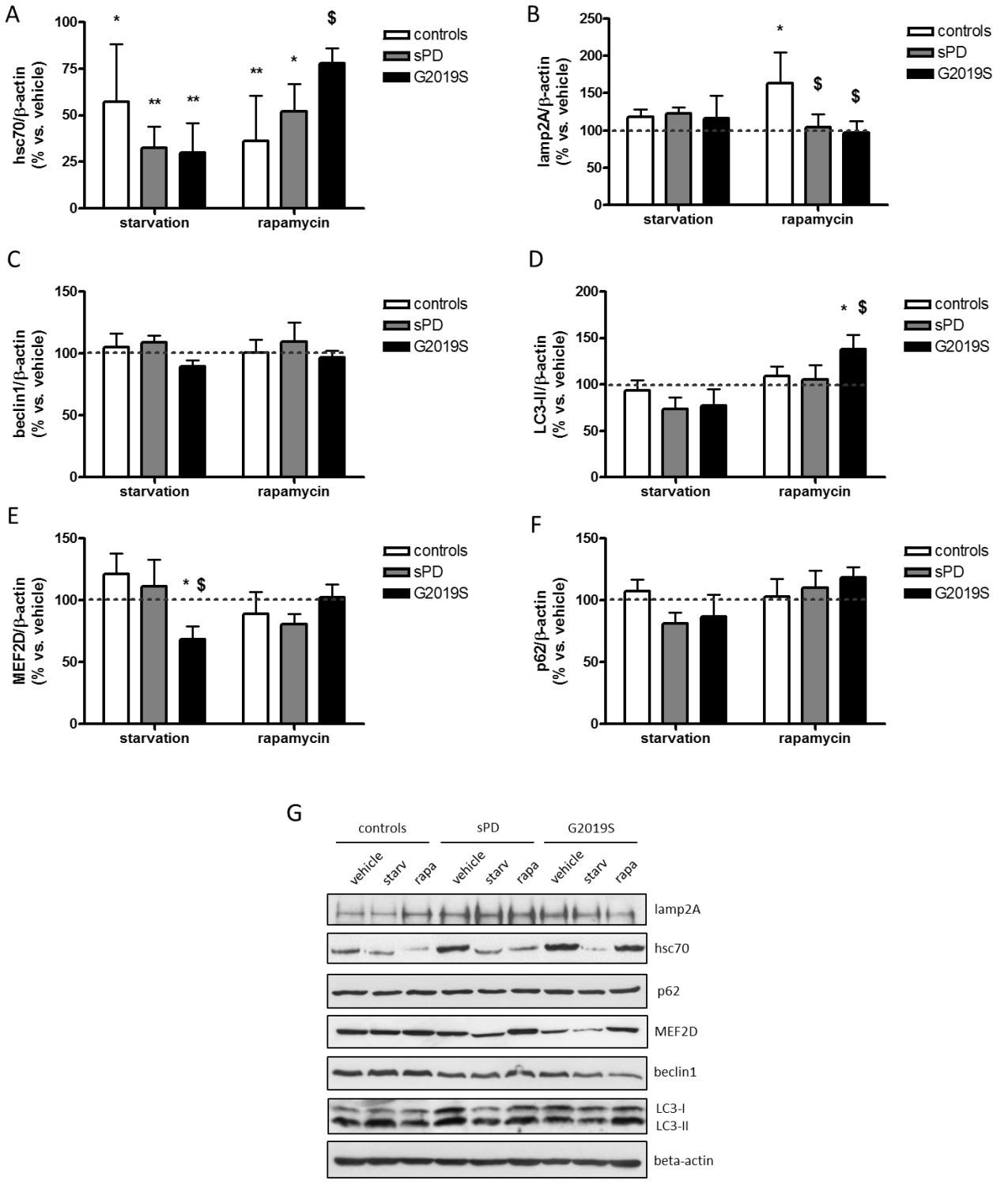

Figure 4. Effects of autophagy inducers on CMA and macroautophagy markers. Protein levels of hsc70 (A), lamp2A (B), beclin1 (C), LC3-II (D), MEF2D (E) and p62 (F) in fibroblasts from healthy controls (ctrls), sporadic PD patients (sPD) and patients with G2019S LRRK2 mutation (G2019S).after 24-hours serum starvation or exposure to 10 μM rapamycin. Protein levels are expressed as % vs. vehicle of the ratio between target protein and beta-actin optical density. Representative Western blot image (G) showing the effects of 24-hours serum starvation (starv) or exposure to 10 μM rapamycin (rapa) on hsc70, lamp2A, beclin1, LC3-II, MEF2D and p62 protein expression. The immunoreactivity of beta-actin, used as internal

standard, was also shown. Results are shown as mean ± standard error of the mean (SEM). Repeated measures ANOVA test, followed by Tukey's post-test; * $p<0.05$, ** $p<0.01$ vs. vehicle; $ $p<0.05$ vs. treated controls (ctrls n = 3; sPD n = 3; G2019S n = 3).

3.3.3 Effects of the autophagy inhibitors ammonium chloride and 3-methyladenine on CMA and macroautophagy

Similarly to the experimental protocol used to assess the effect of autophagy inducers, fibroblasts were exposed to compounds able to inhibit autophagy: ammonium chloride (NH_4Cl), an inhibitor of the lysosomal protease activity, and 3-methyladenine (3-MA), a selective blocker of autophagosome formation. 24-hours cell treatment with 10 mM NH_4Cl did not significantly alter hsc70 or lamp2A protein levels (Figure 5A and 5B), while exposure to 5 mM 3-MA for 24 hours significantly reduced hsc70 protein levels in sPD fibroblasts (-40%, $p < 0.05$, Figure 5A) and increased the levels of lamp2A in control fibroblasts (+100%, $p < 0.05$, Figure 5B). Both the compounds did not affect the levels of beclin1 (Figure 5C), while LC3-II and p62 were significantly increased in all the fibroblasts cells lines after NH_4Cl exposure (Figure 5D and 5F). No effect was observed on MEF2D levels after NH_4Cl or 3-MA exposure (Figure 5E).

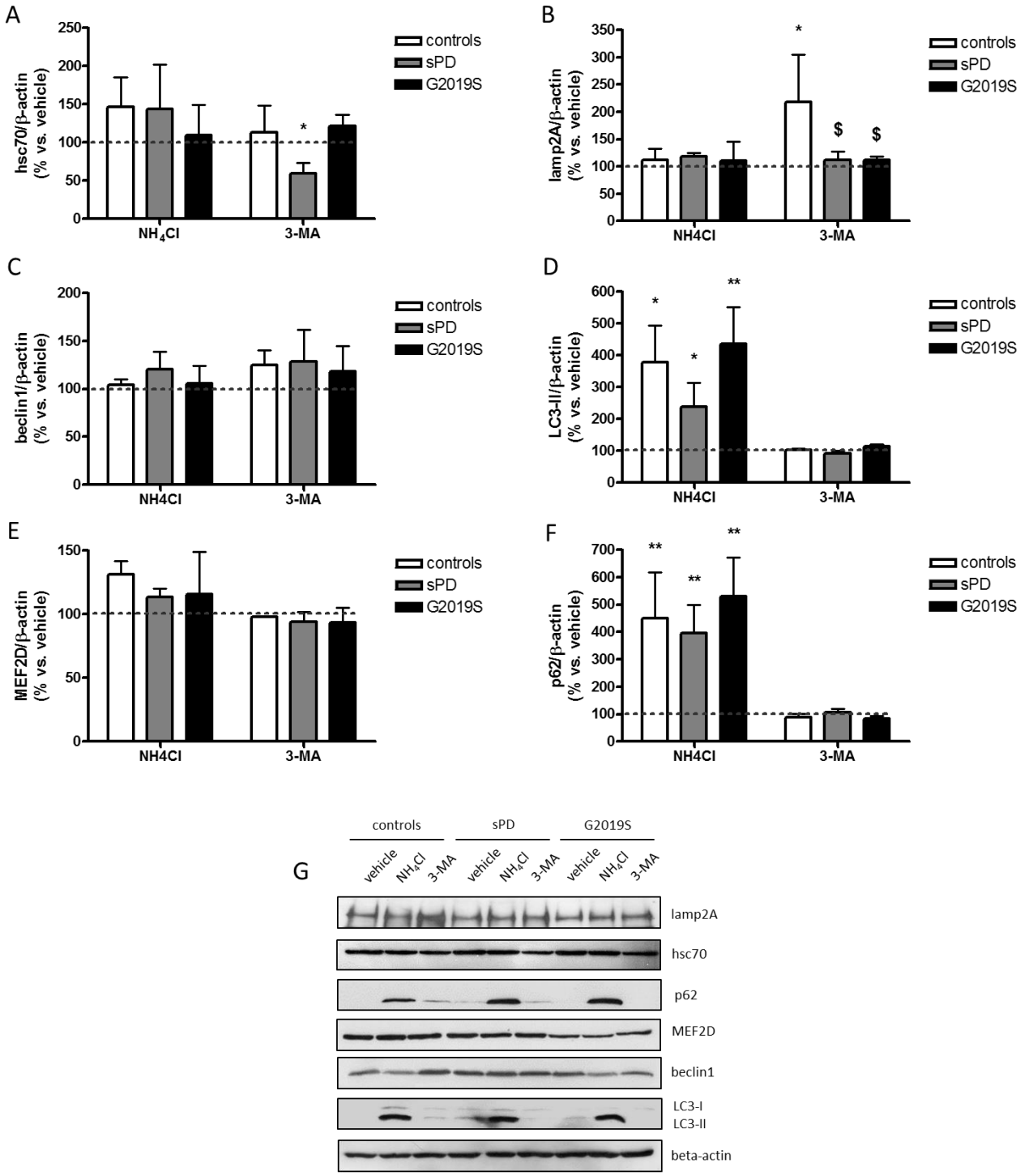

Figure 5. Effects of autophagy inhibitors on CMA and macroautophagy markers. Protein levels of hsc70 (A), lamp2A (B), beclin1 (C), LC3-II (D), MEF2D (E) and p62 (F) in fibroblasts from healthy controls (ctrls), sporadic PD patients (sPD) and subjects with G2019S LRRK2 mutation (G2019S)after 24-hours exposure to 10 mM ammonium chloride (NH_4Cl) or 5 mM 3-methyladenine (3-MA). Protein levels are expressed as % vs. vehicle of the ratio between target protein and beta-actin optical density. Representative Western blot image (G) showing the effects of 24-hours exposure to 10 mM NH_4Cl or 5 mM 3-MA on hsc70, lamp2A, beclin1, LC3-II, MEF2D and p62 protein expression. The immunoreactivity of beta-actin, used as internal standard, was also shown. Results are shown as mean ± standard error of the mean (SEM).

Repeated measures ANOVA test, followed by Tukey's post-test; * $p<0.05$, ** $p<0.01$ vs. vehicle; $ $p<0.05$ vs. treated controls (ctrls n = 3; sPD n = 3; G2019S n = 3).

3.3.4 Ambroxol effects on autophagy

The effect of the chaperone drug ambroxol on autophagy effectors and markers was also tested. According to previous studies from other groups (Maegawa et al., 2009; Luan et al., 2013; McNeil et al., 2014), 30 and 60 μM ambroxol final concentrations were used. After 3-day treatment, ambroxol did not significantly alter the protein levels of hsc70 (Figure 6A), lamp2A (Figure 6B) or beclin1 (Figure 6C). However, a significant 2-fold increase of LC3-II levels was observed in control fibroblasts after exposure to both ambroxol tested concentrations (Figure 6D). Furthermore, ambroxol exposure resulted in a mild increase of LC3-II in sporadic and G2019S LRRK2 PD fibroblasts, which reaches the statistical significance only at 60 μM ambroxol concentration (Figure 6D). A similar trend was observed for p62, whose levels were strongly increased in control fibroblasts and only slightly induced in sPD and G2019S LRRK2 fibroblasts (Figure 6F). Finally, reduced levels of MEF2D were evidenced in sPD fibroblasts after ambroxol exposure while in the other cell lines tested no effects were observed (Figure 6E).

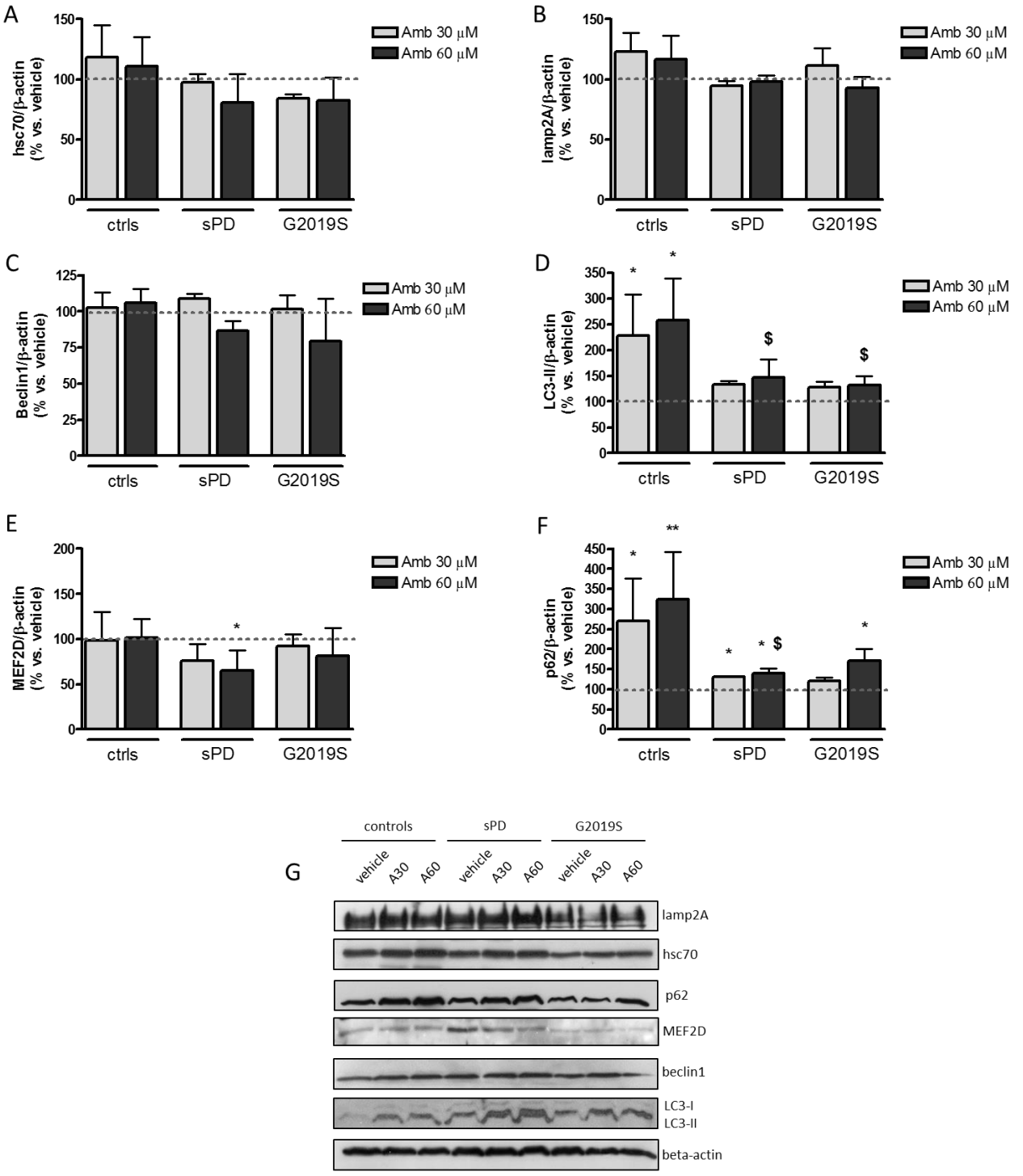

Figure 6. Effects of ambroxol on CMA and macroautophagy markers. Protein levels of hsc70 (A), lamp2A (B), beclin1 (C), LC3-II (D), MEF2D (E) and p62 (F) in fibroblasts from healthy controls (ctrls), sporadic PD patients (sPD) and subjects with G2019S LRRK2 mutation (G2019S) after 3-day exposure to ambroxol (Amb) 30 or 60 μM. Protein levels are expressed as % vs. vehicle of the ratio between target protein and beta-actin optical density. Representative Western blot image (G) showing the effects of ambroxol on hsc70, lamp2A, beclin1, LC3-II, MEF2D and p62 protein expression. The immunoreactivity of beta-actin, used as internal standard, was also shown. Results are shown as mean ± standard error of the

mean (SEM). Repeated measures ANOVA test, followed by Tukey's post-test; * p<0.05, ** p<0.01 vs. vehicle; $ p<0.05 vs. treated controls (ctrls n = 3; sPD n = 3; G2019S n = 3).

3.3.5 Effect of the mitochondrial inhibitor rotenone on CMA

The effects on CMA of the mithocondrial inhibitor rotenone were tested by exposing fibroblasts to two sub-lethal doses of the toxin (0.2 and 1 μM) for 24 hours. 1 μM rotenone resulted in a ~46% reduction of the protein levels of hsc70 in healthy controls, while the same effect was not observed in sPD fibroblasts and even a ~45% increase was observed in G2019S LRRK2 fibroblasts (Figure 7A). No significant alteration of lamp2A protein levels was observed after rotenone exposure (Figure 7B).

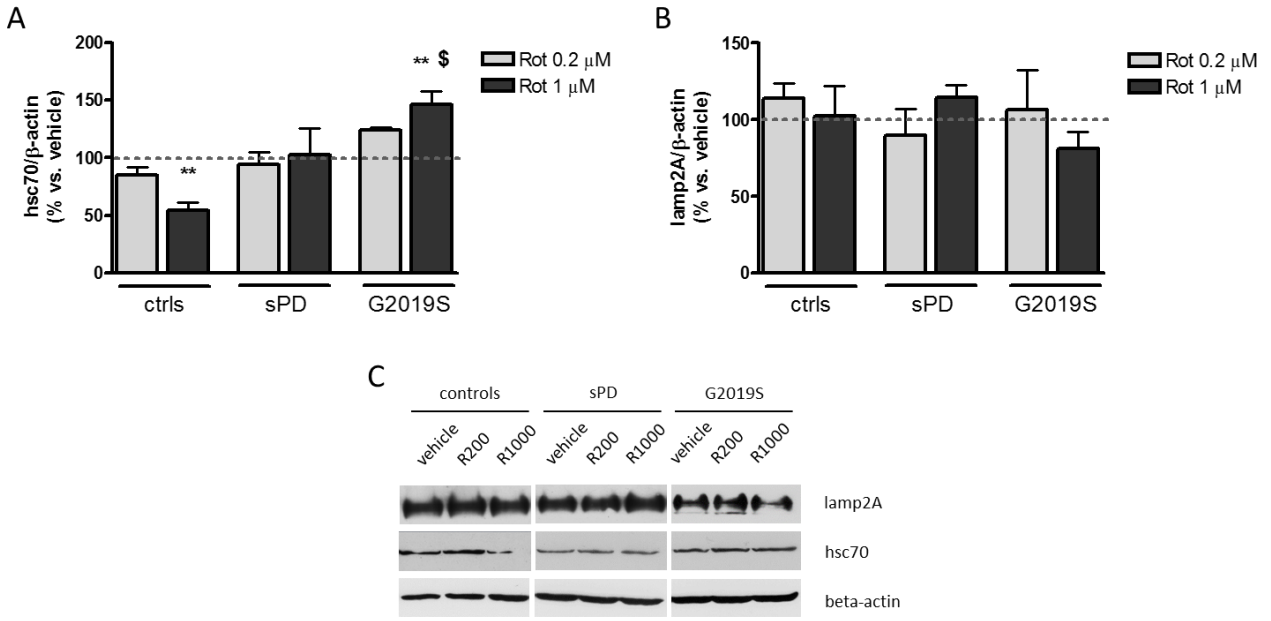

Figure 7. Effects of rotenone on CMA markers. Protein levels of hsc70 (A) and lamp2A (B) in fibroblasts from healthy controls (ctrls), sporadic PD patients (sPD) and subjects with G2019S LRRK2 mutation (G2019S) after 24-hours exposure to rotenone (0.2 and 1 μM). Protein levels are expressed as % vs. vehicle of the ratio between hsc70 or lamp2A and beta-actin optical density. Representative Western blot image (C) showing the effects of 0.2 and 1 μM rotenone (rot) on hsc70 and lamp2A protein expression. The immunoreactivity of beta-actin, used as internal standard, was also shown. Results are shown as mean ± standard error of the mean (SEM). Repeated measures ANOVA test, followed by Tukey's post-test; ** p<0.01 vs. vehicle; $ p<0.05 vs. treated controls (ctrls n = 3; sPD n = 3; G2019S n = 3).

3.4 Discussion

In this study we explored autophagy in fibroblasts from sporadic PD patients and from patients carrying the G2019S mutation on LRRK2 by assessing the levels of CMA effectors, hsc70 and lamp2A, and macroautophagy markers, beclin1 and LC3, as well as of two known substrates of these degradative pathways, MEF2D and p62/SQSTM1. Considering that autophagy is a ubiquitous pathway, we used fibroblasts as a suitable experimental model, already confirmed by a number of published studies (Auberger et al., 2012; Mytilineou et al., 1994; Wiedemann et al., 1999; Musanti et al., 1993; Hoyo et al., 2010), to study possible PD-related autophagy alterations.

The analysis of macroautophagy under basal conditions highlighted a defect in mutant LRRK2 fibroblasts, while no alteration emerged in sporadic cells. Indeed, we found higher levels of the lipidated form of LC3, LC3-II, in G2019S LRRK2 fibroblasts, together with increased levels of p62, suggestive of a reduction in macroautophagy activity or, at least, an increased number of autophagosomes. Moreover, increased p62 levels may impair the delivery of UPS substrates to the proteasome (Korolchuk et al., 2009), suggesting an even more widespread effect of LRRK2 mutations on proteolytic systems derangement. Our results are in line with previous *in vitro* evidences (Alegre-Abarrategui et al. 2009; Gómez-Suaga et al., 2012), while seems to be in contrast with other studies performed in human fibroblasts which failed to found an alteration of LC3-II (Manzoni et al., 2013) or even evidenced an increase of LC3-II accompanied by a decrease of p62 (Bravo-San Pedro et al., 2013). These differences may be explained by the sample size of fibroblast cell lines used in this study, which may represent a bias reflecting the high inter-individual variability.

The susceptibility of patient and control fibroblasts against different autophagy modulators was evaluated in the attempt to identify possible differences among the groups undetectable under basal conditions. No striking difference in macroautophagy markers was observed among the cell lines after serum deprivation, while the selective induction of macroautophagy with rapamycin, an inhibitor of the mammalian target of rapamycin (mTOR), resulted in a significant increase of LC3-II only in G2019S LRRK2 fibroblasts. However, in these cells p62 levels were unaltered,

suggesting that the increased levels of LC3-II are consistent with a different susceptibility of mutant LRRK2 fibroblasts to this compound or with a macroautophagy steady-state defect already occurring in mutant cells. This effect could be explained as an incapacity of G2019S LRRK2 fibroblasts to correctly react to the stimulus that then leads to an autophagic stress, as also suggested in G2019S LRRK2-expressing neuroblastoma cells (Plowey et al., 2008).

While previous works already studied macroautophagy alterations in fibroblasts from sporadic PD patients (Ambrosi et al., 2014) or from patients carrying G2019S mutation on LRRK2 (Bravo-San Pedro et al., 2013; Manzoni et al., 2013; Yakhine-Diop et al., 2014), this is the first study designed to analyze CMA parameters in fibroblasts from sporadic and familial PD patients. Our results indicated that sPD or G2019S LRRK2 fibroblasts do not show alterations of hsc70, lamp2A or MEF2D expression under basal conditions, which may suggest the absence of CMA alterations in the cell lines examined in this work. This observation does not replicate the down-regulation of hsc70 found in peripheral blood mononuclear cells of sporadic PD patients (Sala et al., 2014; Papagiannakis et al., 2015), further reinforcing the view that disease-related autophagy abnormalities may be cell types specific. Nevertheless, alterations of CMA activity may be hard to be detected in standard culture conditions, and, reinforcing this hypothesis, we found different responses of sPD and G2019S LRRK2 fibroblasts with respect to controls after exposure to different autophagy-inducing or -inhibiting conditions.

In this study, serum deprivation was used as non-specific autophagy inducer. As known, nutrient deprivation early activates macroautophagy in cultured cells, with a maximum effect at about 6 hours, while reaches a CMA up-regulation only after 10 hours (Cuervo et al., 1995; Fuertes et al., 2003). The observed reduction of hsc70 protein levels after starvation may be due to a higher degradation rate of this protein which may behave itself as a substrate of CMA (Terlecky et al., 1992). However, as starvation did not produce any effect on the rate-limiting protein of CMA lamp2A, we cannot exclude that the strong hsc70 reduction may be ascribed to the activation of other mechanisms, including the ubiquitin-proteasome system (UPS). Conversely, the observed effects of rapamycin on hsc70 in G2019S LRRK2 fibroblasts compared to controls and the increase

of lamp2A in control fibroblasts suggest again a different susceptibility of mutant LRRK2 and sPD fibroblasts to this drug in terms of CMA activity. Interestingly, a rapamycin-induced reduction of hsc70 has been also observed in human esophageal squamous carcinoma cell lines (Wang et al., 2013a), which can be correlated to a triggered degradation of hsc70 by the cellular degradative systems. Thus, also based on the effects observed for LC3-II, it can be assumed that sPD and G2019S LRRK2 fibroblasts are not differently affected during a general autophagy stimulation as compared to controls, while a more specific stimulus, such as rapamycin, may finely highlight a different reactivity among the cell lines.

The raised levels of LC3-II and p62 after ammonium chloride exposure, an inorganic compound able to inhibit the activity of lysosomal proteases, are indicative of a block of autophagy, as expected. However, no effect was observed on CMA parameters after exposure to this compound with the exception of a slight and not significant increase of hsc70 and MEF2D protein levels in control fibroblasts. In a previous study from our group in SH-SY5Y cells, we demonstrated that ammonium chloride significantly increased alpha-synuclein, MEF2D, and lamp2A protein expression, with no effect on hsc70 (Sala et al., 2013). The lack of effect of ammonium chloride on CMA parameters evidenced in the present study may be ascribed to different biochemical responses of the cellular model used. Conversely, we found an opposite condition after treatment with the macroautophagy inhibitor 3-MA, which blocks autophagosome formation via the inhibition of class III Phosphatidylinositol 3-kinases (PI-3K). Surprisingly, 3-MA did not alter the macroautophagy markers beclin1 and LC3-II or the substrate p62, as expected in response to autophagy inhibition. Our results may be explained by an intriguing dual effect of 3-MA on autophagy. As a matter of fact, 3-MA seems to possess a potent inhibitor effect on autophagy in the first 4 hours, while a prolonged treatment may significantly increase the rate of protein degradation possibly underlying an autophagy induction (Wu et al., 2010). However, another study using the immortalized motoneuron cell line NSC34 showed that 3-MA was able to block autophagic flux up to 24 hours (Rusmini et al., 2013). Anyway, the lack of effect of 3-MA on macroautophagy markers observed in this study may be ascribable to the different cellular model used or to a progressive abatement of

3-MA-induced class III PI-3K inhibition due to the lower concentration used in this study as well as to an involvement of other kinases possibly occurring during long exposure time. On the other hand, the effect of 3-MA on lamp2A was indicative of an induction of CMA in control fibroblasts which is absent in both sPD and G2019S LRRK2 fibroblasts, further suggesting a different responsiveness to autophagy modulation. The observed increase of lamp2A in control cells may be reasonably interpreted as a compensatory up-regulation of CMA or as a general autophagy induction, given the above-mentioned dual role of 3-MA. The observation that 3-MA does not affect hsc70 in control and mutant LRRK2 fibroblasts is in line with our previous findings in SH-SY5Y cells (Sala et al., 2016). However, the decrease of hsc70 observed in sPD fibroblasts is harder to unravel and can be ascribed to an impaired regulation of such protein.

In this study we also intended to explore the effects of ambroxol hydrochloride on autophagy in sPD and G2019S LRRK2 fibroblasts. Ambroxol is a well-known secretolytic agent with claimed antioxidant and anti-inflammatory properties. Recently, it has been reported that ambroxol treatment may improve lysosomal biochemistry (McNeil et al., 2014) and reduce alpha-synuclein levels *in vitro* (McNeil et al., 2014) and in alpha-synuclein transgenic mice (Migdalska-Richards et al., 2016). Our results showed that the levels of CMA effectors hsc70 and lamp2A were not altered by ambroxol exposure, while LC3-II and p62 were strongly increased suggesting a drug-mediated macroautophagy modulation. Interestingly, G2019S LRRK2 fibroblasts showed a mild increase of these proteins after ambroxol treatment as compared with the marked increase observed in control cells, possibly due to a reduced ambroxol effect in mutant LRRK2 fibroblasts characterized by a steady-state increased LC3-II and p62 levels. Furthermore, a similar trend in LC3-II and p62 levels, together with a MEF2D reduction, was observed in sPD fibroblasts, reinforcing the hypothesis of a different sensitivity of PD fibroblasts to the different stimuli tested in this study. Anyway, these results demonstrate a novel autophagy-modulating property of ambroxol, which should be further investigated for potential applications in neurodegenerative disorders.

Finally, the down-regulation of hsc70 observed in control fibroblasts after rotenone exposure is consistent with our previous results in human SH-SY5Y cells and mouse cortical neurons (Sala et

al., 2016). However, the lack of any significant effect on sPD fibroblasts and, more importantly, the opposite increase of hsc70 in G2019S LRRK2 fibroblasts are indicative of a different modulation of this chaperone protein induced by rotenone in the three groups involved in this study. A recent study already showed an increased susceptibility of sporadic PD fibroblasts to rotenone as indicated by a higher necrosis and significantly lower levels of beclin1 in PD cells (Ambrosi et al., 2014). Our study allowed the obtaining of first evidence on the modulatory effect exerted by rotenone on CMA in fibroblasts, confirming the hypothesis that sPD and mutant LRRK2 fibroblasts differently react to the PD-related toxin rotenone.

3.5 Conclusions

Collectively, the increased levels of LC3-II and p62 in fibroblasts from PD patients carrying the G2019S mutation on LRRK2 are consistent with an autophagosome accumulation and may suggest a basal impairment of macroautophagy. More importantly, we demonstrated that both fibroblasts from mutant G2019S LRRK2 PD carriers and fibroblasts from PD patients with no familial history display a different responsiveness to autophagy inducers and inhibitors in terms of CMA and macroautophagy modulation. This altered susceptibility is further highlighted following ambroxol or rotenone exposure, which differently affects macroautophagy and CMA, respectively. Thus, while ALP defects in PD fibroblasts may be difficult to be evidenced under basal conditions, challenging cells with suitable stimuli would be helpful in the identification of disease-related alterations affecting cellular degradative systems. Moreover, this study confirms the usefulness of fibroblasts for investigating the mechanisms underlying PD pathogenesis, a fundamental goal for the development of new biomarkers and therapeutic approaches.

Acknowledgements

This study was carried out within the framework of the Ivascomar project, Cluster Tecnologico Nazionale Scienze della Vita ALISEI, Italian Ministry of Research (MIUR, to CF). We acknowledge the “Cell Line and DNA Biobank from Patients Affected by Genetic Diseases”

(Istituto G. Gaslini), and “Parkinson Institute Biobank” (Milan, http://www.parkinsonbiobank.com/) member of the Telethon Network of Genetic Biobanks funded by Telethon Italy, (http://www.biobanknetwork.org, project No. GTB12001) for providing us with mutant LRRK2 specimens.

Chapter 4:
General discussion and conclusions

Aim of this project was to investigate the role of autophagy-lysosome pathway (ALP) alterations in the pathogenesis of Parkinson's disease (PD). Actually, the involvement of ALP in PD has been highlighted by autoptic evidences (Anglade et al., 1997; Alvarez-Erviti et al., 2010) as well as by a large number of *in vitro* and *in vivo* studies. However, a direct causal relationship between autophagy defects and PD pathogenesis is lacking and the proposed detrimental mechanisms of altered autophagy in the disease are not yet fully unveiled. In particular, chaperone-mediated autophagy (CMA) is probably the most intriguing autophagy pathway which deserves further investigation in PD, given its crucial role in the turn-over of alpha-synuclein. Moreover, one of the main effectors of CMA, hsc70, acts as the carrier of alpha-synuclein to the lysosomes but also possesses anti-aggregant properties suggesting that this chaperone protein of CMA may play a key-role in the pathogenesis of PD.

In the first study we demonstrated that the mitochondrial inhibitor rotenone, a toxin widely used to generate experimental PD models, is able to down-regulate hsc70, mimicking the observations of a reduced hsc70 levels in PD brain samples (Alvarez-Erviti et al., 2010) and in PD lymphomonocytes (Sala et al., 2014; Papagiannakis et al., 2015). This result was confirmed by testing the effects of rotenone in two different cell lines: human neuroblastoma SH-SY5Y cells and mouse cortical neurons. Indeed, SH-SY5Y cells possess a dopaminergic phenotype and are able to reproduce with good approximation the biochemical characteristics of mesencephalic dopaminergic neurons, thus making them one of the most used *in vitro* models of PD. Although SH-SY5Y cells are not representative of the anatomical-physiological and pathological conditions of the disease, they nevertheless have a number of advantages related to the wide availability, low cost, easiness of handling and, above all, the opportunity to study the biochemical pathomechanisms without the potential extra-neuronal interference of an *in vivo* model. On the other side, mouse cortical neurons,

being primary and not tumor-derived cells, are more likely to recapitulate the properties of neuronal cells *in vivo*, although the availability for experiments is more limited.

In this study we also demonstrated that hsc70 down-regulation may be ascribed to the inhibition of mitochondrial complex I rather to a rotenone-induced oxidative stress increase, given the lack of effects on hsc70 expression following hydrogen peroxide exposure. Furthermore, the demonstration that hsc70 knock-down results in an up-regulation of alpha-synuclein underlines the importance of this chaperone protein in the maintenance of an adequate and potentially harmless level of alpha-synuclein.

In the second study we investigated the presence of possible ALP alterations in fibroblasts from sporadic PD patients and from patients with the G2019S mutation on LRRK2. We used fibroblasts since they can be easily obtained and they can be cultured for a long period. While fibroblasts are not neuronal-type cells, they have been reported to reproduce biochemical deficits occurring in degenerating dopaminergic midbrain neurons (Auburger et al., 2012; Hoyo et al., 2010; Wiedemann et al., 1999). We choose to analyze fibroblasts from patients carrying the G2019S LRRK2 mutation as it represents the most common familial form of PD and since it has been already suggested to be able to impair both macroautophagy (Alegre-Abarrategui et al. 2009; Gómez-Suaga et al., 2012) and CMA (Orenstein et al., 2013). Our study confirmed the potential detrimental role of mutant LRRK2 on macroautophagy, based on the increased levels of LC3-II and p62 observed in G2019S LRRK2 fibroblasts as compared to healthy controls, while we failed to evidence any alteration of CMA under basal conditions. However, following exposure of fibroblasts to different autophagy modulators, we were able to unmask several alterations of both CMA and macroautophagy in both sporadic and familial PD fibroblasts.

Anyway, some limits are present in this study. Firstly, while all the three cell lines used represent suitable models of PD, they are a tumour cell line (SH-SY5Y cells), a mouse primary culture (mouse cortical neurons) and a non-neuronal cell type (skin fibroblasts). Thus, we cannot confirm that the observed ALP alterations precisely mirror those occurring in degenerating human nigral neurons. As a matter of fact, cancer cell lines may have different susceptibility to toxins or other

agents and, to overcome this limitation, in the first study we used primary neurons in order to validate and strengthen our results. Secondly, the numerosity of the fibroblast cell lines is likely too little to avoid bias arisen from inter-individual variability or from manipulation activities; anyway, although punch skin biopsies are relatively low invasive, their collection is obviously more difficult as compared to other biological samples, such as peripheral blood.

Collectively, the performed studies contribute to clarify the link between ALP defects and PD and have the ambitious goal to help the development of new tools or experimental paradigms aimed at the identification of PD biomarkers or novel therapeutic targets.

Bibliography

Agarraberes FA, Dice JF.A molecular chaperone complex at the lysosomal membrane is required for protein translocation. J Cell Sci. 2001 Jul;114(Pt 13):2491-9.

Alam ZI, Jenner A, Daniel SE, Lees AJ, Cairns N, Marsden CD, Jenner P, Halliwell B. Oxidative DNA damage in the parkinsonian brain: an apparent selective increase in 8-hydroxyguanine levels in substantia nigra. J Neurochem. 1997 Sep;69(3):1196-203.

Albin RL, Greenamyre JT. Alternative excitotoxic hypotheses. Neurology. 1992;42:733–738. Review.

Alegre-Abarrategui J, Christian H, Lufino MM, Mutihac R, Venda LL, Ansorge O, Wade-Martins R. LRRK2 regulates autophagic activity and localizes to specific membrane microdomains in a novel human genomic reporter cellular model. Hum Mol Genet. 2009 Nov 1;18(21):4022-34.

Alvarez-Erviti L, Rodriguez-Oroz MC, Cooper JM, Caballero C, Ferrer I, Obeso JA, Schapira AH. Chaperone-mediated autophagy markers in Parkinson disease brains. Arch Neurol. 2010 Dec; 67(12):1464-72.

Alvarez-Erviti L, Seow Y, Schapira AH, Rodriguez-Oroz MC, Obeso JA, Cooper JM.Influence of microRNA deregulation on chaperone-mediated autophagy and α-synuclein pathology in Parkinson's disease. Cell Death Dis. 2013 Mar 14;4:e545.

Ambrosi G, Ghezzi C, Sepe S, Milanese C, Payan-Gomez C, Bombardieri CR, Armentero MT, Zangaglia R, Pacchetti C, Mastroberardino PG, Blandini F. Bioenergetic and proteolytic defects in fibroblasts from patients with sporadic Parkinson's disease. Biochim Biophys Acta. 2014 Sep;1842(9):1385-94.

Ambrosi G, Ghezzi C, Zangaglia R, Levandis G, Pacchetti C, Blandini F. Ambroxol-induced rescue of defective glucocerebrosidase is associated with increased LIMP-2 and saposin C levels in GBA1 mutant Parkinson's disease cells. Neurobiol Dis. 2015 Oct;82:235-42.

Anglade P, Vyas S, Javoy-Agid F, Herrero MT, Michel PP, Marquez J, Mouatt-Prigent A, Ruberg M, Hirsch EC, Agid Y. Apoptosis and autophagy in nigral neurons of patients with Parkinson's disease. Histol Histopathol. 1997 Jan; 12(1):25-31.

Auburger G, Klinkenberg M, Drost J, Marcus K, Morales-Gordo B, Kunz WS, Brandt U, Broccoli V, Reichmann H, Gispert S, Jendrach M. Primary skin fibroblasts as a model of Parkinson's disease. Mol Neurobiol. 2012 Aug;46(1):20-7.

Bandyopadhyay U, Kaushik S, Varticovski L, Cuervo AM The chaperone-mediated autophagy receptor organizes in dynamic protein complexes at the lysosomal membrane. Mol Cell Biol. 2008 Sep; 28(18):5747-63.

Beal MF. Mechanisms of excitotoxicity in neurologic diseases. FASEB J. 1992 Dec;6(15):3338-44. Review.

Berman SB, Hastings TG. Dopamine oxidation alters mitochondrial respiration and induces permeability transition in brain mitochondria: implications for Parkinson's disease. J Neurochem. 1999 Sep;73(3):1127-37.

Bertrand E, Lechowicz W, Szpak GM, Dymecki J. Qualitative and quantitative analysis of locus coeruleus neurons in Parkinson's disease. Folia Neuropathol. 1997; 35(2):80-6.

Betarbet R, Canet-Aviles RM, Sherer TB, Mastroberardino PG, McLendon C, Kim JH, Lund S, Na HM, Taylor G, Bence NF, Kopito R, Seo BB, Yagi T, Yagi A, Klinefelter G, Cookson MR, Greenamyre JT. Intersecting pathways to neurodegeneration in Parkinson's disease: effects of the pesticide rotenone on DJ-1, alpha-synuclein, and the ubiquitin-proteasome system. Neurobiol Dis. 2006 May;22(2):404-20.

Betarbet R, Sherer TB, MacKenzie G, Garcia-Osuna M, Panov AV, Greenamyre JT. Chronic systemic pesticide exposure reproduces features of Parkinson's disease. Nat Neurosci. 2000 Dec;3(12):1301-6.

Bjørkøy G, Lamark T, Brech A, Outzen H, Perander M, Overvatn A, Stenmark H, Johansen T.p62/SQSTM1 forms protein aggregates degraded by autophagy and has a protective effect on huntingtin-induced cell death. J Cell Biol. 2005 Nov 21;171(4):603-14.

Bjørkøy G, Lamark T, Pankiv S, Øvervatn A, Brech A, Johansen T. Monitoring autophagic degradation of p62/SQSTM1. Methods Enzymol. 2009;452:181-97

Blandini F, Nappi G, Greenamyre JT. Subthalamic infusion of an NMDA antagonist prevents basal ganglia metabolic changes and nigral degeneration in a rodent model of Parkinson's disease. Ann Neurol. 2001 Apr;49(4):525-9

Bravo-San Pedro JM, Niso-Santano M, Gómez-Sánchez R, Pizarro-Estrella E, Aiastui-Pujana A, Gorostidi A, Climent V, López de Maturana R, Sanchez-Pernaute R, López de Munain A, Fuentes JM, González-Polo RA. The LRRK2 G2019S mutant exacerbates basal autophagy through activation of the MEK/ERK pathway. Cell Mol Life Sci. 2013 Jan;70(1):121-36

Brochard V, Combadière B, Prigent A, Laouar Y, Perrin A, Beray-Berthat V, Bonduelle O, Alvarez-Fischer D, Callebert J, Launay JM, Duyckaerts C, Flavell RA, Hirsch EC, Hunot S. Infiltration of CD4+ lymphocytes into the brain contributes to neurodegeneration in a mouse model of Parkinson disease. J Clin Invest. 2009 Jan;119(1):182-92.

Chartier-Harlin MC, Kachergus J, Roumier C, Mouroux V, Douay X, Lincoln S, Levecque C, Larvor L, Andrieux J, Hulihan M, Waucquier N, Defebvre L, Amouyel P, Farrer M, Destée A. Alpha-synuclein locus duplication as a cause of familial Parkinson's disease. Lancet. 2004 Sep 25-Oct 1;364(9440):1167-9

Chiang HL, Dice JF. Peptide sequences that target proteins for enhanced degradation during serum withdrawal. J Biol Chem. 1988 May 15;263(14):6797-805.

Chiang HL, Terlecky SR, Plant CP, Dice JF. A role for a 70-kilodalton heat shock protein in lysosomal degradation of intracellular proteins. Science. 1989 Oct 20;246(4928):382-5.

Choubey V, Safiulina D, Vaarmann A, Cagalinec M, Wareski P, Kuum M, Zharkovsky A, Kaasik A. Mutant A53T alpha-synuclein induces neuronal death by increasing mitochondrial autophagy. J Biol Chem. 2011 Mar 25;286(12):10814-24

Chong KY, Lai CC, Su CY.Inducible and constitutive HSP70s confer synergistic resistance against metabolic challenges. Biochem Biophys Res Commun. 2013 Jan 11;430(2):774-9.

Cirillo G, Colangelo AM, Berbenni M, Ippolito VM, De Luca C, Verdesca F, Savarese L, Alberghina L, Maggio N, Papa M.Purinergic Modulation of Spinal Neuroglial Maladaptive Plasticity Following Peripheral Nerve Injury. Mol Neurobiol. 2015 Dec;52(3):1440-57.

Colla E, Jensen PH, Pletnikova O, Troncoso JC, Glabe C, Lee MK. Accumulation of toxic α-synuclein oligomer within endoplasmic reticulum occurs in α-synucleinopathy in vivo. J Neurosci. 2012 Mar 7;32(10):3301-5.

Cookson MR. The role of leucine-rich repeat kinase 2 (LRRK2) in Parkinson's disease. Nat Rev Neurosci. 2010 Dec;11(12):791-7.

Coux O, Tanaka K, Goldberg AL. Structure and functions of the 20S and 26S proteasomes. Annu Rev Biochem. 1996;65:801-47.

Cuervo AM, Dice JF, Knecht E. A population of rat liver lysosomes responsible for the selective uptake and degradation of cytosolic proteins. J Biol Chem. 1997 Feb 28; 272(9):5606-15.

Cuervo AM, Dice JF. A receptor for the selective uptake and degradation of proteins by lysosomes. Science. 1996 Jul 26; 273(5274):501-3.

Cuervo AM, Dice JF. Unique properties of lamp2a compared to other lamp2 isoforms. J Cell Sci. 2000 Dec;113 Pt 24:4441-50.

Cuervo AM, Knecht E, Terlecky SR, Dice JF. Activation of a selective pathway of lysosomal proteolysis in rat liver by prolonged starvation. Am J Physiol. 1995 Nov; 269(5 Pt 1):C1200-8.

Cuervo AM, Stefanis L, Fredenburg R, Lansbury PT, Sulzer D. Impaired degradation of mutant alpha-synuclein by chaperone-mediated autophagy. Science. 2004 Aug 27; 305(5688):1292-5.

Cuervo AM, Wong E. Chaperone-mediated autophagy: roles in disease and aging. Cell Res. 2014 Jan;24(1):92-104.

Danzer KM, Haasen D, Karow AR, Moussaud S, Habeck M, Giese A, Kretzschmar H, Hengerer B, Kostka M. Different species of alpha-synuclein oligomers induce calcium influx and seeding. J Neurosci. 2007 Aug 22;27(34):9220-32.

Dauer W, Przedborski S. Parkinson's disease: mechanisms and models. Neuron. 2003 Sep 11;39(6):889-909. Review

de Lau LM, Breteler MM. Epidemiology of Parkinson's disease. Lancet Neurol. 2006 Jun; 5(6):525-35.

Dice JF. Peptide sequences that target cytosolic proteins for lysosomal proteolysis. Trends Biochem Sci. 1990 Aug; 15(8):305-9. Review

Eskelinen EL, Illert AL, Tanaka Y, Schwarzmann G, Blanz J, Von Figura K, Saftig P.Role of LAMP-2 in lysosome biogenesis and autophagy. Mol Biol Cell. 2002 Sep;13(9):3355-68.

Farrer M, Kachergus J, Forno L, Lincoln S, Wang DS, Hulihan M, Maraganore D, Gwinn-Hardy K, Wszolek Z, Dickson D, Langston JW. Comparison of kindreds with parkinsonism and alpha-synuclein genomic multiplications. Ann Neurol. 2004 Feb;55(2):174-9.

Filocamo M, Mazzotti R, Corsolini F, Stroppiano M, Stroppiana G, Grossi S, et al.. Cell Line and DNA Biobank From Patients Affected by Genetic Diseases. Open Journal of Bioresources. 2014;1:e2.

Floor E, Wetzel MG. Increased protein oxidation in human substantia nigra pars compacta in comparison with basal ganglia and prefrontal cortex measured with an improved dinitrophenylhydrazine assay. J Neurochem. 1998 Jan;70(1):268-75

Forno LS. Neuropathology of Parkinson's disease. J Neuropathol Exp Neurol. 1996 Mar;55(3):259-72. Review.

Fuertes G, Martín De Llano JJ, Villarroya A, Rivett AJ, Knecht E. Changes in the proteolytic activities of proteasomes and lysosomes in human fibroblasts produced by serum withdrawal, amino-acid deprivation and confluent conditions. Biochem J. 2003 Oct 1;375(Pt 1):75-86.

Gao HM, Hong JS, Zhang W, Liu B. Distinct role for microglia in rotenone-induced degeneration of dopaminergic neurons. J Neurosci. 2002 Feb 1;22(3):782-90.

Gao X, Carroni M, Nussbaum-Krammer C, Mogk A, Nillegoda NB, Szlachcic A, Guilbride DL, Saibil HR, Mayer MP, Bukau B. Human Hsp70 Disaggregase Reverses Parkinson's-Linked α-Synuclein Amyloid Fibrils. Mol Cell. 2015 Sep 3;59(5):781-93.

Giasson BI, Forman MS, Higuchi M, Golbe LI, Graves CL, Kotzbauer PT, Trojanowski JQ, Lee VM. Initiation and synergistic fibrillization of tau and alpha-synuclein. Science. 2003 Apr 25;300(5619):636-40.

Gibb WR, Lees AJ. The relevance of the Lewy body to the pathogenesis of idiopathic Parkinson's disease. J Neurol Neurosurg Psychiatry. 1988 Jun;51(6):745-52. Review.

Giordano S, Dodson M, Ravi S, Redmann M, Ouyang X, Darley Usmar VM, Zhang J. Bioenergetic adaptation in response to autophagy regulators during rotenone exposure. J Neurochem. 2014 Dec;131(5):625-33.

Gómez-Suaga P, Luzón-Toro B, Churamani D, Zhang L, Bloor-Young D, Patel S, Woodman PG, Churchill GC, Hilfiker S. Leucine-rich repeat kinase 2 regulates autophagy through a calcium-dependent pathway involving NAADP. Hum Mol Genet. 2012 Feb 1;21(3):511-25

Graham DG. Oxidative pathways for catecholamines in the genesis of neuromelanin and cytotoxic quinones. Mol Pharmacol. 1978 Jul;14(4):633-43.

Halliday GM, Li YW, Blumbergs PC, Joh TH, Cotton RG, Howe PR, Blessing WW, Geffen LB. Neuropathology of immunohistochemically identified brainstem neurons in Parkinson's disease. Ann Neurol. 1990 Apr; 27(4):373-85.

Hinault MP, Cuendet AF, Mattoo RU, Mensi M, Dietler G, Lashuel HA, Goloubinoff P. Stable alpha-synuclein oligomers strongly inhibit chaperone activity of the Hsp70 system by weak interactions with J-domain co-chaperones. J Biol Chem. 2010 Dec 3;285(49):38173-82.

Höglinger GU, Oertel WH, Hirsch EC. The rotenone model of parkinsonism--the five years inspection. J Neural Transm Suppl. 2006;(70):269-72.

Hoyo P, Garcia-Redondo A, Bustos F, Molina JA, Sayed Y, Alonso-Navarro H, Caballero L, Arenas J, Agundez JA, Jimenez-Jimenez FJ. Oxidative stress in skin fibroblasts cultures from patients with Parkinson's disease. BMC Neurol. 2010;10:95.

Iwai A, Masliah E, Yoshimoto M, Ge N, Flanagan L, de Silva HA, Kittel A, Saitoh T. The precursor protein of non-A beta component of Alzheimer's disease amyloid is a presynaptic protein of the central nervous system. Neuron. 1995 Feb;14(2):467-75.

Jäger S, Bucci C, Tanida I, Ueno T, Kominami E, Saftig P, Eskelinen EL. Role for Rab7 in maturation of late autophagic vacuoles. J Cell Sci. 2004 Sep 15;117(Pt 20):4837-48.

Jenner P, Olanow CW. Understanding cell death in Parkinson's disease. Ann Neurol. 1998 Sep;44(3 Suppl 1):S72-84. Review.

Jin SM, Lazarou M, Wang C, Kane LA, Narendra DP, Youle RJ. Mitochondrial membrane potential regulates PINK1 import and proteolytic destabilization by PARL. J Cell Biol. 2010 Nov 29;191(5):933-42.

Kabuta T, Furuta A, Aoki S, Furuta K, Wada K. Aberrant interaction between Parkinson disease-associated mutant UCH-L1 and the lysosomal receptor for chaperone-mediated autophagy. J Biol Chem. 2008 Aug 29;283(35):23731-8.

Kaushik S, Cuervo AM. Chaperone-mediated autophagy: a unique way to enter the lysosome world. Trends Cell Biol. 2012 Aug;22(8):407-17.

Kaushik S, Massey AC, Mizushima N, Cuervo AM. Constitutive activation of chaperone-mediated autophagy in cells with impaired macroautophagy. Mol Biol Cell. 2008 May; 19(5):2179-92.

Kiffin R, Christian C, Knecht E, Cuervo AM Activation of chaperone-mediated autophagy during oxidative stress. Mol Biol Cell. 2004 Nov; 15(11):4829-40

Kitada T, Asakawa S, Hattori N, Matsumine H, Yamamura Y, Minoshima S, Yokochi M, Mizuno Y, Shimizu N. Mutations in the parkin gene cause autosomal recessive juvenile parkinsonism. Nature. 1998 Apr 9; 392(6676):605-8.

Korolchuk VI, Mansilla A, Menzies FM, Rubinsztein DC. Autophagy inhibition compromises degradation of ubiquitin-proteasome pathway substrates. Mol Cell. 2009 Feb 27;33(4):517-27.

Krüger R, Kuhn W, Müller T, Woitalla D, Graeber M, Kösel S, Przuntek H, Epplen JT, Schöls L, Riess O. Ala30Pro mutation in the gene encoding alpha-synuclein in Parkinson's disease. Nat Genet. 1998 Feb;18(2):106-8.

Kuzuhara S, Mori H, Izumiyama N, Yoshimura M, Ihara Y. Lewy bodies are ubiquitinated. A light and electron microscopic immunocytochemical study. Acta Neuropathol. 1988; 75(4):345-53.

Kwak S, Masaki T, Ishiura S, Sugita H. Multicatalytic proteinase is present in Lewy bodies and neurofibrillary tangles in diffuse Lewy body disease brains. Neurosci Lett. 1991;128 (1):21–24.

Levine B, Deretic V. Unveiling the roles of autophagy in innate and adaptive immunity. Nat Rev Immunol. 2007 Oct;7(10):767-77.

Levine B, Yuan J. Autophagy in cell death: an innocent convict? J Clin Invest. 2005 Oct;115(10):2679-88. Review.

Lindersson E, Beedholm R, Højrup P, Moos T, Gai W, Hendil KB, Jensen PH. Proteasomal inhibition by alpha-synuclein filaments and oligomers. J Biol Chem. 2004 Mar 26;279(13):12924-34.

Litvan I, Bhatia KP, Burn DJ, Goetz CG, Lang AE, McKeith I, Quinn N, Sethi KD, Shults C, Wenning GK; Movement Disorders Society Scientific Issues Committee. Movement Disorders Society Scientific Issues Committee report: SIC Task Force appraisal of clinical diagnostic criteria for Parkinsonian disorders. Mov Disord. 2003 May;18(5):467-86.

Liu T, Daniels CK, Cao S. Comprehensive review on the HSC70 functions, interactions with related molecules and involvement in clinical diseases and therapeutic potential. Pharmacol Ther. 2012 Dec;136(3):354-74.

Lotharius J, Brundin P. Impaired dopamine storage resulting from alpha-synuclein mutations may contribute to the pathogenesis of Parkinson's disease. Hum Mol Genet. 2002 Oct 1;11(20):2395-407. Review.

Lowe J, McDermott H, Landon M, Mayer RJ, Wilkinson KD. Ubiquitin carboxyl-terminal hydrolase (PGP 9.5) is selectively present in ubiquitinated inclusion bodies characteristic of human neurodegenerative diseases. J Pathol. 1990 Jun; 161(2):153-60.

Luan Z, Li L, Higaki K, Nanba E, Suzuki Y, Ohno K. The chaperone activity and toxicity of ambroxol on Gaucher cells and normal mice. Brain Dev 2013;35:317-22.

Mader BJ, Pivtoraiko VN, Flippo HM, Klocke BJ, Roth KA, Mangieri LR, Shacka JJ.Rotenone inhibits autophagic flux prior to inducing cell death. ACS Chem Neurosci. 2012 Dec 19;3(12):1063-72.

Maegawa GH, Tropak MD, Buttner JD, Rigat BA, Fuller M, Pandit D, et al. Identification and characterization of ambroxol as an enzyme enhancement agent for Gaucher disease. J Biol Chem 2009;284:23502-16.

Mak SK, McCormack AL, Manning-Bog AB, Cuervo AM, Di Monte DA. Lysosomal degradation of alpha-synuclein in vivo. J Biol Chem. 2010 Apr 30;285(18):13621-9.

Manzoni C, Mamais A, Dihanich S, McGoldrick P, Devine MJ, Zerle J, Kara E, Taanman JW, Healy DG, Marti-Masso JF, Schapira AH, Plun-Favreau H, Tooze S, Hardy J, Bandopadhyay R, Lewis PA. Pathogenic Parkinson's disease mutations across the functional domains of LRRK2 alter the autophagic/lysosomal response to starvation. Biochem Biophys Res Commun. 2013 Nov 29;441(4):862-6.

Massey AC, Kaushik S, Sovak G, Kiffin R, Cuervo AM. Consequences of the selective blockage of chaperone-mediated autophagy. Proc Natl Acad Sci U S A. 2006 Apr 11; 103(15):5805-10.

Matsuda N, Sato S, Shiba K, Okatsu K, Saisho K, Gautier CA, Sou YS, Saiki S, Kawajiri S, Sato F, Kimura M, Komatsu M, Hattori N, Tanaka K. PINK1 stabilized by mitochondrial depolarization recruits Parkin to damaged mitochondria and activates latent Parkin for mitophagy. J Cell Biol. 2010 Apr 19;189(2):211-21.

McNaught KS, Belizaire R, Isacson O, Jenner P, Olanow CW. Altered proteasomal function in sporadic Parkinson's disease. Exp Neurol. 2003 Jan; 179(1):38-46.

McNaught KS, Olanow CW. Proteolytic stress: a unifying concept for the etiopathogenesis of Parkinson's disease. Ann Neurol. 2003;53 Suppl 3:S73-84; discussion S84-6.

McNeill A, Magalhaes J, Shen C, Chau KY, Hughes D, Mehta A, Foltynie T, Cooper JM, Abramov AY, Gegg M, Schapira AH. Ambroxol improves lysosomal biochemistry in glucocerebrosidase mutation-linked Parkinson disease cells. Brain. 2014 May;137(Pt 5):1481-95.

Migdalska-Richards A, Daly L, Bezard E, Schapira AH. Ambroxol effects in glucocerebrosidase and α-synuclein transgenic mice. Ann Neurol. 2016 Nov;80(5):766-775.

Mizushima N, Noda T, Yoshimori T, Tanaka Y, Ishii T, George MD, Klionsky DJ, Ohsumi M, Ohsumi Y. A protein conjugation system essential for autophagy. Nature. 1998 Sep 24;395(6700):395-8.

Mizushima N. The role of the Atg1/ULK1 complex in autophagy regulation. Curr Opin Cell Biol. 2010 Apr;22(2):132-9. Review.

Murphy MP. How mitochondria produce reactive oxygen species. Biochem J. 2009 Jan 1;417(1):1-13. Review.

Musanti R, Parati E, Lamperti E, Ghiselli G. Decreased cholesterol biosynthesis in fibroblasts from patients with Parkinson disease. Biochem Med Metab Biol. 1993;49(2):133–142.

Mytilineou C, Werner P, Molinari S, Rocco A, Cohen G, Yahr MD. Impaired oxidative decarboxylation of pyruvate in fibroblasts from patients with Parkinson's disease. J Neural Transm Park Dis Dement Sect.1994;8(3):223–228.

Narendra D, Tanaka A, Suen DF, Youle RJ. Parkin is recruited selectively to impaired mitochondria and promotes their autophagy. J Cell Biol. 2008 Dec 1;183(5):795-803.

Nedelsky NB, Todd PK, Taylor JP.Autophagy and the ubiquitin-proteasome system: collaborators in neuroprotection. Biochim Biophys Acta. 2008 Dec;1782(12):691-9.

Nicklas WJ, Vyas I, Heikkila RE. Inhibition of NADH-linked oxidation in brain mitochondria by 1-methyl-4-phenyl-pyridine, a metabolite of the neurotoxin, 1-methyl-4-phenyl-1,2,5,6-tetrahydropyridine. Life Sci. 1985 Jul 1;36(26):2503-8.

Obeso JA, Marin C, Rodriguez-Oroz C, Blesa J, Benitez-Temiño B, Mena-Segovia J, Rodríguez M, Olanow CW. The basal ganglia in Parkinson's disease: current concepts and unexplained observations. Ann Neurol. 2008 Dec;64 Suppl 2:S30-46. Review.

Olney JW. Brain lesions, obesity, and other disturbances in mice treated with monosodium glutamate. Science. 1969 May 9;164(3880):719-21.

Orenstein SJ, Kuo SH, Tasset I, Arias E, Koga H, Fernandez-Carasa I, Cortes E, Honig LS, Dauer W, Consiglio A, Raya A, Sulzer D, Cuervo AM. Interplay of LRRK2 with chaperone-mediated autophagy. Nat Neurosci. 2013 Apr;16(4):394-406.

Outeiro TF, Putcha P, Tetzlaff JE, Spoelgen R, Koker M, Carvalho F, Hyman BT, McLean PJ. Formation of toxic oligomeric alpha-synuclein species in living cells. PLoS One. 2008 Apr 2;3(4):e1867

Paisan-Ruiz C, Jain S, Evans EW, et al. Cloning of the gene containing mutations that cause PARK8-linked Parkinson's disease. Neuron. 2004;44(4):595–600.

Papagiannakis N, Xilouri M, Koros C, Stamelou M, Antonelou R, Maniati M, Papadimitriou D, Moraitou M, Michelakakis H, Stefanis L. Lysosomal alterations in peripheral blood mononuclear cells of Parkinson's disease patients. Mov Disord. 2015 Nov;30(13):1830-4.

Pemberton S, Madiona K, Pieri L, Kabani M, Bousset L, Melki R. Hsc70 protein interaction with soluble and fibrillar alpha-synuclein. J Biol Chem. 2011 Oct 7;286(40):34690-9.

Pemberton S, Melki R. The interaction of Hsc70 protein with fibrillar α-Synuclein and its therapeutic potential in Parkinson's disease. Commun Integr Biol. 2012 Jan 1;5(1):94-5.

Plowey ED, Cherra SJ 3rd, Liu YJ, Chu CT. Role of autophagy in G2019S-LRRK2-associated neurite shortening in differentiated SH-SY5Y cells. J Neurochem. 2008 May;105(3):1048-56.

Polymeropoulos MH, Lavedan C, Leroy E, Ide SE, Dehejia A, Dutra A, Pike B, Root H, Rubenstein J, Boyer R, Stenroos ES, Chandrasekharappa S, Athanassiadou A, Papapetropoulos T, Johnson WG, Lazzarini AM, Duvoisin RC, Di Iorio G, Golbe LI, Nussbaum RL. Mutation in the alpha-synuclein gene identified in families with Parkinson's disease. Science. 1997 Jun 27;276(5321):2045-7.

Prigione A, Piazza F, Brighina L, Begni B, Galbussera A, Difrancesco JC, Andreoni S, Piolti R, Ferrarese C.Alpha-synuclein nitration and autophagy response are induced in peripheral blood cells from patients with Parkinson disease. Neurosci Lett. 2010 Jun 14;477(1):6-10.

Reggiori F, Tucker KA, Stromhaug PE, Klionsky DJ.The Atg1-Atg13 complex regulates Atg9 and Atg23 retrieval transport from the pre-autophagosomal structure. Dev Cell. 2004 Jan;6(1):79-90.

Rogers JD, Brogan D, Mirra SS. The nucleus basalis of Meynert in neurological disease: a quantitative morphological study. Ann Neurol. 1985 Feb;17(2):163-70.

Rusmini P, Crippa V, Giorgetti E, Boncoraglio A, Cristofani R, Carra S, Poletti A. Clearance of the mutant androgen receptor in motoneuronal models of spinal and bulbar muscular atrophy. Neurobiol Aging. 2013 Nov;34(11):2585-603.

Saggu H, Cooksey J, Dexter D, Wells FR, Lees A, Jenner P, Marsden CD. A selective increase in particulate superoxide dismutase activity in parkinsonian substantia nigra. J Neurochem. 1989 Sep;53(3):692-7.

Sala G, Arosio A, Stefanoni G, Melchionda L, Riva C, Marinig D, Brighina L, Ferrarese C. Rotenone upregulates alpha-synuclein and myocyte enhancer factor 2D independently from lysosomal degradation inhibition. Biomed Res Int. 2013;2013:846725.

Sala G, Brighina L, Saracchi E, Fermi S, Riva C, Carrozza V, Pirovano M, Ferrarese C. Vesicular monoamine transporter 2 mRNA levels are reduced in platelets from patients with Parkinson's disease. J Neural Transm (Vienna). 2010 Sep;117(9):1093-8.

Sala G, Marinig D, Riva C, Arosio A, Stefanoni G, Brighina L, Formenti M, Alberghina L, Colangelo AM, Ferrarese C. Rotenone down-regulates HSPA8/hsc70 chaperone protein in vitro: A new possible toxic mechanism contributing to Parkinson's disease. Neurotoxicology. 2016 May;54:161-9.

Sala G, Stefanoni G, Arosio A, Riva C, Melchionda L, Saracchi E, Fermi S, Brighina L, Ferrarese C. Reduced expression of the chaperone-mediated autophagy carrier hsc70 protein in lymphomonocytes of patients with Parkinson's disease. Brain Res. 2014 Feb 10;1546:46-52.

Sala G, Trombin F, Mattavelli L, Beretta S, Tremolizzo L, Andreoni S, Calabrese E, Sanvito L, Ferrarese C. Lack of evidence for oxidative stress in sporadic amyotrophic lateral sclerosis fibroblasts. Neurodegener Dis. 2009;6(1-2):9-15.

Schapira AH, Gu M, Taanman JW, Tabrizi SJ, Seaton T, Cleeter M, Cooper JM. Mitochondria in the etiology and pathogenesis of Parkinson's disease. Ann Neurol. 1998 Sep;44(3 Suppl 1):S89-98.

Scott RC, Juhász G, Neufeld TP. Direct induction of autophagy by Atg1 inhibits cell growth and induces apoptotic cell death. Curr Biol. 2007 Jan 9; 17(1):1-11.

Serpell LC. Alzheimer's amyloid fibrils: structure and assembly. Biochim Biophys Acta. 2000 Jul 26;1502(1):16-30. Review.

Sherer TB, Kim JH, Betarbet R, Greenamyre JT. Subcutaneous rotenone exposure causes highly selective dopaminergic degeneration and alpha-synuclein aggregation. Exp Neurol. 2003 Jan;179(1):9-16.

Sian J, Dexter DT, Lees AJ, Daniel S, Agid Y, Javoy-Agid F, Jenner P, Marsden CD. Alterations in glutathione levels in Parkinson's disease and other neurodegenerative disorders affecting basal ganglia. Ann Neurol. 1994 Sep;36(3):348-55

Silva PN, Furuya TK, Braga IL, Rasmussen LT, Labio RW, Bertolucci PH, Chen ES, Turecki G, Mechawar N, Payão SL, Mill J, Smith MC. Analysis of HSPA8 and HSPA9 mRNA expression and promoter methylation in the brain and blood of Alzheimer's disease patients. J Alzheimers Dis. 2014;38(1):165-70.

Singh R, Kaushik S, Wang Y, Xiang Y, Novak I, Komatsu M, Tanaka K, Cuervo AM, Czaja MJ. Autophagy regulates lipid metabolism. Nature. 2009 Apr 30;458(7242):1131-5.

Singleton AB, Farrer M, Johnson J, Singleton A, Hague S, Kachergus J, Hulihan M, Peuralinna T, Dutra A, Nussbaum R, Lincoln S, Crawley A, Hanson M, Maraganore D, Adler C, Cookson MR, Muenter M, Baptista M, Miller D, Blancato J, Hardy J, Gwinn-Hardy K. alpha-Synuclein locus triplication causes Parkinson's disease. Science. 2003 Oct 31;302(5646):841.

Sonia Angeline M, Chaterjee P, Anand K, Ambasta RK, Kumar P. Rotenone-induced parkinsonism elicits behavioral impairments and differential expression of parkin, heat shock proteins and caspases in the rat. Neuroscience. 2012 Sep 18;220:291-301.

Spillantini MG, Divane A, Goedert M. Assignment of human alpha-synuclein (SNCA) and beta-synuclein (SNCB) genes to chromosomes 4q21 and 5q35. Genomics. 1995 May 20;27(2):379-81.

Stricher F, Macri C, Ruff M, Muller S. HSPA8/HSC70 chaperone protein: structure, function, and chemical targeting. Autophagy. 2013 Dec;9(12):1937-54.

Tanaka K, Mizushima T, Saeki Y. The proteasome: molecular machinery and pathophysiological roles. Biol Chem. 2012 Apr;393(4):217-34. Review.

Tansey MG, McCoy MK, Frank-Cannon TC. Neuroinflammatory mechanisms in Parkinson's disease: potential environmental triggers, pathways, and targets for early therapeutic intervention. Exp Neurol. 2007 Nov;208(1):1-25. Review.

Terlecky SR, Chiang HL, Olson TS, Dice JF. Protein and peptide binding and stimulation of in vitro lysosomal proteolysis by the 73-kDa heat shock cognate protein. J Biol Chem. 1992 May 5;267(13):9202-9.

Tetzlaff JE, Putcha P, Outeiro TF, Ivanov A, Berezovska O, Hyman BT, McLean PJ. CHIP targets toxic alpha-Synuclein oligomers for degradation. J Biol Chem. 2008 Jun 27;283(26):17962-8.

Thakur P, Nehru B. Long-term heat shock proteins (HSPs) induction by carbenoxolone improves hallmark features of Parkinson's disease in a rotenone-based model. Neuropharmacology. 2014 Apr;79:190-200.

Venda LL, Cragg SJ, Buchman VL, Wade-Martins R. α-Synuclein and dopamine at the crossroads of Parkinson's disease. Trends Neurosci. 2010 Dec;33(12):559-68.

Vicencio JM, Ortiz C, Criollo A, Jones AW, Kepp O, Galluzzi L, Joza N, Vitale I, Morselli E, Tailler M, Castedo M, Maiuri MC, Molgó J, Szabadkai G, Lavandero S, Kroemer G. The inositol 1,4,5-trisphosphate receptor regulates autophagy through its interaction with Beclin 1. Cell Death Differ. 2009 Jul;16(7):1006-17.

Vogiatzi T, Xilouri M, Vekrellis K, Stefanis L. Wild type alpha-synuclein is degraded by chaperone-mediated autophagy and macroautophagy in neuronal cells. J Biol Chem. 2008 Aug 29;283(35):23542-56.

Wang BS, Yang Y, Yang H, Liu YZ, Hao JJ, Zhang Y, Shi ZZ, Jia XM, Zhan QM, Wang MR.
PKCι counteracts oxidative stress by regulating Hsc70 in an esophageal cancer cell line. Cell Stress Chaperones. 2013a May;18(3):359-66.

Wang Q, Hu W, Lei M, Wang Y, Yan B, Liu J, Zhang R, Jin Y. MiR-17-5p impairs trafficking of H-ERG K+ channel protein by targeting multiple er stress-related chaperones during chronic oxidative stress. PLoS One. 2013b Dec 30;8(12):e84984.

Webb JL, Ravikumar B, Atkins J, Skepper JN, Rubinsztein DC. Alpha-Synuclein is degraded by both autophagy and the proteasome. J Biol Chem. 2003 Jul 4;278(27):25009-13.

Wiedemann FR, Winkler K, Lins H, Wallesch CW, Kunz WS. Detection of respiratory chain defects in cultivated skin fibroblasts and skeletal muscle of patients with Parkinson's disease. Ann N Y Acad Sci.1999;893:426–429.

Winslow AR, Chen CW, Corrochano S, Acevedo-Arozena A, Gordon DE, Peden AA, Lichtenberg M, Menzies FM, Ravikumar B, Imarisio S, Brown S, O'Kane CJ, Rubinsztein DC. α-Synuclein impairs macroautophagy: implications for Parkinson's disease. J Cell Biol. 2010 Sep 20; 190(6):1023-37.

Wong AS, Cheung ZH, Ip NY. Molecular machinery of macroautophagy and its deregulation in diseases. Biochim Biophys Acta. 2011 Nov;1812(11):1490-7. Review.

Wu G, Wang X, Feng X, Zhang A, Li J, Gu K, Huang J, Pang S, Dong H, Gao H, Yan B. Altered expression of autophagic genes in the peripheral leukocytes of patients with sporadic Parkinson's disease. Brain Res. 2011 Jun 7;1394:105-11.

Wu YT, Tan HL, Shui G, Bauvy C, Huang Q, Wenk MR, Ong CN, Codogno P, Shen HM. Dual role of 3-methyladenine in modulation of autophagy via different temporal patterns of inhibition on class I and III phosphoinositide 3-kinase. J Biol Chem. 2010 Apr 2;285(14):10850-61.

Wu F, Xu HD, Guan JJ, Hou YS, Gu JH, Zhen XC, Qin ZH. Rotenone impairs autophagic flux and lysosomal functions in Parkinson's disease. Neuroscience. 2015 Jan 22;284:900-11.

Xilouri M, Brekk OR, Landeck N, Pitychoutis PM, Papasilekas T, Papadopoulou-Daifoti Z, Kirik D, Stefanis L.Boosting chaperone-mediated autophagy in vivo mitigates α-synuclein-induced neurodegeneration. Brain. 2013 Jul;136(Pt 7):2130-46.

Xilouri M, Brekk OR, Polissidis A, Chrysanthou-Piterou M, Kloukina I, Stefanis L. Impairment of chaperone-mediated autophagy induces dopaminergic neurodegeneration in rats. Autophagy. 2016 Nov;12(11):2230-2247.

Xilouri M, Vogiatzi T, Vekrellis K, Park D, Stefanis L. Abberant alpha-synuclein confers toxicity to neurons in part through inhibition of chaperone-mediated autophagy. PLoS One. 2009;4(5):e5515.

Yakhine-Diop SM, Bravo-San Pedro JM, Gómez-Sánchez R, Pizarro-Estrella E, Rodríguez-Arribas M, Climent V, Aiastui A, López de Munain A, Fuentes JM, González-Polo RA. G2019S LRRK2 mutant fibroblasts from Parkinson's disease patients show increased sensitivity to neurotoxin 1-methyl-4-phenylpyridinium dependent of autophagy. Toxicology. 2014 Oct 3;324:1-9.

Yang Q, She H, Gearing M, Colla E, Lee M, Shacka JJ, Mao Z. Regulation of neuronal survival factor MEF2D by chaperone-mediated autophagy. Science. 2009 Jan 2;323(5910):124-7.

Zarranz JJ, Alegre J, Gómez-Esteban JC, Lezcano E, Ros R, Ampuero I, Vidal L, Hoenicka J, Rodriguez O, Atarés B, Llorens V, Gomez Tortosa E, del Ser T, Muñoz DG, de Yebenes JG. The new mutation, E46K, of alpha-synuclein causes Parkinson and Lewy body dementia. Ann Neurol. 2004 Feb;55(2):164-73.

Zhang J, Hattori N, Leroy E, Morris HR, Kubo S, Kobayashi T, Wood NW, Polymeropoulos MH, Mizuno Y. Association between a polymorphism of ubiquitin carboxy-terminal hydrolase L1 (UCH-L1) gene and sporadic Parkinson's disease. Parkinsonism Relat Disord. 2000 Oct 1;6(4):195-197

Zimprich A, Biskup S, Leitner P, et al. Mutations in LRRK2 cause autosomal-dominant parkinsonism with pleomorphic pathology. Neuron. 2004;44(4):601–607